Håkon Furnes Havre
Ulrik Lien
Mattias Myklebust Ness

Network Design for Zero Emission Passenger Vessel Services

Master's thesis in Industrial Economics and Technology Management
Supervisor: Kjetil Fagerholt
Co-supervisor: Kenneth Løvold Rødseth
June 2022

Master's thesis

NTNU
Norwegian University of Science and Technology
Faculty of Economics and Management
Dept. of Industrial Economics and Technology Management

NTNU
Norwegian University of
Science and Technology

Håkon Furnes Havre
Ulrik Lien
Mattias Myklebust Ness

Network Design for Zero Emission Passenger Vessel Services

Master's thesis in Industrial Economics and Technology Management
Supervisor: Kjetil Fagerholt
Co-supervisor: Kenneth Løvold Rødseth
June 2022

Norwegian University of Science and Technology
Faculty of Economics and Management
Dept. of Industrial Economics and Technology Management

NTNU
Norwegian University of
Science and Technology

NTNU | Norwegian University of Science and Technology

Department of Industrial Economics & Technology Management

TIØ4905 - Managerial Economics and Operations Research

Network Design for Zero Emission Passenger Vessel Services

Authors:

Håkon Furnes Havre
Ulrik Lien
Mattias Myklebust Ness

Supervisors:

Kjetil Fagerholt
Kenneth Løvold Rødseth

June, 2022

Preface

This master's thesis is written in the spring of 2022, and marks the end of our Master of Science in Industrial Economics and Technology Management at the Norwegian University of Science and Technology (NTNU), Department of Industrial Economics and Technology Management. The thesis builds upon our project report, written in the fall semester of 2021 within the subject of Managerial Economics and Operations Research. Both the project report and this master thesis is a part of the *Enabling Zero Emission Passenger Vessel Services* (ZEVS) research project, lead by the Institute of Transport Economics (TØI) and including 13 partners from both public and private sector.

We would like to express our deepest gratitude towards our two supervisors, Prof. Dr. Kjetil Fagerholt (NTNU) and Dr. Kenneth Løvold Rødseth (TØI). Their guidance and support has been essential for the success of this master thesis. Additionally, we would like to thank the partners of the ZEVS project, providing us with real world data and insights.

Håkon Furnes Havre, Ulrik Lien & Mattias Myklebust Ness

Trondheim, June 2022

Abstract

This thesis studies the possibility of replacing conventional High-Speed Passenger Vessels (HSVs) with battery-electric HSVs. On a general level, we investigate if technical and economic challenges may be alleviated by appropriate planning of services. We propose a novel Mixed-Integer Programming (MIP) model that considers both operator and passenger costs for a battery-electric HSV service, in which strategic, tactical, and operational decisions are determined. The strategic decisions comprise the vessel type and fleet size, along with locations for charging infrastructure. Tactical decisions include route choices and their associated service frequencies, whereas speed choices along different sailing legs, charging and waiting times are examples of operational decisions. The problem is too complex to be solved to optimality for realistic instances in a commercial solver, and we thus propose a heuristic Decomposition Based solution method. This heuristic is based on fixing the strategic decisions in the MIP and individually solving the subsystems that become independent due to the fixation. We implement and solve the decomposed version of the MIP heuristically for both a battery-electric and conventional vessel service, using data from an existing service in Norway. We solve for both energy carriers to estimate the abatement costs of transitioning to a Zero-Emission (ZE) service, and observe how (if) route choices are affected by this shift. In addition to solving for all the ports in the studied area, we also create high-demand and short-distanced instances to observe the effects on the solution. The results show that the ZE systems have higher total costs than the conventional in all the test instances. The abatement costs in the short distanced instance were lower than the two others, however, indicating that transferring to ZE operations is more costly for services covering large geographical areas. Another important result is a general divergence in tactical decisions between conventional and ZE solutions. The conventional vessels manage to complete longer routes within the given time period, while the ZE vessels are better suited for shorter routes due to their needs for frequent charging. The results also show that demand patterns have great influence on the route structures and frequency choices. From a managerial point of view, our thesis demonstrates the value of replanning existing services to account for technological and economic limitations induced by the transition. In particular, we find that continuing the operation of routes and frequencies optimal for conventional vessels, is not only costly, but in many cases not possible for ZE operations. A general remark, however, is that the future is promising for ZE transportation systems where said limitations are taken into account.

Sammendrag

Denne masteroppgaven studerer mulighetene for å erstatte konvensjonelle hurtigbåter med batteri-elektriske hurtigbåter. På et generelt nivå, undersøker vi hvorvidt tekniske og økonomiske utfordringer kan omgås ved god planlegging av transporttilbudet. Vi innfører en ny blandet heltallsmodell med mål om å minimere summen av operatørens og passasjerenes kostnader knyttet til et batteri-elektrisk hurtigbåttilbud. I modellen tas både strategiske, taktiske og operasjonelle beslutninger. De strategiske beslutningene omfatter båttype, flåtestørrelse og plassering av elektrisk ladeinfrastruktur på land. De taktiske beslutningene består av rute- og frekvensvalg, mens seilingshastighet samt lade- og ventetider er eksempler på operasjonelle avgjørelser. Problemformuleringen er for kompleks til å løses eksakt med kommersiell programvare, og vi presenterer derfor en heuristisk løsningsmetode basert på en dekomponering av problemet. Dekomponeringen skjer ved å fiksere de strategiske beslutningene i den blandete heltallsmodellen, for deretter å individuelt løse de uavhengige subsystemene som oppstår. Vi implementerer og løser heuristikken både for batteri-elektriske og konvensjonelle hurtigbåter, ved hjelp av data innhentet fra et reelt hurtigbåtsamband i Florø, Norge. Vi løser problemet både for konvensjonelle hurtigbåter og nullutslippsbåter for å kunne estimere kostanden ved en overgang til nullutslippsløsninger, samt for å undersøke hvordan (dersom) løsningen forandrer seg. I tillegg til å løse problemet for alle havnene i Florøområdet, lager vi også to instanser med færre havner, hvor disse selektert på bakgrunn av henholdsvis høy etterspørsel og korte reiseavstander til Florø. Resultatene viser at nullutslippsløsningene totalt sett er dyrere i alle instanser. Overgangskostnaden (abatement cost) var derimot lavere i instansen med kortere reiseavstander til Florø enn i de to andre instansene, noe som indikerer at en overgang til nullutslippsbåter er dyrere for hurtigbåtsamband som dekker større geografiske områder. Et annet viktig resultat er en generell divergens mellom de taktiske beslutningene tatt i nullutslippsløsningene og i de konvensjonelle løsningene. Konvensjonelle hurtigbåter kan fullføre lengre ruter innenfor en gitt tidsperiode, mens nullutslippsbåter egner seg bedre til kortere ruter, da de må lades hyppig. Resultatene viser også at etterspørselsmønsteret har stor innvirkning på rutestruktur og frekvensvalg. Fra en beslutningstakers synsvinkel, bidrar denne masteroppgaven til å belyse verdien av å replanlegge eksisterende hurtibåtssamband for å ta hensyn til tekniske og økonomiske begrensninger tilknyttet overgangen til nullutslipp. Spesielt, ser vi at en videreføring av gode ruter og frekvenser for konvensjonelle hurtigbåter, ikke bare er dyrt for nullutslippsbåter, men i mange tilfeller ikke gjennomførbart. En generell betraktning er likevel at fremtiden er lovende for hurtigbåtssamband basert på nullutslippsteknologi, når nevnte tekniske og økonomiske begrensinger hensyntas.

Table of Contents

List of Figures

List of Tables

Abbreviations and Terminology

Abbreviations frequently used throughout the thesis

ZEVSNDP	Zero-Emission Passenger Vessel Service Network Design Problem
ZEVRPP	Zero Emission Route Planning Problem
MIP	Mixed Integer Programming
LP	Linear Programming

Definitions of frequently used terms

Route	Set of ports being visited by the vessel service
Butterfly route	Route allowing for single stops in all ports except one, the central hub
Subroute	Subset of the ports visited in the route, served by the same vessels and experiencing the same service frequency
Central hub	Port with multiple visits in a butterfly route, possibly included in multiple subroutes
Butterfly wing	A cyclic part of a butterfly route, originating and ending in the central hub
Time period	A predefined time interval during the day
Service frequency	How many times during the time period the least visited port in the (sub)route is visited
Rotation	In this thesis, a rotation contains predefined fixed decisions. These are the route with its subroute configuration, the frequency in each subroute, vessel type, number of vessels in each subroute and infrastructure layout

Chapter 1

Introduction

The transport sector accounts for a large proportion of global emissions and has thus become a target in recent climate resolutions. According to the International Energy Agency (2022), the sector needs a 20% emission decrease already by 2030 in order to reach the Paris agreement goal of net zero by 2050. As a result, Norway, a forerunner of the electrification of cars (Energi og Klima, 2022), has planned for additional reductions in the transport sector. Public transportation is an area of particular interest because it is under the jurisdiction of the regional government, and thus directly influenced by governmental policies. A recent emission reduction measure has been the electrification of car ferries. The first battery-electric ferry launched in 2015 (Fjellstrand AS, 2014), and a subsequent ramp-up has resulted in 70 of 130 electrified ferry connections at present (Klima- og miljødepartementet, 2022). The electrification of ferries has fueled other Zero-Emission (ZE) initiatives within waterborne public transportation in Norway. For instance, the first ZE High-Speed Passenger Vessel (HSV) is scheduled for launch this June. An HSV is defined as a passenger vessel operating at speeds higher than 20 knots (Norwegian Ministry of Foreign Affairs, 1994), and the government has presented a concrete target for HSV services in their most recent climate plan (Klima- og miljødepartementet, 2022). That is, future “governmental tenders require low and zero-emission High-Speed Passenger Vessel (HSV) services, where feasible, from 2025”.

Norway has the world’s second-longest coastline, which makes HSVs an integral part of the country’s public transportation service (Klima- og miljødepartementet, 2021). Norwegian district politics are based on accommodating and facilitating occupancy in rural areas, and commuter services are subsidized in order to provide a functional alternative to private transportation. People have consequently become dependent and accustomed to waterborne public transportation, and public HSVs are crucial to retain coastal communities (Norwegian Ministry of Foreign Affairs, 1994). There is great variation in the features and purposes of the services. On the one hand, the commuter connection between Nesoddtangen and Lysaker, a service close to Oslo, spends eight minutes across the Oslofjord. On the other hand, we find the service between Bergen and Selje, a stretch along the western coast of Norway. This connection takes approximately five hours and is often subject to harsh weather and waves reaching up to eight meters. These examples illustrate that the HSVs in Norway operate under varying conditions. Indeed, connections in Norway differ so much that some HSVs are specifically designed for the routes they operate.

The high-speed requirements make HSVs an energy-intensive mode of transport. They are thus prime candidates for a ZE-transition, but the varying operating conditions are a complicating factor. As a matter of fact, Sundvor et al. (2021) found that while 70% of current HSVs in operations could be replaced by hydrogen-driven vessels, only 15% could be operated by battery-electric HSVs without imposing changes to the current operational pattern. As battery-electric vessels have a higher technology readiness level than hydrogen-powered vessels, it timely to study the implications of these changes. This serves as a motivation for this thesis. In particular, we base the report on the overreaching hypothesis that the replacement potential of ZE HSVs is excelled with better planning of services.

We consider a route design problem for an HSV service. The HSVs in the problem use battery electric energy carriers, as opposed to the current vessel services, which rely on fossil energy sources. As a result, new challenges arise regarding, e.g., vessel range, locations for installing onshore infrastructure, and when and where to receive additional energy. Henceforth, we refer to the problem as the Zero-Emission Passenger Vessel Service Network Design Problem (ZEVSNDP). The ZEVSNDP aims to minimize the total system costs of an HSV service, which comprise both operator and passenger costs. The decisions are divided into strategic, tactical, and operational decisions. The *strategic* decisions comprise the vessel type and number of vessels to acquire, along with the locations where infrastructure is installed. The *tactical* decisions include route and frequency choices. Finally, the speed levels along each leg, and the number of passengers to pick up during port calls are examples of *operational* decisions. By solving the ZEVSNDP, we aim to investigate the consequences of choosing ZE vessels over conventional vessels, an analysis that may prove useful for planning future public transportation systems.

We initially formulate the ZEVSNDP as a Mixed-Integer Linear Programming (MILP) model. In the mathematical formulation, we combine more aspects in our modeling approach than previously found in the literature. More specifically, we optimize speed levels along the chosen route, include time-dependent charging, frequency-dependent demand, and diverse route structures, at the same time. A drawback of the initial mathematical formulation is, however, the need for a pre-generated set of candidate routes as input. This, combined with the exponential solution times of the model, motivates the use of a Decomposition Based (DB) heuristic. The solution method is based on fixing the strategic decisions in the ZEVSNDP and individually solving the subsystems that become independent as a result of the fixation. The DB heuristic is able to generate and evaluate promising solutions to the ZEVSNDP, thus finding good solutions using relatively short runtimes.

The MIP-model and the proposed heuristic have been tested on a real-life instance for the geographical area in and around Florø. This is a Norwegian coastal city with approximately 10 000 inhabitants, located in the western part of Norway. Florø is the central stop of several HSV connections, and we use data from current connections as input to our test case. The area consists of 20 ports, served by different routes and schedules. We create novel route structures for these ports and minimize the total system costs. We also create instances that contain subsets of all the ports in the area. More specifically, we consider services only visiting ports near Florø and services only visiting ports with high demand to and from Florø. Further, we rewrite the ZEVSNDP and DB heuristic to account for conventional vessels, to compare ZE solutions to conventional solutions and thus calculate abatement costs of a future transition. The case study shows that the ZE service is the more expensive choice in all cases, but the abatement costs are far lower in the service only visiting the near ports.

This thesis, along with our project report (Havre et al., 2021) are, to our knowledge, the first contributions within operations research that optimize a ZE HSV service. We add a novel MIP to the literature that combines more detailed and realistic modeling choices than previously found in related problems. The problem definition and model formulation are generalized and may be applied in the planning of any battery-electric HSV connection. Moreover, small adjustments make the model applicable for other energy carriers, such as hydrogen. Further, our proposed solution method, the DB heuristic, returns realistic solutions for a real-life instance in Norway. We provide important analyses and decision support from these solutions, such as the impact of variation in future CO_2-taxation schemes and electricity prices. The work thus becomes an essential step toward future maritime transport systems.

The thesis consists of 11 chapters. Chapter 2 further elaborates on the context of the problem, whereas Chapter 3 describes the problem at hand. Further, Chapter 4 presents literature touching upon the same subjects as the ZEVSNDP. Chapter 5 presents the mathematical formulation of the problem, while Chapter 6 explains the DB heuristic. Chapter 7 presents the implementation and instances used, whereas Chapter 8 describes the performance of the DB heuristic and important results. Finally, Chapter 9 summarizes the thesis, while Chapter 10 outlines future extensions to the ZEVSNDP.

Chapter 2

Background

The transitioning into Zero-Emission (ZE) technologies for High Speed Passenger Vessels (HSVs) is attracting broad interest, and since the delivery of our project thesis (Havre et al., 2021) this winter, numerous new projects have been launched world-wide. This chapter provides a background on High Speed Passenger Vessels (HSVs), future propulsion technologies and initiatives within the field. The chapter is an extension of the background provided in Havre et al. (2021).

The chapter is organized as follows. Section 2.1, introduces the fast ferry market and presents both international and national progress on Zero-Emission (ZE) technologies for passenger vessels. Section 2.2 elaborates on the Enabling Zero Emission Passenger Vessel Services (ZEVS) project, of which this thesis is a part. Thereafter, Section 2.3 describes potential energy carrier technologies relevant for HSVs. Finally, Section 2.4 presents examples of both completed and ongoing ZE vessel initiatives, including both car ferries and vessels exclusively serving passengers.

2.1 High Speed Passenger Vessels

HSVs have emerged as important alternatives in commuter transport worldwide. There are several connections that serve as good examples of areas with high demand for transport by HSVs. In San Fransisco, there was a passenger increase of 85% from 2012-2017 in the local commuter connections. Due to rail and highway being at capacity, this is a segment local authorities seek to expand. They plan for a long-term goal of 44 operational vessels within 2035, compared to a current fleet of 14 (WETA, 2018). In Dar Es Salaam, several fast ferry companies connect coastal islands to the mainlands. One of the main carriers, Azam Marine run four departures between the islands a day, carrying up to 600 passengers per departure (Azam Marine, 2022). Yet another area relying on fast ferry services is the Sydney bay. Here, the carriers spend 18 minutes as opposed to one hour with terrestrial modes of transport (NRMA, 2022). In the Hong Kong area, HSVs connect main ports as well as smaller islands (Wang et al., 2008). Recently, three HSVs were delivered to Hong Kong from Brødrene Aa AS, a Norwegian shipyard (Brødrene Aa AS, 2017). Brødrene Aa have long traditions with the construction of HSVs for the Norwegian market.

Even though HSVs have experienced increased attraction and usage, they exhibit an energy intensive use profile, and high emissions per passenger-kilometer (pkm). The IMO (2020) expects an increase in CO_2-emissions of 90-130% in the sector by 2050, from 2008 levels. This estimate assumes a "business as usual" scenario, accounting for an atmospheric temperature increase of below two degrees Celsius. The same study emphasizes the adoption of low-carbon alternative fuels to reach the target of a 50% reduction in greenhouse gas emissions by 2050. The stage is, in other words, set for alternative propulsion technologies in the maritime sector, and HSVs are important candidates due to their high emissions per passenger-kilometer. To illustrate, HSVs consume approximately five times the energy per passenger-kilometer compared to scheduled flights. The numbers amount to 13.2 MJ/pkm and 2.7 MJ/pkm, respectively (Ianssen et al., 2017). As of yet, there are, to our knowledge, no operating HSVs worldwide utilizing ZE propulsion systems, which further motivates the research within applicable technologies.

In Norway, a leading European ZE market, there has been rapid development within ZE technologies for the maritime sector in general, and car ferries in particular. The world's first electrical car ferry, MF Ampere, was launched in Norway in 2015. According to Sundvor et al. (2021), Norway has electrified 70 of its approximately 130 car ferry connections as of 2021. Moreover, the first liquid hydrogen car ferry, MF Hydra, was launched in 2021. The world's first battery-electric HSV, MS Medstraum, is scheduled for launch later in 2022. Sundvor et al. (2021) find that 60% of the current Norwegian fleet of conventional HSVs can be replaced with battery-electric or hydrogen-based HSVs. This conclusion is based on existing routes and calculated vessel range for candidate energy carriers. They further highlight that 22 of the current conventional routes are incompatible with both battery-electric and hydrogen as energy carriers. This is due to high energy demands and strict schedules. Thus, for Norway to reach its goal of zero emissions within the public transportation sector, optimizing timetables and route structures is necessary. The modeling of such an optimization problem is indeed the purpose of this report.

2.2 Enabling Zero Emission Passenger Vessel Services

One of the initiatives with the intent of improving knowledge and insight into fossil-free HSVs, is the Enabling Zero Emission Passenger Vessel Services (ZEVS) project. It is overseen by the Norwegian Institute of Transport and consists of six parts, or Work Packages (WPs). The WPs are shown in Figure 2.1. This report will contribute to WP4, focusing on assessing routes and schedules for novel HSV technologies. The overall goal of the ZEVS-initiative is to remedy lacking research on ZE HSVs, and develop a decision-support tool for the governmental electives responsible for addressing the transition to ZE transportation. The project will have a particular focus on how schedules and routing is affected by ZE technologies. In a broader perspective, ZEVS focuses on how society is affected by these emerging technologies. The six WPs address different aspects of the problem and are synthesized into a roadmap at the end of the project. Areas such as ZE infrastructure and attributes of different vessel types will thus be covered in different WPs.

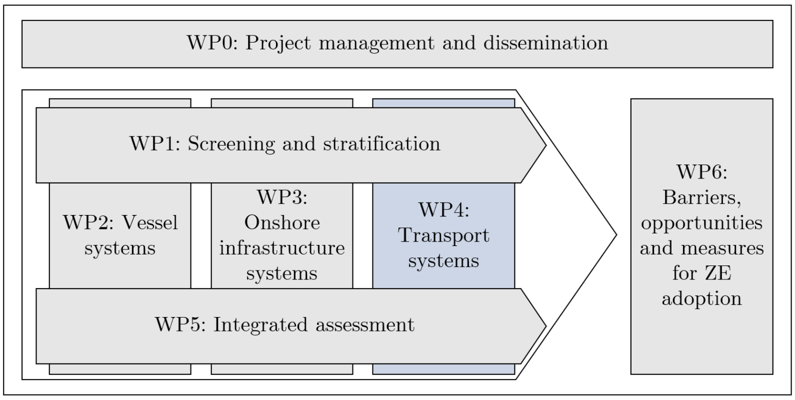

Figure 2.1: An overview of the ZEVS project structure

As shown in Figure 2.1, the different WPs are interlinked and depend on each other. WP1 contributes with feasibility studies of existing routes and services, in order to locate current ZE candidates. WP2 inspects the current vessel types and attempts to predict energy usage and emissions of current and novel vessel technologies, using available public information. WP3 results in an optimization model for ZE infrastructure, as well as studies on different types of energy carriers. Additionally, energy consumption profiles are developed in order to understand the demand for novel power resources, e.g., hydrogen. WP4 considers the operational service. Specifically, it addresses whether or not ZE services are in conflict with economic efficient operations, and if ZE services can be introduced while simultaneously improving economic efficiency through better planning of services. The deliverable from this WP is an optimization model with the objective of minimizing passenger, operational and damage costs while accounting for the constraints of a more frequent recharging/refill system. The two final WPs serve as an assessment of the former WPs and produce a final product. WP5 further inspects the routes and their feasibility for ZE operations, given the results from WP2 to WP4. WP6 evaluates the political viability of the proposed measures and presents future steps of action. Regional governments are also invited to review the former models and construct incentive schemes to accelerate the transition. Finally, a roadmap outlining required actions for a transition to ZE in the HSV sector is produced.

2.3 Energy Carriers

This section describes three energy carriers relevant for HSVs, both in the short and long-term. In Subsection 2.3.1, battery-electric technology, which is the chosen energy carrier in the mathematical model in Chapter 5, is described. Further, in Subsection 2.3.2, the use of hydrogen in HSVs is outlined. Finally, we elaborate on ammonia as an energy carrier. Ammonia has not received as much attention as the two other carriers, but is nevertheless relevant in a longer time horizon. Figure 2.2 shows the energy densities (kWh/kg) of the different technologies. The numbers are found in Brown (2017) and Sundvor et al. (2021), and illustrate an important variation between the proposed energy carriers.

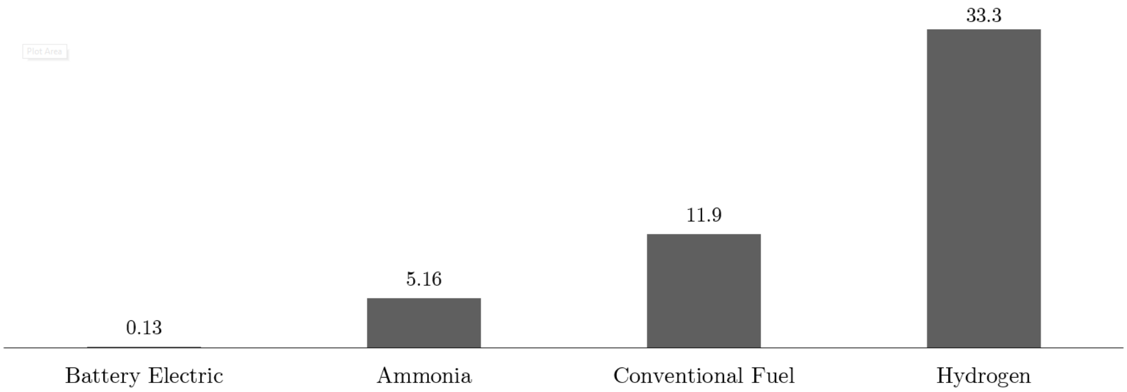

Figure 2.2: The energy density (kWh/kg) of different technologies

2.3.1 Battery-electric

Current battery technologies restrict the number of feasible routes for battery replacements. Batteries have lower energy storage per kilogram than, for instance, diesel and thus require substantial battery weight in order to store enough energy for longer routes. This limits the feasible routes for battery-electric ferries to 16% of the current routes along the Norwegian coastline when assuming today's battery technologies (Sundvor et al., 2021).

Nevertheless, there are several advantages with electric propulsion systems compared to the conventional motors used in HSVs today. Firstly, an electric system is more robust to the varying amount of thrust experienced by HSVs due to acceleration and deceleration occurring when docking frequently. Moreover, electrical motors require less maintenance than conventional propulsion systems, reducing operational costs (Ianssen et al., 2017). Additionally, the route layout of high-speed passenger vessels with frequent stops enables the opportunity for regular charging. An adaption of battery-electric HSVs is also advantageous for the passengers aboard, as they are less exposed to the noise from conventional engines.

However, some challenges remain. The power available for charging is dependent on local grid capacities, which are often limited compared to the HSV's energy demand. This issue is especially relevant on islands and in rural areas (DNV GL, 2019). Besides, there are substantial costs of installing infrastructure for charging. This adds to the investment cost related to replacing the vessel itself or retrofitting an electric drive train.

2.3.2 Hydrogen

Hydrogen is an energy carrier that may be produced without emissions. Due to safety issues, hydrogen tanks are required to be placed on open decks, and filled in safe distances from where passengers embark and disembark. According to Sundvor et al. (2021), it takes approximately 20 minutes to fill a hydrogen tank of 450 kilograms.

One may produce hydrogen using various methods. 95% of the hydrogen used today is made through a reformation of natural gas or other fossil fuels. On a global scale, this leads to 830 million tons of CO_2-emissions per year, which equals the emissions of the UK and Indonesia, combined (Agency, 2019). This approach may, however, experience reduced emissions in the future with carbon capture and storage technology. Another procedure for hydrogen production is through electrolysis, which yields hydrogen by separating water molecules using an electric current. Electrolysis consumes a lot of energy and is thus not preferred economically. However, the technique is without emissions, given that the initial energy is fossil-free. There are two main ways of utilizing the energy in the hydrogen, once aboard the HSV (DNV GL, 2019). The most energy-efficient method is through fuel cells. This is a process where fuel (i.e., hydrogen) in combination with air is separated into protons and electrons. The electrons traverse an external circuit, thus converting chemical energy into electric energy (US Department of Energy, 2021). The second method of hydrogen usage is through direct combustion with air. The overall efficiencies are 50-60% and 40-50% for the two approaches, respectively.

There are some challenges related to hydrogen as an energy carrier. First of all, it is difficult to store efficiently. There are two ways of storing hydrogen on a vessel: either as a compressed gas or as a liquid. The reason for this is that although hydrogen has a high energy density by weight (Figure 2.2), its energy density by volume is low without compression or cooling (Zittel et al., 1996). According to DNV GL (2019), the liquid form is more expensive than the compressed form due to temperature and insulation requirements. On the other hand, compressed hydrogen requires special tanks to avoid the hydrogen molecules exuding into the insulation material, as this may cause metal embrittlement and gas leakages. This poses safety issues, as hydrogen is highly flammable. Moreover, there is presently limited infrastructure facilitating maritime hydrogen use.

2.3.3 Ammonia

Ammonia has a long history of industrial use. It has been used for over 100 years in the fertilizer industry, and was also experimented with as a supplement to coal fuel on an omnibus during the second world war (Kobayashi et al., 2019). More recently, ammonia has received increased attention as an energy carrier due to the aforementioned challenges related to hydrogen. Moreover, ammonia can be produced emission-free, liquefies at higher temperatures, and is 50% more energy-dense per unit volume than liquid hydrogen (DNV GL, 2019). As liquid ammonia shares approximately the same vaporization temperature as propane, it can be transported using existing infrastructure and containers developed for propane.

There are, however, some drawbacks with ammonia as an energy carrier. In short, the technology is premature and must be heavily researched and tested before it is commercially viable. DNV GL (2019) estimates that ammonia only will be used in subsidized pilot projects in the next 5-10 years. Difficulties to be overcome are, e.g., a high ignition temperature, low flammability, and the fact that most of the production today is from natural gas. Like hydrogen, ammonia is dependent on the advancement of carbon capture and storage to become emission-free. Due to hydrogen and ammonia demonstrating a lower readiness level for HSVs, we formulate the ZEVSNDP for a battery-electric energy carrier.

2.4 Zero Emission Initiatives

As mentioned in the introduction of this chapter, there has been rapid developments in the HSV sector. These developments in particular include novel ZE alternatives. Since Havre et al. (2021)

put forth their preliminary research to the area, numerous projects have been launched, and some of these are planning for operation within the coming months. In the following, we present forerunners to emission free HSVs, namely ferries powered by ZE propulsion in Norway. Subsequently, we present the world's first ZE HSV, the TRaM initiative (Rogaland Fylkeskommune, 2021). We lastly present some world-wide ZE HSV projects scheduled for operation in the near and distant future.

2.4.1 MF Ampere

The world's first battery-powered electric ferry MF Ampere (Figure 2.3), launched in 2015. It operates 34 departures on weekdays between Lavik and Oppedal, a car ferry connection in western Norway. The ferry has contributed to emission reductions, and the operator, Norled, estimated a reduction of three million liters of diesel and a corresponding 8 100 tons of CO_2 by late 2018. Additionally, they estimated a reduction in operating costs by 80% due to reduced fuel consumption and maintenance (Norled, 2018). The ferry's capacity is 120 cars, and it can serve a total of 350 passengers per departure. Two lithium-ion batteries provide MF Ampere with a total capacity of 1 000 kWh. The ferry holds a top speed of 14 knots and an operating speed of 10 knots (Fjellstrand AS, 2014). The introduction of MF Ampere was an inflection point for the transition to ZE car ferries, and by the end of 2021, 70 of approximately 130 ferries are planned to be powered by electricity (Energi og Klima, 2021a).

2.4.2 MF Hydra

Another great leap within the car ferry industry is planned for the autumn of 2022, as MF Hydra (Figure 2.4) is set to become the world's first hydrogen-powered ferry. The vessel already commenced operation during the autumn of 2021, but is currently operated on battery cells. It took longer than expected to complete documentation and practical details, resulting in a delay of operation on hydrogen. MF Hydra serves the route between Hjelmeland and Skipavik in southwestern Norway, together with the battery-powered MF Nesvik (Teknisk Ukeblad, 2021). MF Hydra is designed to use three energy sources: two 200 kW hydrogen-powered fuel cells, a battery of 1 360 kWh, and a diesel-powered generator of 440 kW. The hydrogen cells are intended to continuously power the batteries, whereas the diesel generator is installed as backup. One expects the hydrogen to account for approximately 50% of the energy production in the batteries, whereas the remaining energy demand is provided by onshore charging stations. MF Hydra shows how vessels also may utilize multiple energy carriers to enable the transition away from fossil fuels.

Figure 2.3: MF Ampere, photo courtesy of Norled

Figure 2.4: MF Hydra, photo courtesy of Norled

2.4.3 MS Medstraum

Even though car ferries and lower-speed passenger vessels have transitioned to ZE energy carriers, there is yet no HSV in operation powered by sustainable energy sources. However, one initiative, Transport: Advanced and Modular (TrAM) is in its final stages and plans the launch of an electrical HSV during the summer of 2022. This initiative is coordinated by Kolumbus, the operator of public transport in Rogaland, which has resulted in the construction of the world's first battery-electric HSV, MS Medstraum (Figure 2.5). The vessel will operate the connection between Stavanger and Byøyene in Rogaland county and accommodate up to 150 passengers and 20 bicycles. Medstraum will have a battery capacity of 1 500 kWh, with a maximum charging power of 2 000 kW. The vessel is designed for an operating speed of 23 knots (Rogaland Fylkeskommune, 2021).

2.4.4 Zero-Emission High Speed Vessel initiatives

Since Havre et al. (2021), numerous new Zero-Emission (ZE) alternatives for HSVs have been launched. These are mainly in urban areas, and a subset are briefly introduced below.

In *Auckland, New Zealand*, there are high ambitions for a fleet of ZE HSVs. They aim to operate an entirly electric fleet of HSVs by 2030 (Bunkerspot, 2022). As a stepping-stone, they have scheduled the launch of two electric passenger fast ferries, ready for operation in 2024. According to Bunkerspot (2022), the current service consumes around 13 million liters of diesel a year, which emit 34 000 tons of CO_2. The ferries scheduled for 2024 will have a capacity of 200 passengers, a length of 24 meters and a maximum sailing speed of 25 knots. They are further designed in a way that supports a future retrofitting of larger batteries.

In *San Francisco, US*, there are plans for the launch of a 75-passenger hydrogen powered fast ferry named *Sea Change* (Voanews, 2022). The ferry is planned for operation this June, and sail at a max speed of 20 knots. The vessel is powered by hydrogen fuel cells, which subsequently convert hydrogen into electricity. This will be the first HSV in the world completely powered by hydrogen.

Stockholm, Sweden are currently planning for a ZE HSV named Beluga24 (Marine Link, 2022). The Beluga24 exhibits a new design, based on hydrofoil technology. As a result, the manufacturers estimate a reduction in energy usage by 50 % as compared to conventional catamarans used today. The Beluga24 is expected delivered in 2023, with a commence in passenger service in early 2024.

In *London, UK*, the transport company Uber and river transport company Thames Clipper have cooperated on a low-emission project (Offshore Energy, 2022). It is set out to be a passenger service on the river Thames, operated with both electricity and biofules. The former is intended for use within central London, whereas the latter will be used outside. The vessels will use excess power from the biofueled engines to recharge the batteries, contrary to current technologies, which need to dock in order to charge. The project expects its first launch in the autumn of 2022, and subsequent strengthenings are planned for the spring of 2023. The operators have, as of yet, committed to achieve net-zero emissions by the end of 2025.

Figure 2.5: Concept image of Medstraum, illustration courtesy of Kolumbus

Figure 2.6: Concept image of electric fast ferry in Auckland, photo courtesy of Danfoss

Chapter 3

Problem Definition

This chapter presents the Zero-Emission Passenger Vessel Service Network Design Problem (ZEVSNDP), studied in this thesis. ZEVSNDP is relevant for all coastal areas offering water-borne public transportation to its inhabitants. The problem is typically encountered by operators, already operating a vessel service or planning a new one. The problem is particularly relevant for a transition from conventional marine diesel operations to Zero-Emission (ZE) solutions. The ZEVSNDP is, similarly to the ZEVRPP presented in Havre et al. (2021), applicable to a broad range of energy carriers, as discussed in Chapter 2. Due to current technical limitations within other energy carriers, the model formulated in Chapter 5 is based upon battery-electric vessels. To provide a thorough understanding of the problem at hand, this chapter explains the relevant aspects of it as follows: Section 3.1 presents the problem input and relevant assumptions while Section 3.2 explains the problem objective, the different decisions that are made and the belonging restrictions. To further exemplify the problem, Section 3.3 presents an overview of the problem's key components.

3.1 Problem Input and Assumptions

The coastal area considered in the problem is populated by a set of ports. We assume that every pair of ports within this set has a predefined demand for transportation for a given time period throughout the day. The varying demand within the port pairs is illustrated in Figure 3.1. The figure shows four ports (A-D) with a given demand for transportation between them for three time periods throughout a day.

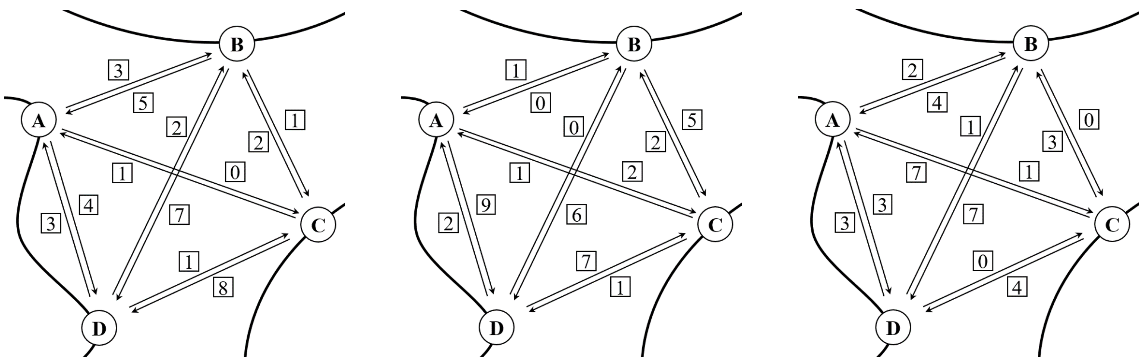

(a) Period 1 (b) Period 2 (c) Period 3

Figure 3.1: Demand between ports A-D for three time periods throughout a day

Although a fixed total demand for transportation is assumed, the fraction of the number of passengers choosing the vessel service as their desired mode of transportation, is influenced by the perceived frequency of the service. We define the service frequency as the experienced possibility to travel from a port to another. That is, if a route has two vessels, and these sail two round trips each, a passenger may travel from a port to another a total of four times over the planning horizon. We assume that the demand for the use of the vessel service is dependent of this frequency, where a higher service frequency increases the popularity and usability of the service. The dependency between experienced frequency and the willingness to use the vessel service as one's preferred mode of transportation is thus an important input to the problem.

All passengers not served by the vessel service are assumed to choose alternative modes of transportation to fulfill their demands for travel. A passenger not using the vessel service may thus stem from three different phenomena. Firstly, as mentioned above, the service frequency may be too low for the passenger to consider the service as an adequate option for traveling. Secondly, the vessel chosen for the service may not have sufficient passenger capacity to accommodate all demand, leaving passengers behind at port calls. Thirdly, the selected route may not visit the port the passenger is traveling to or from. All three reasons elicit unmet demand, causing passengers to choose alternative transportation methods. Consequently, the cost of alternative transport, which varies between port pairs, is thus an important input to the ZEVSNDP.

Further, an important input to the problem is the candidate vessel types. The candidate vessel types are the selection of vessel types the problem may choose to invest in, and utilize in its route. Each vessel is associated with an investment cost, an hourly crew cost, a passenger capacity, an energy storage capacity (e.g. battery size), and an energy consumption profile. A large set of predefined vessel types is assumed, ensuring broad coverage of sailing speeds, passenger capacities and energy storage capabilities. The available vessels may be easily altered to fit other energy carriers, such as conventional fossil fuels, hydrogen, or ammonia.

Another category of important input to the problem is linked to the onshore infrastructure necessary to provide the vessels with energy. This may be filling stations for hydrogen or, as in the model discussed in this thesis, electrical charging stations. Such infrastructure must be placed in at least one of the ports, and investment costs and available power (determining the charging speed) in the area, constitute important input.

The final critical input to the ZEVSNDP is, as in many problems regarding public transportation, the *passengers' value of time*. This is important, because the passenger cost is closely connected to the travel time multiplied by the value per time unit. A longer travel time, consisting of both waiting time in port and sailing time, has a greater cost than a shorter one, and vice versa for a shorter travel time. The precise level of the passengers' value of time depends on multiple factors, as discussed by Wardman (2001), and could hence be difficult to determine. The conversion between time and monetary units for the passengers does, however, enable a single objective problem, which is the minimization of total system costs.

An important assumption in the ZEVSNDP is the limitation of only choosing one vessel type. This aspect of the problem is introduced to reduce the problem complexity and to obtain more realistic solutions. To be able to treat every departure within a port pair equally, we prohibit different vessel types. If a route could be served by two different vessel types, one could imagine a scenario where one of the vessels had a large capacity and the other a very small capacity. If the vessels sailed one round trip each, the passengers should by our definition experience a service frequency of two. However, if the small vessel always would fill up, many would have to wait for the large vessel, reducing the actual service frequency to one. To mitigate this effect, only one vessel type is allowed.

3.2 Objective, Decisions and Restrictions

The objective of the ZEVSNDP is, similar to the ZEVRPP, to minimize the total system cost. That is, to minimize the sum of operator and passenger costs for the vessel service. The operator costs are defined as the sum of the vessel investment costs, the crew cost, the infrastructure investment costs and the energy cost of the vessel service. The passenger costs are defined as the sum of the passengers' cost of alternative transportation, the cost of waiting in port and the passengers' sailing time costs. The entire cost structure is illustrated in Figure 3.2.

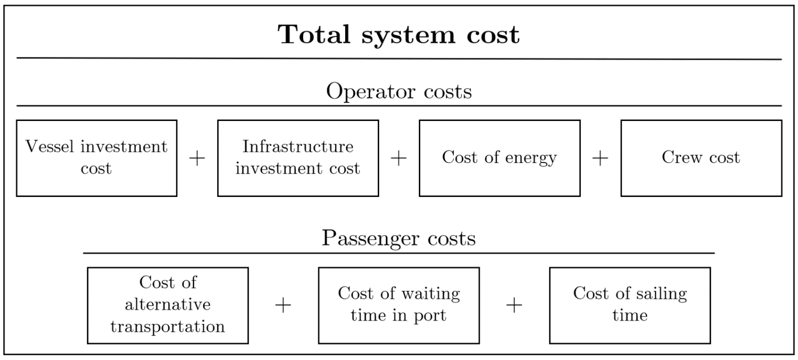

Figure 3.2: Overview of the total system costs minimized in the ZEVSNDP

The ZEVSNDP contains many different decisions. An essential one is the selection of which route to sail. This route may, as opposed to the fixed cyclical routes in the ZEVRPP (Havre et al., 2021), take on many different structures. A route defines a sequence of ports, enabling diverse route structures such as *simple cycle*, *butterfly* and *chain routes*. Simple cycle routes only allow for one stop in each port per round trip, whereas butterfly routes have a central hub, occasionally referred to as *the butterfly port*, where multiple stops are allowed. Where Reinhardt and Pisinger (2012) only let the central hub have two visits per round trip, we extend the definition of the butterfly route to allow for multiple visits in the central hub. This allows for more than two *wings* in the butterfly route, with routes bearing resemblance to a *flower*, rather than a butterfly. A third route structure, denoted the chain route (Thun et al., 2017), is an extension to the butterfly route. This structure allows for multiple central hubs in one route, suitable for routes along a coastline or in a fjord, allowing port stops in both directions. An illustration of the three route structures is found in Figure 3.3. The set given as input to the ZEVSNDP may contain many variations of these route structures, varying between time periods.

An essential part of a route is its (optional) division into subroutes. This allows a route to be operated in separate smaller routes, each having its own number of vessels in use and service frequency. This is highly relevant for routes with a butterfly structure, where separate vessels are able to serve the different wings of a route, utilizing the central port as a transit hub. To exemplify this further, we consider Figure 3.3b, and a situation where ports 1, 2, 3 and 5 comprise a subroute and ports 4, 5, 6 and 7 comprise another one. The route would then be operated as two separate ones, allowing for different sailing frequencies in the two wings. Passengers travelling from port 3 to port 6 would have to change vessel in port 5.

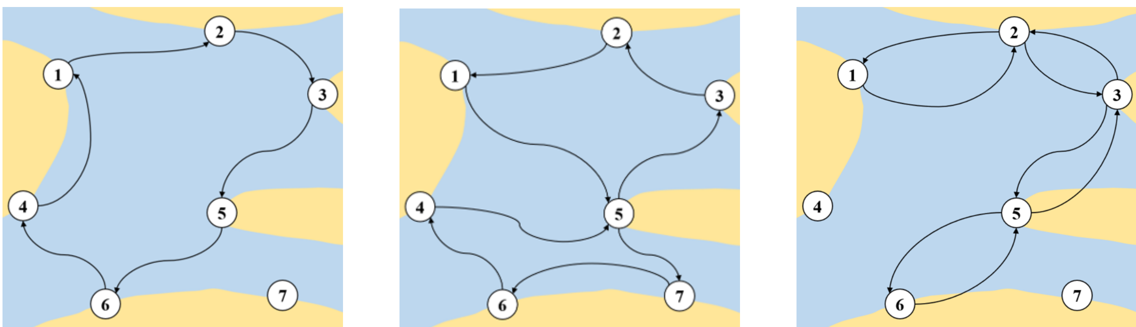

(a) Simple cycle route **(b)** Butterfly route **(c)** Chain route

Figure 3.3: Examples of different route decisions in the ZEVSNDP

The ZEVSNDP is a complex problem with a multitude of decisions made on every stage of the planning hierarchy, as illustrated in Figure 3.4. Starting from the top, the problem includes several important strategic decisions. These decisions are the vessel type and number to acquire, in addition to which port(s) to install onshore infrastructure in. These decisions have a large impact on the future passenger vessel system due to their long time horizons. Both vessel and infrastructure investments set the boundaries for future flexibility in the service offered. The tactical decisions in the problem are which route to select, as described above, and for each subroute, the decision of how many vessels to use and with which frequency to sail. The inclusion of subroutes in the problem offers a large combination of frequency decisions within otherwise similar routes. These decisions are possible to redo, but should however stay somewhat constant to provide predictability and continuity for passengers using the service. The same applies for the utilization of acquired vessels. The last group of decisions are the operational decisions, constituting of passenger flow (how many passengers to transport within each port pair), the speed on each sailing leg of the chosen route, and the time usage throughout the time period, e.g., how much time to spend sailing, charging and waiting in the different ports. The decisions regarding time usage are key decisions in calculating a correct passenger cost for a candidate route. Spending time charging with many passengers on board increases their travel time, while charging with an empty boat has no effect on their costs. Furthermore, the length of the charging time is an important decision as it determines the battery level when leaving the port, deciding the possible energy usage and thus the possible sailing speed. The last relation stems from the fact that maintaining a higher sailing speed requires a higher power output per distance unit. This last point showcases the large degree of interdependence between the operational decisions. The operational decisions are easier to change, but do however have to stay within the boundaries set by the strategic and tactical decisions.

We would like to emphasize that the main focus of the problem is to consider the strategic decisions and provide managerial support for these decisions. Vessel type, the number of vessels, and where to install charging infrastructure are decisions with significant impact, and thus primary focus when planning for ZE passenger vessel services at low system costs. However, the tactical and operational decisions play an important role as feedback variables. Strategic choices limit the solution space for the tactical and operational decisions, and feedback from this limitation's impact on the objective value is critical to quantify the strategic solutions. Optimizing the decisions on all planning levels simultaneously could lead to better overall solutions. On this basis, both the operational, tactical and strategic decisions are important in the ZEVSNDP, although the main focus is on the latter.

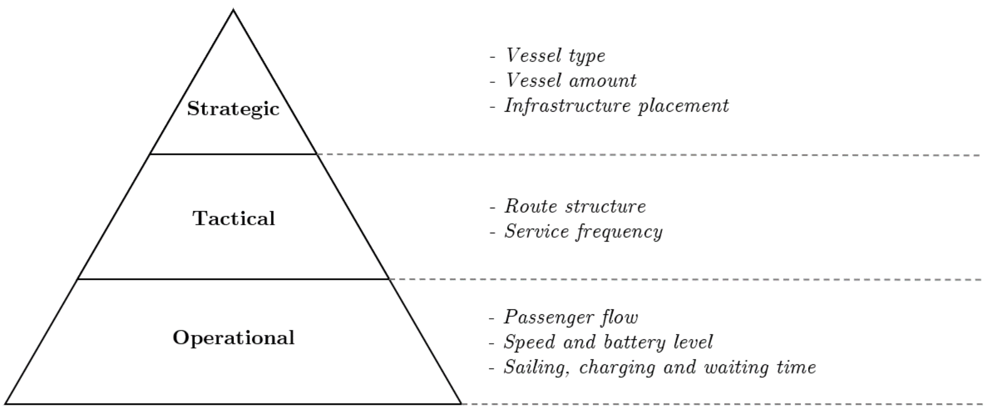

Figure 3.4: Overview of strategic, tactical and operational decisions in the ZEVSNDP

There are four main types of restrictions in the ZEVSNDP problem. Firstly, a main restriction is the enforcement of only allowing the use of vessels and infrastructure already invested in. This restriction links the strategic and operational decisions, thus securing realistic solutions. Secondly, the number of passengers that could be transported is restricted by the vessels' capacities and the demand for transportation. Thirdly, the route and speed selection is restricted by the battery capacities of the vessels. A vessel's battery level must at all times be below a maximum and above a minimum level to ensure safe operations and prolong battery lifetime. This is an important restriction in the ZEVSNDP, ensuring that the problem acquires appropriate vessels, with a suiting battery capacity, to serve the route in question. The fourth type of restrictions is the limitations on time usage with respect to service frequency and the number of vessels. The number of vessels and the frequency of service define the schedule of the route. All these scheduled trips must be completed within the planning horizon.

3.3 Numerical Example

To further explain and exemplify the ZEVSNDP, we introduce a toy-sized numerical example in this section. The example does not contain all relevant input parameters described in Section 3.1, but introduces key parameters to provide a good understanding of the core problem. To reduce complexity and avoid the question of optimality, cost parameters are disregarded in this example. We do, however present a feasible solution to the problem, providing an understanding of what such a solution could look like. Questions regarding optimality and costs are more thoroughly discussed in Chapter 8.

Assume a coastal area populated by four ports, A, B, C and D. The ports and the distances between them are illustrated in Figure 3.5. The distances are subsequently used to calculate the sailing time between ports, and the energy usage required to maintain a certain speed level between them.

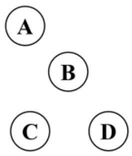

(a) Ports

	A	B	C	D
A	0	7	18	20
B	7	0	8	8
C	18	8	0	8
D	20	8	8	0

(b) Distances in nautical miles

Figure 3.5: Overview of ports and distances in the numerical example

Further, we assume that we consider three time periods, each lasting four hours, throughout a day, giving the total planning length a duration of twelve hours. Each period has a specified demand for transportation, dependent on the offered service frequency. As visible from Table 3.1, the possible service frequencies to choose from are either one or two, where a frequency of one implies a lower demand for the passenger vessel service, as described in Section 3.1. If a frequency of one is chosen, the difference between the demand with a frequency of two (maximum frequency) and the demand at a frequency of one, is treated as unmet, forcing alternative transportation for the passengers in question. It is worth noting that the demand between certain port pairs is zero and that some port pairs have a higher demand in one direction in one period, and in the other direction in a different period. The last point is interesting for the sailing direction of a route, and will be discussed further in Chapter 8.

	A	B	C	D
A	0	80	10	90
B	50	0	20	35
C	10	70	0	60
D	25	30	15	0

(a) Period 1, $f = 1$

	A	B	C	D
A	0	70	0	10
B	10	0	25	50
C	0	45	0	30
D	0	40	20	0

(b) Period 2, $f = 1$

	A	B	C	D
A	0	35	5	65
B	60	0	0	0
C	30	40	0	25
D	15	30	15	0

(c) Period 3, $f = 1$

	A	B	C	D
A	0	90	14	98
B	55	0	22	40
C	12	75	0	65
D	28	35	18	0

(d) Period 1, $f = 2$

	A	B	C	D
A	0	74	0	12
B	12	0	30	58
C	0	52	0	36
D	5	45	24	0

(e) Period 2, $f = 2$

	A	B	C	D
A	0	42	8	70
B	70	0	4	0
C	34	40	0	25
D	18	30	24	0

(f) Period 3, $f = 2$

Table 3.1: Demand for transportation between port pairs for different time periods and service frequencies (f)

The next input in this numerical example is the set of available routes to choose from in each time period. To avoid introducing unnecessary complexity to this example, all three time periods are assigned the same set of candidate routes to choose from. The set of routes could contain a multitude of different route structures, but we have decided to limit the set to four distinct routes in this example, visible in Figure 3.6.

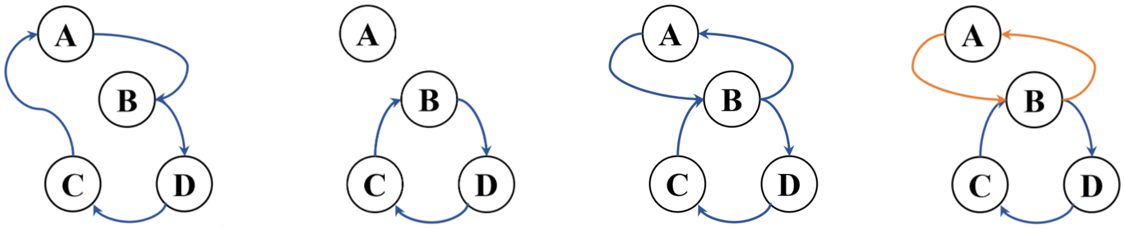

(a) Route 1 **(b)** Route 2 **(c)** Route 3 **(d)** Route 4

Figure 3.6: Set of routes provided as input to the problem in every time period

Each route has some characteristics worth studying closer. Route 1 is a classical cyclical route, similar to those studied in the ZEVRPP (Havre et al., 2021). The route visits every port once before looping around and starting over. Route 2, on the other hand, does not stop in every port, as it never visits port A. This is a fully feasible route, as there is no requirement to visit all ports. Demand either to or from port A is considered covered by alternative modes of transportation. Apart from skipping port A, route 2 shares the cyclical structure of route 1. Route 3 is a butterfly route. This implies that the vessels stop in port B twice during a cycle through the route. Route 3 does however only constitute of one subroute, meaning that passengers travelling through port B do not change vessel, but stay onboard the entire time from their origin to their destination. The division into subroutes is the only difference between route 3 and route 4. Route 4 consists of two separate subroutes. This does, unlike route 3, imply that passengers travelling through port B have to disembark their vessel in B and wait for the next one bringing them to A. It is important to note that the division into multiple subroutes has a few consequences for the strategic decisions in the ZEVSNDP problem. Firstly, all subroutes must be connected to a port with charging infrastructure to ensure that the vessels are able to charge without leaving their subroute. Secondly, the number of vessels acquired can not be less than the number of subroutes. This follows from the fact that each subroute is operated separately. To illustrate, one could imagine one vessel sailing in a "figure eight" in route 3, while route 4 must consist of two separate circles, with at least one vessel in each.

Returning to the numerical example, the next important input is the set of candidate vessel types to choose from. This set could potentially contain a large number of vessel types, but is in this numerical example limited to three different vessel types, shown in Table 3.2. The table includes the passenger capacity, the battery size and the vessel type's power demand to maintain three different speed levels. Observe the correlation between vessel size and power demand and the convex relation between speed level and power demand. A speed level of 25 knots requires more than double the power output compared to a speed level of 15 knots.

Vessel type	Passengers	Battery	Speed levels (knots) with power demand		
v_1	100	1000 kWh	15 kn: 500 kW	20 kn: 800 kW	25 kn: 1200 kW
v_2	150	2000 kWh	15 kn: 550 kW	20 kn: 900 kW	25 kn: 1350 kW
v_3	150	3000 kWh	15 kn: 600 kW	20 kn: 1000 kW	25 kn: 1400 kW

Table 3.2: Overview of candidate vessel types for the numerical example

The last crucial input parameter to this numerical example is the available charging power in each port. This power is decisive for the speed a vessel can charge its battery with. Variations in available power could be caused by geography, such as the port being on an island, or simply varying grid capacity due to other power intensive consumers in the area. It is important to note that although this charging power is available in the grid, an investment must still be made for the vessel service to utilize it. An overview of the available charging power in the four ports is found in Table 3.3.

Port	A	B	C	D
Available charging power	1000 kW	2000 kW	1500 kW	1000 kW

Table 3.3: Available charging power in the different ports

This numerical example has many possible solutions. If we choose exactly one vessel type, one route and one service frequency (per subroute), we are well on our way to a feasible solution. As fulfilling demand is not a restriction in the problem, the only main restrictions to obey are that the vessel(s) need to be able to sail the chosen frequency within the time period we are planning for, and have a large enough battery to make it to the next charging station. To illustrate how this could be a problem, we present two different ways a solution could be infeasible. We consider a solution for an arbitrary period with the following strategic and tactical decisions: The chosen route is route 1 and the selected service frequency is 2. The vessel acquisition is 1 vessel of type v_1, and the only port with charging infrastructure is port A.

1. Time usage exceeds length of planning period
To obtain a service frequency of 2, the single vessel must sail the route twice. This implies a total sailing distance of 82 nautical miles in period 2. Sailing at its maximum speed level of 25 knots, this would take the vessel 3 hours and 17 minutes to complete. We are still within the limits of our time period. The power demand for v_1 to maintain a speed of 25 knots is 1200 kW. Sailing for 3 hours and 17 minutes would imply a total energy consumption of 3 936 kWh. To charge this amount of energy with a charging power of 1 000 kW in port A, would take a total of 3 hours and 56 minutes on its own. A total time usage of 7 hours and 13 minutes is far more than the planning period allows for, and the solution is thus infeasible.

2. Battery capacity insufficient to reach next charging point
A vessel of type v_1 has a battery size of 1 000 kWh. If we assume that this is fully charged upon leaving port A, it has to have sufficient energy stored to be able to reach back to port A, following the route. As the power demand profile is convex, we assume that the vessel sails at its lowest speed level, 15 knots. To complete one round trip of 41 nautical miles, it has to sail for 2 hours and 44 minutes at this speed. With a power demand to maintain 15 knots of 500 kW, this would imply a total energy usage for the single round trip of 1 367 kWh. It is clearly an infeasible solution as the energy usage from charging point to charging point exceeds the battery capacity onboard.

To conclude this numerical example, we present a feasible solution to the problem. As mentioned above there exist many such solutions, but an example could be to select route 4 for period 1 and 3 and route 2 for period 2. The selected vessel type is v_3 and we acquire 2 vessels. This enables a service frequency of 2 for route 2 in period 2, and a service frequency of 1 in each of the subroutes of route 4 for the two other periods. Charging infrastructure is built in port B, providing charging for all routes. This solution holds both the feasibility criteria discussed above.

Chapter 4

Literature Review

The purpose of this chapter is to provide insights into literature focusing on the same areas within Operations Research (OR) as the Zero-Emission Passenger Vessel Service Network Design Problem (ZEVSNDP). We also aim to support and discuss our modeling choices, by highlighting experiences from optimization models considering problems with similarities to the ZEVSNDP.

This thesis builds upon Havre et al. (2021), as does this literature review. To our knowledge, Havre et al. (2021) are the first to contribute towards decision support for a Zero-Emission (ZE) High Speed Passenger Vessel (HSV) Service. This report is an extension to the model they present, where several new aspects are taken into account. The most notable novelties are a construction heuristic for generating rotation structures, the support for other route structures in addition to cyclical routes, and multiple time periods. Rotation generation is in short a composition of essential decisions, such as vessel type, frequency and route. Consequently, we extend their literature search with two new searches; one focusing on Network Design Problems and another focusing on OR-literature applying the concept of rotation generation. The material collection was mainly performed with aid of the search engine Scopus (Elsevier, 2021). For a more thorough description of the general search process when collecting material for public transport literature (Section 4.1) and sub-problem literature (Section 4.2), we refer to Section A.1 and Section A.2 in Appendix A, respectively.

This chapter is outlined as follows. Section 4.1 presents literature within public transport, with a novel search procedure and additional reviews for network design. As mentioned, the ZEVSNDP encompasses several sub-problems that have been sparsely studied in public transport planning. A review of literature considering these sub-problems is presented in Section 4.2. In Section 4.3, we present the reviews of literature on rotation generation, while Section 4.4 summarizes important aspects of the reviewed problems. Lastly, we present our contributions to the field in Section 4.5.

4.1 Public Transport Problems

In this section we present the most relevant findings from OR-literature within public transport. A forerunner in this field is the publication from Ceder and Wilson (1986), where public transport problems are divided into five parts. In a more recent publication, Ceder (2007) refines the categories into the *Transit Network Planning problem* (TNP). The TNP contains the sub-problems *Transit Network Design* (TND), *Timetable Development or Frequency Setting* (FS), *Vehicle Scheduling Problem* (VSP) and *Driver Scheduling Problem* (DSP). This categorization was used as an inspiration for the search procedure in our project report (Havre et al., 2021), which may be found in Section A.1 in Appendix A, whereas the review of said literature is presented in Section 4.1. We commence this section with an additional search for TND problems, and present this procedure along with a review of articles found in the search. An overview of the articles reviewed in this section is found in Table 4.1.

Article	Type of problem	Considerations relevant to our problem
Chuah et al. (2016)	BPP	Route generation using clustering
Buba and Lee (2019)	UTNDP	Network design
Liu et al. (2022)	UETNP	Network design and charging location problem
Arbex and da Cunha (2015)	TNDFSP	Frequency setting
Shang et al. (2019)	VSP	The average waiting time for passengers
Rinaldi et al. (2018)	VSP	Energy consumption and charging
Klier and Haase (2015)	TNP	Endogenous demand
Aslaksen et al. (2020)	FSNDP	Ferries sailing in cyclical sequences
Lai and Lo (2004)	FNDP	The cost of passenger time
Aslaksen et al. (2021)	C-DAR-FS	Inspect solutions under varying demand

Table 4.1: Results from the literature search within Public Transport problems. The articles found in the specific search for Network Design Problems are listed above the dashed line.

4.1.1 Review of public transport literature

In this subsection, we firstly perform additional reviews of the Public Transport Problems that focus on Transit Network Design. In order to focus specifically on literature from Network Design Problems, we conducted a search using Scopus as search engine (Elsevier, 2021). The search scanned the title, abstract and keywords of the articles in Scopus, and returned those that matched the words of a carefully designed search string.

To steer the search towards literature on Network Design Problems, we put an "AND"-operator between "Network" and "Design", meaning that both words must be included in the search. Further, we included the group of similar words "Route" and "Routing". These were themselves separated by an "OR"-operator in order to include papers that had either of these. The group was then included in the search string with an "AND"-operator, such that problems where routes, and the generation of routes, were considered. In order to exclusively focus on optimization problems, the keyword "Optimization" was added to the search string, separated with an "AND"-operator. Lastly, the keyword "Passenger" was added, in order to find articles within public transportation. This search left us with 237 documents. A filtering where articles within subjects that were deemed irrelevant, such as "Astronomy", "Social Sciences" and "Medicine" was performed, and the abstracts of the resulting articles were read. These procedures left us with 134 documents for further inspection. After a more thorough read through of these articles, we were left with 11 articles. Three of these are presented below, whereas the rest were excluded due to a too heavy focus on the development of heuristics in order to solve the Network Design Problem.

Chuah et al. (2016) present the Bus Planning Problem (BPP), and exploit taxi data in order to discover weaknesses in the current public transportation system in Singapore. Based on the clustering of taxi rides, they propose novel bus routes in areas that have high degree of taxi service. Similarly to the ZEVSNDP, the authors base their model on existing route structures, when seeking to improve the public transportation system. Chuah et al. (2016) formulate an optimization model that minimizes the travel distances of empty buses. The resulting model consists of directed cycle graphs. The authors argue that the formulated problem is NP-hard, and develop a heuristic method in order to obtain a solution, i.e., new bus routes. These are chosen from the clusters with the highest number of taxi tours.

Buba and Lee (2019) consider the Urban Transit Network Design Problem (UTNDP), for homogeneous buses. The UTNDP is a complex problem, which is mainly caused by the building-bricks of the transit time, e.g., in-vehicle/vessel waiting time, transfer time and transfer penalties. The authors attempt at simultaneously deciding a set of transit routes and service frequencies for each of these. This is similar to the approach in the ZEVSNDP, where the routes and frequency decisions are made simultaneously. In the newtork design, Buba and Lee (2019) construct feasbile routes on urban roads with predifined stops, a clear parallel to the ZEVSNDP. The problems also share the multiobjective of optimizing from both the passengers' and the operator's perspectives. Specifically, Buba and Lee (2019) optimize passenger total travel time along with operator costs.

Contrarily to the ZEVSNDP, the authors disregard constraints such as bus capacity and fleet size. The problem is solved using the particle swarm algorithm.

Liu et al. (2022) take the UTDNP a step further by considering electric buses. They formulate the Urban Electric Transit Network Problem (UETNP), in which they simultaneously decide bus route layout, service frequency of the routes and the location and size of electrical charging stations. As Buba and Lee (2019) and ZEVSNDP, they seek a solution to the multiobjective and trade off between passenger inconvenience and operator costs. The problem is a combination of the Charging Station Location Problem (CSLP) and the Transit Network Design Problem (TNDP). More specifically, the buses need to satisfy all demand, and the frequencies need to be assigned such that the buses have sufficient capacity. Further, the buses must be assigned to a charging station in order to serve their demand for energy. The authors thus argue that the problem is NP-hard, because it is harder than the general NDP, which is NP-hard. To solve the problem, they design a Pareto Artificial Fish Swarm Algorithm (PAFSA) that iteratively searches for network layouts, and a Genetic Algorithm that finds charging locations in the network returned by the PAFSA.

Shang et al. (2019) study a VSP, in which they minimize both operator costs and passenger waiting costs. In general, they consider a multi-depot bus network with a set of predefined routes that must be served. The authors allow each route in the network to take a frequency between a lower and an upper bound. Furthermore, they show how the average passenger waiting time depends on the chosen frequency. The choice of frequency and use of frequency-dependent passenger waiting times are two properties also found in the ZEVSNDP. To calculate the cost of waiting, Shang et al. (2019) introduce a parameter representing the waiting cost per passenger. This parameter is in the objective function multiplied with the number of waiting passengers and their frequency-dependent average waiting time. Additionally, the objective function has multiple objectives and minimizes both the operator costs as well as the passenger waiting costs. The resulting model is nonlinear because the objective function is neither convex nor concave. This enforces an alternative solution method, and the problem is solved heuristically.

Rinaldi et al. (2018) consider a VSP for electric and hybrid buses in a single depot case, where the charging infrastructure is installed at the depot. Accordingly, Rinaldi et al. (2018) consider charging constraints as a part of the scheduling problem. In the model formulation, they use discrete time steps and declare that a bus can either charge or serve a trip in each time step. If the bus charges during a time step, it starts the next time step with a full battery. As a result, the problem does not capture the relationship between the time spent charging and the battery level, as the ZEVSNDP does. The objective of their model is to minimize the operator costs, which include both the cost of charging and serving a route. They implement and solve a Mixed-Integer Linear Programming model exact.

Arbex and da Cunha (2015) consider a multi-objective Transit Network Design and Frequency Setting Problem (TNDFSP). More specifically, they determine an optimal set of routes and the number of times each route is served. The objective function minimizes both the operator costs and the passenger inconvenience costs in the transit network, similarly to the ZEVSNDP. The authors state that the two objectives are in conflict with each other, leading to a set of Pareto optimal solutions. This means that it is not possible to improve one of the objectives without deteriorating the other. As mentioned in the introduction of this section, Ceder (2007) state that the TNP consists of five sub-problems, where network design and frequency setting are two of these. Arbex and da Cunha (2015) indicate that previous literature mainly focuses on solving these sub-problems independently, due to their complexity. They further argue that solving both the TND and the FS problem simultaneously is NP-hard and thus propose a heuristic to solve the problem. The challenges of solving a TND and FS problem simultaneously is also experienced in the ZEVSNDP.

Klier and Haase (2015) study a TNP with flexible demand. Flexible, or endogenous, demand, entails a variation in demand based on the passengers' perceived value of the service. An efficient service with short waiting times increases demand, whereas few departures decrease demand. This trait is also incorporated in the ZEVSNDP. The passengers in the network may either walk or use public transport. Walking and transit (driving) arcs in the network are connected by nodes. Together, a passenger's route from start to stop constitutes a path, and Klier and Haase (2015) predict the expected travel time along the different paths in the networks. Using the characteristics of travel time, such as walking, waiting, and transit time, the authors predict the expected demand. Finally, by using the expected demand, they attempt to determine the optimal paths and frequencies in order to maximize the total number of expected public transit passengers, subject to a budget constraint. Attempts to solve the model in a commercial solver were unsuccessful.

Aslaksen et al. (2020) present a Ferry Service Network Design Problem (FSNDP) that considers the generation of schedules for autonomous ferries. They study a set of homogeneous ferries, where each vessel repeats a cyclical sequence of port visits. To solve the problem, the authors propose a two-step approach, where they first generate routes and corresponding frequencies using a construction heuristic. Their model then determines the optimal combination of routes, frequencies and vessels that maximizes perceived customer satisfaction. They call the combination of routes, frequencies and vessels for a *rotation*, which we will further elaborate on in Section 4.3. It is worth noting that Aslaksen et al. (2020) require a minimum frequency between ports in their model formulation, which is also the case in ZEVSNDP, where the frequency is bounded below by a minimum level.

In a continuation of the article presented above, Aslaksen et al. (2021) consider the Combined Dial-a-Ride (DAR) and Fixed Schedule problem (C-DAR-FS). C-DAR-FS seeks to determine the optimal assignment mix of vessels to dynamic and fixed schedules. More specifically, they first create a schedule for the fixed vessels, as described in Aslaksen et al. (2020). They then create a simulation that decides whether a requested passenger trip is best suited for a fixed schedule or a dynamic on-call service. The overall goal of the problem is to maximize user utility by minimizing time spent in the system and maximizing the number of met trip requests. The purpose of the model is to evaluate the relationship between fleet size and composition under various demand scenarios. Aslaksen et al. (2021) find that scheduled services are cost-efficient in busy ports and may serve substantial demand. DAR services, on the other hand, are best suited in situations with low demand.

Lai and Lo (2004) study an FNDP and consider the optimal fleet size, routing, and scheduling of two ferry services. Their objective is to minimize both the operator and passenger costs related to passenger waiting and transit time. This is the same objective as in the ZEVSNDP. Lai and Lo (2004) argue that although the objective is to maximize profit, the service must consider passenger inconveniences. Several competing services exist in the considered area, and a lesser service would shift the passengers towards competitors, thus reducing profits. The model is formulated as a mixed-integer multiple origin-destination network flow problem with ferry capacity constraints. It incorporates two types of networks: a network describing the flow of passengers and a network describing the movement of vessels. In the former, passenger flow in the system, e.g., waiting, is described along with discrete time intervals and different locations in space. In the latter, waiting and sailing are described over the same dimensions as the passenger-flow network. The flow variables in both networks are decided simultaneously at run time. The authors argue that the passenger-flow and vessel-movement networks may be further divided into sub-networks in order to handle different ferry types and different demand scenarios. The model also incorporates an idea of different fare revenues in the short and long run. In the short run, the revenue is fixed, due to few alternatives of transport. In the long run, however, the revenue is a function of several variables, among them service quality, job relocation, and the number of competing or alternative transport methods. The option of using alternative transportation is also included in the ZEVSNDP.

4.2 Sub-problem Related Literature

As stated in the introduction of this chapter, the ZEVSNDP consists of sub-problems that are not covered solely by reviewing articles within public transport problems. Accordingly, more narrow and targeted literature searches were conducted to gain insight into other sub-problems. The relevant sub-problems for further investigation were scheduling/assignments to a route, vessel speed optimization, and, lastly, infrastructure location problems. The search procedure is described in Section A.2 in Appendix A, while the reviews are presented in the following. Table 4.2 shows an overview of the reviewed articles.

Article	Type of problem
Li et al. (2008)	SDVSP
Sassi and Oulamara (2014)	EVSCP
Zhang et al. (2021)	Optimal Charging Location and EVS
Andersson et al. (2015)	Route optimization incl. speed optimization
Ritari et al. (2021)	Route optimization incl. speed optimization
Fagerholt et al. (2010)	Route optimization incl. speed optimization
Villa et al. (2020)	Electric Infrastructure Location Problem
Rogge et al. (2018)	EVS-FMC

Table 4.2: Results from the literature searches for the relevant sub-problems to the ZEVSNDP

Li et al. (2008) study a truck scheduling problem of solid waste collection. The problem considers the collection of waste in fixed routes originating from a single depot and the offloading of the collected waste in recycling facilities. The problem minimizes the total operating and fixed truck costs when serving a set of predetermined collection trips. Contrary to the ZEVSNDP, the planning period is defined for recurring time windows early in the morning. The time windows are in the range from one to three hours, and the trucks are without capacity constraints due to limited collecting time. The problem with this is that without operational decision support, there is a need for an immense fleet in order to cover all the routes. Li et al. (2008) thus seek to decrease maintenance costs by reducing the fleet size and at the same time serve demand. The problem is a special case of the Single Depot Vehicle Scheduling Problem. However, it is constrained by balanced unloading at the depots. Balanced unloading means that the different depots should be served by a balanced amount of vehicles. This feature is important in order to secure a stable number of jobs at every recycling facility. On the other hand, this requirement makes the problem more complex.

Sassi and Oulamara (2014) approach the Electric Vehicle Scheduling and Optimal Charging Problem (EVSCP), in which they seek to optimize the allocation of fixed tours to electric vehicles while minimizing charging costs. In the problem, they take a set of electric and combustion engine vehicles as input, a set of tours, and a given electrical charging infrastructure. They present a Mixed-Integer Programming (MIP) model with two terms in a lexicographical objective function. The most important term seeks to maximize the traveled distance, and this value then bounds the second term, which is the minimization of charging costs. The problem is restricted by the placement of chargers, battery capacity, and the electric vehicles' driving range. The EVSCP and the ZEVSNDP mainly share properties with regards to the constraints, as the ZEVSNDP considers vessel range and battery capacity. On the other hand, the route is given in advance in the EVSCP, whereas the route is designed in the ZEVSNDP. Another important distinction is that the energy consumption depends on the speed along the legs in the ZEVSNDP. In the EVSCP, the consumption is constant along each tour, implying constant speed. Additionally, the ZEVSNDP determines the location of chargers, while these are fixed in the EVSOCP.

Zhang et al. (2021) consider the assignment of electric buses to pre-defined routes and decide the charging technology that should be installed at terminal stations. They approach the problem by first solving an operational, lower-level problem before sending the solution to a tactical, higher-level problem afterwards. In the lower-level problem, they decide the optimal assignment of buses to serve the fixed routes, and they determine the charging schedule for the buses. The charging schedule depends on the charging technology installed at the terminal stations, which is decided in the higher-level problem. The charging technology could either be fast or slow. In order to create a relationship between battery level and charging schedule, Zhang et al. (2021) introduce discrete time periods of 10 minutes. The fast charging takes one time period, whereas the slow charging takes 12 time periods. They further assume constant speed on the given routes. This is a simplification compared to the ZEVSNDP because it includes the possibility of sailing in linear combinations of discrete speed levels. Accordingly, the energy consumption must thus be calculated for each discrete speed level in the ZEVSNDP. In the objective of the operational problem Zhang et al. (2021) minimize the investment cost for buses and the operational cost of charging. The latter is only related to the battery degradation, which depends on the State of Charge (SoC), i.e., the battery level of the bus. Thus, Zhang et al. (2021) diverge from our approach, where the operational cost of charging depends on the electricity prices. Further, the objective of the higher-level model is to minimize the cost of investing in the different charging technologies.

Andersson et al. (2015) look at fleet deployment in liner shipping, and present a case study for Roll-on Roll-off shipping. Unlike foregoing literature on the subject, they include speed optimization in the planning of routes, which previously was accomplished after the route generation phase. The problem consists of a heterogeneous fleet of ships that either serve trade routes (routes with cargo onboard) or ballast routes (empty, re-positioning routes). The sailing speed of the vessels affects the transit time and the fuel consumption per distance unit. The authors thus attempt to reduce the number of ballast routes while choosing speed levels that minimize fuel consumption. To incorporate more speed options, they allow for linear combinations of the discrete speed levels, a similar approach as in the ZEVSNDP. Andersson et al. (2015) further explain how the linear combinations overestimate both the sailing times and the fuel consumption. This is caused by the interpolated value of speed being greater than or equal to the actual speed, leading to a higher estimate. The problem's objective is to minimize total costs (exclusively sailing costs), where the sailing speeds along the routes affect the fuel consumption and thus the costs. The problem is solvable for short planning horizons for commercial MIP-solvers. To solve for longer horizons, the authors propose a rolling horizon heuristic.

Ritari et al. (2021) study the adoption of batteries as an energy carrier in vessels. Specifically, they explore how large-capacity batteries affect operational measures such as routing, speed, and fleet deployment, compared to conventional vessels. The study consists of two problems. Firstly, the Emission Control Area (ECA) routing problem is extended with ZE legs. An ECA is an area that enforces strict emission regulations. Routing problems considering conventional vessels operating in ECAs have yielded routes that sail around the ECA, resulting in increased emissions. The second problem consists of optimizing the trade-off between speed and battery capacity on ZE legs. The problem is a MIP with quadratic constraints, which are mainly caused by the quadratic emission profile of slow vessels. The study emphasizes that a 25-100 times lower energy density in lithium-ion batteries compared to hydrocarbon fuels, makes the technology incapable of providing the total energy demand. The trade-off between battery capacity and speed in ZE areas has received limited attention in the literature. The authors thus intend to fill out the operational and design decision gaps. They conclude with a 50% lower optimal speed on battery-powered legs, and that variation in speeds between sailing segments results in higher overall fuel consumption.

Fagerholt et al. (2010) study the problem of reducing fuel emissions by optimizing the speed on each leg for given shipping routes. Fuel consumption is directly linked to emissions, hence the authors seek to minimize the amount of fuel consumed. In contrast to the ZEVSNDP, Fagerholt et al. (2010) study vessels powered by conventional fuel, while we mainly focus on ZE technologies. A comparison could still be drawn to the ZEVSNDP, where the energy consumption depends on the speed in the same manner as the fuel consumption in their article. In the problem presented by Fagerholt et al. (2010), the vessels must arrive at each port in the route within specified time windows. This forces the vessels to sail faster than their minimum speed level on every leg, which would have been a trivial solution. They propose three models to solve the problem. The first model proposes speed on each leg as the decision variable. In the second problem, time is the decision variable. They show that both these approaches lead to non-linear models due to the fuel consumption being a cubic function of speed. Their last model proposes the discretization of arrival time at each port. The model must then decide on a discrete arrival time, which affects the fuel consumption due to speed-dependent arrival. To solve the last model, a shortest path algorithm is proposed. They also compare the third model with the solution to the non-linear problems, solved in a commercial non-linear solver. The third model has a lower run time than the two preceding models and provides quasi-optimal solutions.

Villa et al. (2020) introduce the Electric Riverboat Charging Station Location Problem (ERCSLP). The ERCSLP considers the charging of electric riverboats that sail through rural areas on the Amazon river. In these areas, there are no electric grid connections, and the proposed charging stations are therefore supplied with solar power. The boats sail fixed routes along the river and have predefined stops (nodes). Villa et al. (2020) allow the boats to choose different battery sizes, where larger batteries store more energy but are heavier and result in a higher energy consumption.

The boats sail at a constant speed, meaning that energy consumption between nodes only depends on the battery size. The authors argue that the time to charge one kWh is a non-linear function that depends on the battery size. The charging power depends on the charger installed at the charging stations, where the model can choose between fast or slow charging at different costs. The non-linear charging function is modeled as a piece-wise linear function to make the final MIP-model linear. The model's objective is to minimize the investment costs, which include both the vessel battery and the charging infrastructure. Villa et al. (2020) solve the MIP to optimality using a commercial solver.

In the Electric Vehicle Scheduling Fleet Size and Mix problem with Optimization of Charging Infrastructure (EVS-FMC), Rogge et al. (2018) study the challenge of substituting conventional buses with electric buses. In particular, they address the scheduling of bus routes using electrical buses while at the same time accounting for their range limitations, charging times, and the whole system's charging infrastructure. The buses are constrained from operation when charging, similarly to the ZEVRPP. Further, the cost of investing in charging infrastructure is minimized, as in our problem. On the other hand, Rogge et al. (2018) assume that charging only occurs in a given depot, as opposed to the ZEVRPP, where the location of charging infrastructure is a decision variable. The overall goal of the EVS-FMC is to minimize the total cost of ownership, which also includes the investment in buses and operational costs. Other key decisions in the problem are the selection of a sufficient number of vehicles in order to serve all trips and the number of chargers to install in the depot.

4.3 Rotation Generation

The ZEVSNDP proposes a solution method to the Network Design Problem by applying the concept of a *rotation*. This concept is frequently mentioned in the literature, and most notably in Aslaksen et al. (2020). In this section, we present a review of literature incorporating the generation of rotations. We direct the search by inspecting literature mentioned in Aslaksen et al. (2020), and by later work that cite Brouer et al. (2014). Table 4.3 presents the reviewed articles.

Article	Type of problem
Brouer et al. (2014)	LSNDP
Thun et al. (2017)	LSNDP
Aslaksen et al. (2020)	FSNDP

Table 4.3: Results from the literature search within rotation generation

Brouer et al. (2014) study the Liner-Shipping Network Design Problem (LSNDP), which entails the generation of a set of non-simple cyclic sailing routes for a fleet of container vessels. The authors formulate a Mixed-Integer Programming (MIP) model, that maximizes the revenues and minimizes the costs of liner shipping operations. The model is designed for handling butterfly rotations (routes), which complicates the assignment of transhipment costs. In liner-shipping literature, a *service* consists of a route and the frequency with which it is served. Brouer et al. (2014) define a *rotation* as a specific configuration of such a service, with a specific vessel class, number of vessels and their sailing speed. The authors advocate for the modeling of butterfly routes, because these are often used in practice. They allow one butterfly route per rotation, and designate a master port, i.e., a port that is visited more than once. The authors provide a column generation approach in order to solve the problem, and design an auxiliary problem that finds the optimal route, which maximizes the net revenue contribution from each sailing.

Thun et al. (2017) study the LSNDP and propose a branch-and-price algorithm to solve the problem for different route instances. The authors study different route layouts, e.g., butterfly routes and complex routes, i.e., where ports may be visited an arbitrary number of times. They define a service (rotation), as a given sequence of ports to visit, the vessel type serving these ports and the number of vessels used. Associated with the service is a set of possible delivery patterns, which describes the amount of goods loaded and unloaded at each port. The services are planned at a weekly format, and the model minimizes the total weekly cost of all services. The solution method uses a branch-and-price method, where a master problem (LSNDP) seeks to find the delivery pattern with the lowest cost, whereas the subproblem finds new services and delivery patterns.

Aslaksen et al. (2020) also use the concept of a rotation, as mentioned in Section 4.1. They approach the rotation generation heuristically, using two route heuristics and one rotation heuristic. Their rotation constitute of a route, number of vessels and associated frequencies. The routes and rotations are generated a priori, i.e., serve as an input to the FSNDP. The routes in their first heuristic follow five rules, e.g., a maximum number of ports, and adjoining pairs. The second route heuristic limits the number of routes by comparing those generated by the first heuristic. Finally, the rotation heuristic finds suitable frequencies and number of vessels to accompany the generated routes.

4.4 Synthesis

This section synthesises the main findings from the reviewed literature. Further, it compares aspects from already existing literature to the ZEVSNDP. An overview of the literature review in tabular form is found in Section A.3 in Appendix A.

There are, in general, two main categories of objective functions in the reviewed problems: multi-objectives minimizing both operator and passenger costs, and the sole minimization of operator costs. The public transit problems typically consider the former alternative. According to Lai and Lo (2004), it is typical to consider both costs in public transit network design studies because competing modes of transport become more attractive when the passenger costs increase. They, along with Shang et al. (2019), consider both the passenger waiting and transit time in their objective function. Arbex and da Cunha (2015) add to previous work by considering a transit penalty, penalizing the number of transits in their network in addition to the waiting and travel times. Aslaksen et al. (2020), on the other hand, seek to maximize customer service quality through rapid departures while minimizing excess transit time. The latter is the difference between actual transit time and the transit time in a direct link. We find the papers that penalize transit and waiting times the most relevant, as this is the approach used in the ZEVSNDP.

Three of the reviewed papers consider speed in their respective problems. Fagerholt et al. (2010) examine how speed optimization can save fuel costs. In particular, the paper leverages the cubic relationship between speed and fuel consumption (above a given minimum speed) to arrive at optimal speeds for each sailing leg. Andersson et al. (2015) further elaborate on this topic, as they formulate an approximation of speed based on a linearization of a set of discrete speed levels. Using the convexity of the speed-fuel relationship, they show that special ordered sets are unnecessary for the approximation to be valid, thus reducing complexity. Ritari et al. (2021) introduce renewable technologies to speed optimization. They study the trade-off between speed and battery size and make use of the same relationship between speed and energy consumption as Fagerholt et al. (2010) and Andersson et al. (2015). As the ZEVSNDP also makes use of a linear approximation of speed, based on discrete values, we find Andersson et al. (2015) especially relevant. Further, the trade-off between speed and battery size in Ritari et al. (2021) is also relevant when optimizing battery-electric HSVs, for apparent reasons.

With regards to the problems incorporating continuous time, Andersson et al. (2015) also use time windows in order to decide when a ship can enter and leave a port. However, due to the linear approximation of speed in this paper, time also becomes continuous due to the relationship between time and speed. Rogge et al. (2018) similarly have a time window as in Andersson et al. (2015). They further incorporate charging in their problem, in which the vehicle is out of operation. The use of allowed time windows still pertains. Arbex and da Cunha (2015) use a matrix describing the travel times between the nodes in the problem. They note that travel time is not constant but varies with congestion, e.g., in peak hours. However, they simplify the problem by assuming fixed timing between nodes. Finally, Shang et al. (2019) use a time variable to compute the total waiting time. We find Andersson et al. (2015) relevant due to their dependency between speed and time. Additionally, the relationship between continuous-time and charging as presented by Rogge et al. (2018) is also important in the ZEVSNDP.

In the inspected literature, routes are generated mainly in two fashions. In some problems, they are constructed simultaneously as the other decision variables are set. These problems often require heuristic solution methods. Pregenerating the routes is also a possibility. Buba and Lee (2019), Arbex and da Cunha (2015) and Chuah et al. (2016) all try to decide optimal routes simultaneously as other decision variables. As a result, Buba and Lee (2019) solve the UTDNP using a particle swarm algorithm, while Arbex and da Cunha (2015) propose yet another heuristic solution method. Chuah et al. (2016), also use a heuristic solution method in order to construct the route networks, but employ a genetic algorithm to decide the charging location once the network is constructed. Another approach to solving the Network Design Problems, is the application of branching methods. Brouer et al. (2014) create a column generation approach for instance, whereas Thun et al. (2017) use a branch-and-price framework. The ZEVSNDP, employs yet another approach, the pregeneration of rotations. The concept of rotations is well-known within the liner shipping literature, where it may be referred to as a service. Brouer et al. (2014) include vessel class, number of vessels, and a sailing speed in their services. Thun et al. (2017), on the other hand, include a route in their service, but leave out the speed. Further, they attach a delivery pattern to the rotations, which describes the loading and unloading of goods. The two aforementioned authors do not pregenerate the rotations, but construct these in an iterative manner. Aslaksen et al. (2020), similarly to the ZEVSNDP generate a set of rotations that are used as input in the optimization problem. Aslaksen et al. (2020) include route, number of vessels and frequency in their rotations. In this paper, the rotations consider the route, the division into multiple subroutes, the frequency in each subroute, the vessel type, the fleet size and the location of charging infrastructure.

4.5 Our Contribution

Throughout our project and master thesis, we contribute to the research on route planning and feasibility of electric High-Speed passenger vessels (HSVs). In our project thesis (Havre et al., 2021), we introduced the Zero-Emission Route Planning Problem (ZEVRPP), which to our knowledge, is the first problem providing decision support for a ZE passenger vessel service. It is, moreover, a contribution to the steady increase of problems considering ZE energy carriers in the transportation sector.

The ZEVSNDP continues the novelties introduced in the ZEVRPP. In particular, the ZEVSNDP combines numerous fields and sub-problems within operations research and serves as an example of how decisions on multiple planning levels may be combined in a single problem. In particular, the combination of frequency setting (tactical decision) and sailing speed optimization (operational decision) is a novel procedure within public transport problems. Both of these decisions have implications for the perceived passenger inconvenience, and thus the passenger cost.

The ZEVSNDP captures several important aspects of future public transit systems. Specifically, it considers the relationship between frequency and demand. Furthermore, it addresses the consequences of ZE energy carriers. This includes the relationship between the battery level and the sailing speeds, e.g., when to save energy by slowing down. The speed optimization is a trade-off between energy cost for the operator and transit time cost for the passenger. All in all, the ZEVSNDP displays various implications caused by the objective of minimizing the total system cost.

In the ZEVSNDP, we extend our approach with regards to route design. Where the ZEVRPP only handles one predefined, cyclic route, we construct a set of routes in the ZEVSNDP, and account for both simple cyclic routes and butterfly routes. In the latter route structures, we allow passengers to transit in a central hub, if they are traveling from one butterfly subroute to another. Brouer et al. (2014) argue that butterfly routes are common in liner shipping, and our communication with route planners for HSVs in Norway show that this is also the case for some HSV connections. The inclusion of said route structures thus adds a more realistic model to the field. Further, the ZEVSNDP is defined for multiple planning periods, compared to the single planning period of the

ZEVRPP. As a result, the ZEVSNDP contributes to a more granular decision making process. The literature on Zero-Emission transport problems is currently scarce, and this thesis makes advances by jointly considering technical and operational measures to lower costs of energy transitions.

Chapter 5

Mathematical Formulation

In this chapter we define a Mixed-Integer Programming model of the ZEVSNDP. As explained in Chapter 3, the mathematical model is formulated for battery electric vessels, but could easily be altered to allow other energy carriers. In Section 5.1, we clarify the modeling approach and the assumptions made during the model formulation process. Further, the notation used in the ZEVSNDP is presented in Section 5.2, before the full mathematical formulation is presented in Section 5.3. In Section 5.4, we describe how we linearize the non-linear terms in the formulation. Section 5.5 concludes the chapter by presenting a mathematical formulation for a service powered by conventional marine diesel fuel. This model is used as a benchmark for the Zero-Emission model in Chapter 8.

5.1 Modeling Approach and Assumptions

The mathematical formulation of the ZEVSNDP chooses from a set of predefined candidate routes in each period. A proposal for generating such a set is elaborated on in Chapter 6. Further, as described in Chapter 3, a route could consist of multiple subroutes. In each time period, only one route may be chosen, and all the subroutes in this route must be served. An optimal vessel investment is determined in the model in order to serve the routes for all periods. This is a one-time investment across all time periods, meaning that the number of vessels restrains the allocation of vessels in the different time periods. For simplicity, we only allow one vessel type to be chosen across all routes and time periods. For conventional vessels within the public transport sector, especially in Norway, the vessel type is usually designed for the route it is supposed to serve. Accordingly, choosing only one vessel type is a reasonable model assumption. In addition, this approach simplifies the allocations of vessels in different time periods, further discussed in Chapter 3.

In the model, it is assumed that every port has the possibility of installing charging infrastructure, but at different costs based on the state of the available electrical grid. The available charging power may vary between ports, for example due to different electricity demands in the area. Further, it is assumed that charging happens at constant power, meaning there is a linear relationship between time spent charging and the battery level. This is in contrast to Villa et al. (2020), where the relationship between charging time and State of Charge (SoC) is non-linear. We do, however, find it to be a reasonable assumption within the SoCs allowed in the model. Lastly, the infrastructure location is a strategic decision that cannot be changed from one time period to another.

Each subroute in a route visits a set of ports. The sequence in which the ports are visited is described by a set of sailing legs, meaning that a subroute consists of both a set of ports and a set of legs. The port from which a leg originates is known in advance based on how the route and subroutes are defined. To model this relationship, we introduce a parameter, A_{prcik}, which is equal to 1 if port i is the origin of leg k. This parameter is used in the model presented in Section 5.3 to connect a port to the specific sailing leg in a subroute. Suppose that we know that charging infrastructure is installed in port i. To ensure charging is only allowed at the beginning of sailing leg k originating from i, we need a conversion between the port name and leg number. This mapping is stored in the A_{prcik} parameter. The relation between port name and sailing leg number may vary across all subroutes c, routes r and time periods p.

The modeling of demand is an important aspect of the ZEVSNDP. In general, the demand within all port pairs for all time periods is known in advance. For the ZEVSNDP to handle the demand data, it must be altered to account for ports being in different subroutes and when in the subroutes these are visited. To do so we introduce a demand parameter for each subroute c (in route r in time period p), D_{prckl}, describing the demand from the port at the beginning of leg k to the port at the beginning of leg l within a subroute. This is possible, because the visiting order of the ports within a subroute is known in advance. Further, the model should comply with passengers wanting to travel from one subroute to another. This is accomplished by routing the passengers through the nearest port linking the two subroutes, e.g., the central hub of a butterfly route.

To exemplify, consider Figure 5.1 and Figure 5.2. The figures show six ports served by a butterfly route with two subroutes, A and BC. In both Figure 5.1 and Figure 5.2 wing B and C are considered the same subroute with two visits to the central hub. Figure 5.1 illustrates the case where a passenger wants to travel from port 1, situated in subroute A, to port 3 situated in subroute BC. This is done by letting the passenger transit in the square port, the central hub. This is accomplished by altering the demand parameter for subroute A, i.e., increasing the demand from the passenger's origin port to the central hub. At the same time the demand parameter increases artificially in subroute BC, where the passenger is routed from the central hub to its final destination port. Figure 5.2 shows another case where the demand parameter is altered to facilitate efficient passenger transportation. If the given passenger wants to travel from port 5 at the beginning of leg $k_{BC} = 3$ to port 6 at the beginning of leg $k_{BC} = 2$, it is inconvenient to first sail the remaining subroute. Instead, we allow the passenger to exit at the central hub and wait for the next vessel, and follow the same approach as in Figure 5.1. The demand increases from port 5, at the beginning of leg $k_{BC} = 3$, to the port at the beginning of leg $k_{BC} = 4$, the central hub. Accordingly, the demand increases from the port at the beginning of leg $k_{BC} = 1$, again the central hub, to port 6, situated at the beginning of leg $k_{BC} = 2$.

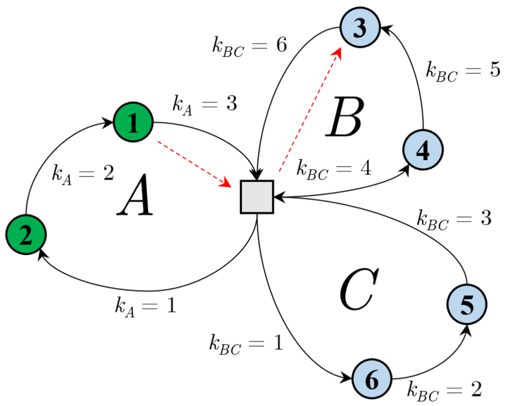

Figure 5.1: Illustration of a how a passenger that wants to travel between different subroutes is routed

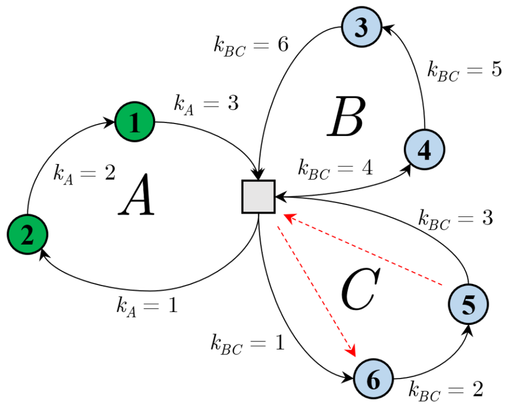

Figure 5.2: Illustration of how a passenger could disembark at a central hub and wait for the next vessel

In each subroute, the model can choose from a set of service frequencies. As described in Chapter 3, the frequency is defined as the number of times the least visited port is visited during the planning period. The demand in each subroute is assumed to depend on the frequency, due to passengers choosing other means of transportation, if the service frequency is too low. This approach is similar to that of Klier and Haase (2015). The frequency in the subroute is also assumed to influence the passenger waiting time in port. In the formulation of the ZEVSNDP, a similar approach as that of Shang et al. (2019) is used, where the average waiting time for the passenger is calculated in advance for each possible frequency. The calculation of average waiting time is provided below, where W_{prcf}, further described in Section 5.2, is the average waiting time for a given frequency f, and $\overline{T}_p$ is the length of the time period.

$$W_{prcf} = \frac{\overline{T}_p}{2f}$$

Passengers preferring other means of transportation are considered unmet demand in the model. This could occur, as described above, when the passenger finds the service frequency insufficient, but it could also occur if the chosen vessels have inadequate capacity to bring all passengers. A third possibility leading to unmet demand, is when either the port of origin or destination is not included in the chosen route. From the set of candidate routes the model can choose from, there is not a requirement that all ports in the area must be visited. This is the case, because we want the model to choose not to visit ports if this is economically efficient. If a port is not visited, the number of passengers the cannot be served is known in advance from the demand matrix. Hence, the cost of passengers using other means of transportation due to a port not being visited is calculated in advance for each potential route choice in each period.

The modeling of time and sailing speed is important in the ZEVSNDP, similarly to the ZEVRPP (Havre et al., 2021), and the modeling approach is similar. The sailing time along each leg is computed in advance for a discrete number of speeds. A vessel can then be assigned a speed which is a linear combination of the discrete speed levels. Accordingly, a vessel may choose between infinitely many speed levels between the lowest and highest discrete speed level. This approach is the same as in Andersson et al. (2015), and slightly overestimates the actual sailing time of the distance. The time usage per nautical mile, sailing at a speed of 25 knots, is illustrated in Figure 5.3. Note from the figure that the linear combination of the time usage at 20 and 30 knots is overestimated compared to the exact sailing time at 25 knots. Energy consumption is also speed dependent. Hence, we apply the same linearization technique when describing the energy consumption on each arc. Accordingly, we introduce a parameter that defines the energy consumption on each arc for each vessel at each discrete speed level. Therefore, the option of choosing linear combinations of the speed levels also applies to the energy consumption. The linear approximation of energy usage is illustrated in Figure 5.4. The overestimation is also observed for the energy consumption.

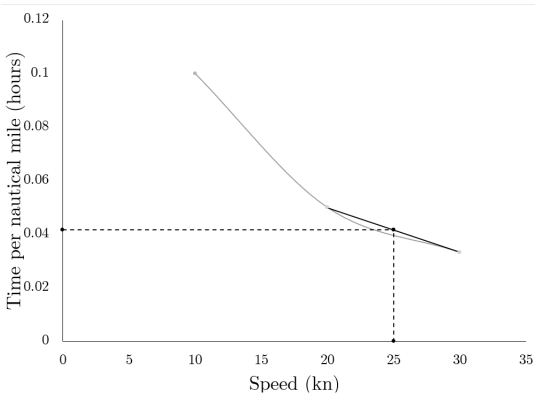

Figure 5.3: Illustration of the time usage per nautical mile at different speed levels. The linear approximation leads to an overestimation of the time usage

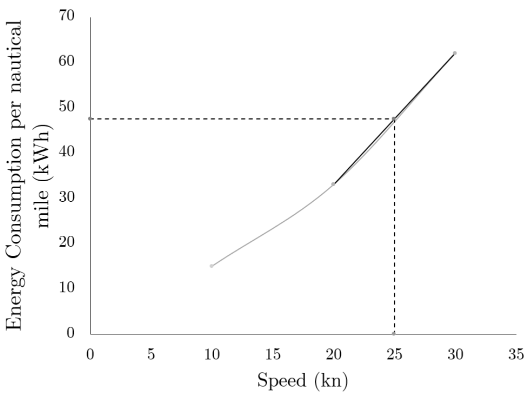

Figure 5.4: Illustration of the energy usage per nautical mile at different speed levels. The linear approximation leads to an overestimation of the energy usage

5.2 Notation

In this section, we elaborate on the notation used to formulate the mathematical model for the ZEVSNDP. Firstly, the sets used in the formulation are introduced. Secondly, the parameters are presented, before the decision variables are introduced. The last part of this section is a summary of all notation used in the mathematical formulation.

Sets

Let each period within the planning horizon be represented by an index $p \in \mathcal{P}$, and let each period be of length $\overline{T}_p$. In each period p, a single route may be chosen from a set of potential candidate routes, $\mathcal{R}_p$. Further, a route r consists of a set of subroutes $\mathcal{C}_r$. A subroute c contains a set of legs, $\mathcal{K}_c$ and ports, $\mathcal{I}_c$, where the set of ports in a subroute is a subset of all ports, $\mathcal{I}$. Further, let $\mathcal{F}_c$ be the set of potential service frequencies in each subroute. In order to uphold this frequency, a vessel type, v, is chosen from a set of available vessel types $\mathcal{V}$. Each potential vessel type, v, has a set of discrete speed levels, $\mathcal{S}_v$, which in the model may be linearly combined to achieve continuous speed selection, as described in Section 5.1.

Parameters

The time of sailing a leg k, in a subroute c (in a route r in time period p), with a vessel v, at speed s, is computed in advance and given as input to the model through the parameter T_{prckvs}. Further, a vessel will have a minimum waiting time in each port $\underline{T}_i^W$, representing time spent on disembarking and embarking passengers. The objective function punishes a longer sailing time between ports, compared to the fastest way to travel from the origin port to the destination port along the route. Hence, the travel time from the port at the beginning of leg k, to the port at the beginning of leg l, in subroute c (in a route r in time period p), sailed with the fastest available vessel type at its highest speed level, is represented by T_{prckl}^U. Lastly, let W_{prcf} represent the passenger waiting time in a port, dependent on the frequency f in subroute c (in a route r in time period p) as discussed in Section 5.1.

Let D_{prckl} denote the maximum demand for transportation from the port at the beginning of leg k, to the port at the beginning of leg l, within subroute c (in a route r in time period p). As explained in Section 5.1, passengers with origin and destination in different subroutes are routed through the nearest port shared by the two subroutes. Hence, the demand to ports that serve as hubs in the route is higher than the number of passengers having the hub as their final destination. In each subroute a frequency f is chosen. Lower frequencies lead to passengers preferring other means of transportation, while higher frequencies make the service more attractive. Thus, D_{prcklf} is introduced to represent the frequency-dependent demand for passengers with origin port at the beginning of leg k, with destination port at the beginning of leg l, in subroute c, when served with frequency f, in time period p. Note that the maximum demand for transportation, D_{prckl}, is equal to the demand for transportation at the highest available service frequency, $|\mathcal{F}_c|$, implying $D_{prckl} = D_{prckl|\mathcal{F}_c|}$. Lastly, the served demand is restricted by the capacity of the chosen vessel type, v, denoted Q_v.

A vessel must at all times demonstrate a battery level above a lower bound, $\underline{B}_v$, and below a maximum bound, $\overline{B}_v$. The energy consumption when sailing a leg k, in subroute c (in a route r in time period p), with vessel type v, at speed level s, is denoted E_{prckvs}. In Section 5.1, we elaborated on the procedure of using the sailing legs to denote the visiting order of the ports. This approach makes the port at the start of a leg dependent on how the set of legs in a subroute is defined. Further, each subroute must contain a port with charging infrastructure installed, to ensure feasibility of the route. Since the location of infrastructure is a strategic decision that cannot be changed across time periods, we need to know the port i where leg k starts in each subroute c, in a route r in time period p. To do so, we introduce the parameter A_{prcik}, where an entry equals 1 if leg k starts at port i in subroute c. Lastly, P_i denotes the potential charging power that could be installed in port i.

As explained in Chapter 3, the problem considers both the operator and the passenger costs. The first of the operator's costs is the vessel investment cost for each vessel type C_v^{FC}. Further, there is an investment cost, C_i^{INF}, for installing infrastructure in port i. We let C_{pi}^{VC} denote the energy cost per kWh in period p in port i. This cost is assumed to fluctuate throughout the day and differ between locations, which is the reasoning behind the p and i indices. In comparison to the ZEVRPP (Havre et al., 2021)), where the crew cost was incorporated in the investment cost for the vessel, the ZEVSNDP has an extra term in its objective function that accounts for the crew cost of each time period. Hence, we let C_v^{CREW} denote the crew cost of using a vessel of type v for one hour. When considering the passenger costs, there is a cost incurred by passengers choosing other means of transportation. Let C_{prckl}^{ALT2} denote the cost of one such passenger demanding transportation from the port starting at leg k, to the port starting at leg l, in subroute c (in a route r in time period p). As described in Section 5.1, there is no requirement to include all ports in the selected route. The cost of unmet demand due to not visiting a port r in time period p is computed directly and labeled C_{pr}^{ALT1}. Lastly, we denote C^{PW} and C^{SW} as the value of passenger time while waiting in port and the value of passenger time while sailing, respectively.

Variables

When considering the variables in the mathematical formulation, we let three variables denote the strategic decisions taken for all periods. Let α_i be a binary variable, equalling 1 if infrastructure is installed at port i, and 0 otherwise. Further, let δ_v be equal to 1 if vessel type v is chosen. The last strategic decision in the ZEVSNDP is the acquired number of vessels of type v, denoted by the integer variable y_v.

In each period p, three tactical decisions are considered. These are 1) the route to sail in each period, 2) where to allocate the acquired vessels across all subroutes, and 3) with which frequency to serve each subroute. Let β_{pr} denote a binary variable equal to 1 if route r is chosen in time period p. Let g_{prcv} take the value of the number of vessels of type v used in subroute c in route r in period p, bounded by the strategic decision of total fleet size. This variable allows vessels to stay idle during a period, if the model finds it optimal. Lastly, let z_{prcf} be another binary variable, equal to 1 if frequency f is chosen for subroute c in route r in time period p.

As already highlighted in Section 5.1, sailing time is an important aspect of the ZEVSNDP and is considered an operational decision in the model. Let $x_{prckvfs}$ denote the weight variable for the speed level s for a vessel of type v on leg k when subroute c is served with frequency f, in a route r in time period p. As explained in Section 5.1, linear combinations of the discrete speed levels are allowed to permit more speed choices than those defined by $\mathcal{S}_v$. Further, let $c_{prcikvf}$ and $w_{prcikvf}$ denote the charging time and waiting time in port i before sailing leg k with a vessel of type v in subroute c served with frequency f (in a route r in time period p), respectively. The sailing time, charging time and waiting time when a vessel of type v has completed a full round trip, in a subroute c (in a route r in time period p), with frequency f, equals the round trip time, t_{prcvf}^{RT}. Additionally, we introduce t_{prckl} to be the transit time from the port at the beginning of leg k, to the port at the beginning of leg l, in subroute c, in route r, in time period p. Lastly, let b_{prckv} denote the battery level before sailing leg k, with a vessel of type v, in subroute c, in route r, in time period p.

Another operational aspect of the ZEVSNDP is the number of passengers picked up when visiting a port. Let $q_{prcklvf}$ be the number of passengers picked up in the port at the beginning of leg k, with destination port at the beginning of leg l, in subroute c, in route r, in time period p, served with frequency f, and vessel type v. To make sure the capacity onboard a vessel is not exceeded, we let l_{prcklv} denote the number of passengers on board a vessel of type v, on leg k, with destination port at the beginning of leg l, in subroute c in route r, in time period p. Lastly, let u_{prckl} denote the number of passengers using other means of transportation from the port at the beginning of leg k, with destination port at the beginning of leg l, in subroute c, when route r is chosen in time period p. These variables only consider the passengers that use other means of transportation, but potentially could use the vessel service. The unmet demand due to either the origin or destination port not being visited in the route, is already incorporated in C_{pr}^{ALT1} as described above.

Summary of Notation

Sets

$\mathcal{P}$	Set of planning periods
$\mathcal{R}_p$	Set of potential routes in period p
$\mathcal{C}_r$	Set of subroutes in route r
$\mathcal{K}_c$	Set of legs in route c
$\mathcal{I}$	Set of all ports
$\mathcal{I}_c$	Set of ports in route c
$\mathcal{F}_c$	Set of potential frequencies in subroute c
$\mathcal{V}$	Set of available vessel types
$\mathcal{S}_v$	Set of discrete speed levels for vessel type v

Parameters

$\overline{T_p}$	Length of planning period p
T_{prckvs}	Sailing time of leg k in subroute c in route r in period p with speed s and vessel type v
$\underline{T}_i^W$	Minimum waiting time in port i to allow passengers to enter and exit the vessel
T_{prckl}^U	Travel time from port at the beginning of leg k to port beginning at leg l in subroute c in route r in period p with the fastest vessel type available, sailing at its fastest speed level, with no charging or waiting time beyond the minimum requirements
W_{prcf}	Average waiting time at frequency f in time period p for subroute c in route r
D_{prckl}	Maximum demand from port at the beginning of leg k to port at the beginning of leg l in subroute c in period p with route r
D_{prcklf}	Demand from port at the beginning of leg k to port at the beginning of leg l in subroute c in period p with route r at frequency f
Q_v	Passenger capacity of vessel type v
E_{prckvs}	Energy consumption on leg k in subroute c in route r in period p with vessel type v sailing at speed s
$\overline{B}_v$	Maximum battery level of vessel type v
$\underline{B}_v$	Minimum battery level of vessel type v
P_i	Available charging power in port i
A_{prcik}	1 if leg k starts at port i in subroute c in route r in period p, 0 otherwise
C_v^{FC}	Fixed cost per vessel of type v
C_i^{INF}	Fixed cost of investing in charging infrastructure in port i
C_v^{crew}	Crew cost of using vessel v for one hour
C_{pi}^{VC}	Cost per unit of energy charged in port i in period p
C_{pr}^{ALT1}	Alternative cost per passenger not transported due to unvisited ports in route r in period p
C_{prckl}^{ALT2}	Alternative cost per passenger not transported between port at the beginning of leg k to port at the beginning of leg l in subroute c in route r in period p
C^{PW}	Value of passenger time while waiting at port
C^{SW}	Value of passenger time while sailing

Variables

α_i	1 if charging infrastructure is built in port i, 0 otherwise
δ_v	1 if vessel type v is chosen, 0 otherwise
y_v	Number of vessels of type v bought
β_{pr}	1 if route r is chosen in period p
g_{prcv}	Number of vessel v used in subroute c in route r in period p
z_{prcf}	1 if frequency f is chosen for subroute c and route r in period p, 0 otherwise
$x_{prckvfs}$	Weight variable for speed s for vessels of type v on leg k in subroute c in route r served with freqeuncy f in period p
l_{prcklv}	Number of passengers traversing leg k with destination port at the end of leg l in subroute c with a vessels of type v in route r in period p
$q_{prcklvf}$	Number of passengers picked up in port at the beginning of leg k with destination at the port in the beginning of leg l in subroute c with route r in period p with frequency f with vessel type v
u_{prckl}	Unmet demand between port at the beginning of leg k and port at the beginning of leg l in subroute c with route r in period p
t^{RT}_{prcvf}	Total round trip time in subroute c for a vessel of type v with route r served with frequency f in period p
$c_{prcikvf}$	Charging time in port i before traversing leg k in subroute c served with frequency f with a vessel of type v in route r in period p
$w_{prcikvf}$	Time spent in port i before sailing leg k in subroute c when served with frequency f with a vessel of type v in route r in period p
t_{prckl}	Transit time from port at the beginning of leg k to port at the beginning of leg l in subroute c in route r in period p
b_{prckv}	Battery level when starting on leg k for vessels of type v in subroute c route r in period p

5.3 Mathematical Formulation

After introducing the notation in Section 5.2, we formulate a mathematical formulation of the ZEVSNDP in this section. In Subsection 5.3.1, we introduce and explain each term of the objective function, while Subsection 5.3.2 elaborates on the constraints for the ZEVSNDP. In multiple of the constraints presented we make use of Big-M notation. Appropriated values for the different Big-Ms could be found in Appendix B.

5.3.1 Objective function

$$\begin{aligned}\min z = &\sum_{v\in\mathcal{V}} C_v^{FC} y_v + \sum_{i\in\mathcal{I}} C_i^{INF}\alpha_i + \sum_{p\in\mathcal{P}}\sum_{r\in\mathcal{R}_p}\sum_{c\in\mathcal{C}_r}\sum_{i\in\mathcal{I}_r}\sum_{k\in\mathcal{K}_c}\sum_{v\in\mathcal{V}}\sum_{f\in\mathcal{F}_c} C_{pi}^{VC} P_i c_{prcikv} f z_{prcf} \\
&+ \sum_{p\in\mathcal{P}}\sum_{r\in\mathcal{R}_p}\sum_{c\in\mathcal{C}_r}\sum_{v\in\mathcal{V}} C_v^{CREW}\overline{T}_p g_{prcv} + \sum_{p\in\mathcal{P}}\sum_{r\in\mathcal{R}_p} C_{pr}^{ALT1}\beta_{pr} \\
&+ \sum_{p\in\mathcal{P}}\sum_{r\in\mathcal{R}_p}\sum_{c\in\mathcal{C}_r}\sum_{k\in\mathcal{K}_c}\sum_{l\in\mathcal{K}_c} C_{prckl}^{ALT2} u_{prckl} \\
&+ C^{PW}\sum_{p\in\mathcal{P}}\sum_{r\in\mathcal{R}_p}\sum_{c\in\mathcal{C}_r}\sum_{f\in\mathcal{F}_c} W_{prcf} z_{prcf} (\sum_{k\in\mathcal{K}_c}\sum_{l\in\mathcal{K}_c} q_{prcklvf}) \\
&+ C^{SW}\sum_{p\in\mathcal{P}}\sum_{r\in\mathcal{R}_p}\sum_{c\in\mathcal{C}_r}\sum_{k\in\mathcal{K}_c}\sum_{l\in\mathcal{K}_c}\sum_{f\in\mathcal{F}_c} (t_{prckl} - T_{prckl}^{U}) D_{prcklf} z_{prcf}\end{aligned} \tag{5.1}$$

The objective function (5.1) aims, as explained in Chapter 3, to minimize the sum of the operator and the passenger costs. The first four terms cover the operator costs, while the last four terms encompass the passenger costs. The first term in (5.1) represents the vessel investment cost, namely the vessel price multiplied by the number of acquired vessels. The second term consists of the infrastructure investment cost in each port, multiplied by the binary variable indicating if infrastructure is installed in port i or not, yielding the total infrastructure investment cost. The third term is the variable cost of charging. This cost is computed by multiplying the electricity price with the available power and charging time in a port i, summed over all selected frequencies in all selected subroutes and routes, in all time periods. The last operator cost, described by the fourth term in (5.1), is the crew cost. This is calculated by multiplying the number of vessels used in a time period, g_{prcv} with the length of the period, $\overline{T}_p$ and the hourly cost, C_v^{CREW}. Finally, we sum the aforementioned product over all periods, routes, subroutes and vessel types, to obtain the total crew cost.

The fifth and sixth terms represent the alternative cost of using other means of transportation. The former captures the alternative cost of not visiting a port in the chosen route r in period p. The cost parameter, C_{pr}^{ALT1} is known in advance for a given route, as explained in Section 5.2. We therefore sum over all periods and routes while multiplying the parameter with the binary variable β_{pr}, indicating whether a route is chosen in the time period. The sixth term calculates the cost of passengers using other means of transportation, when both origin and destination port is served by the chosen route. The seventh term computes the passengers' cost of waiting in port, which depends on the frequency, as elaborated on in Section 5.1. The last term in the objective function encompasses the passengers' costs of sailing, where the actual transit time, t_{prckl} is compared to the benchmark T_{prckl}^{U} and the difference is penalized. It should be noted that the third, seventh and eighth terms in the objective function are non-linear. These terms are linearized in Section 5.4, in order to solve the model in a commercial MILP-solver.

5.3.2 Constraints

In this subsection we present and explain the constraints for the ZEVSNDP. The constraints capturing the behaviour of the strategic and tactical decisions are presented first as Constraints

(5.2)-(5.7). Secondly, the constraints necessary to connect time usage are presented as Constraints (5.8)-(5.15). Thirdly, to make sure the battery level is at sufficient levels at all times, the battery constraints are presented as Constraints (5.16)-(5.20). Lastly, we present the passenger flow constraints as Constraints (5.23)-(5.30), to ensure correct handling of demand, pick-up of passengers and the number of people on board on each leg.

Constraints linking strategic and tactical decisions

Constraint (5.2) makes sure we only choose one vessel type for the ZEVSNDP. Next, Constraints (5.3) allow the model to only invest in vessels of the chosen vessel type v.

$$\sum_{v\in\mathcal{V}} \delta_v = 1 \tag{5.2}$$

$$y_v \leq M^1 \delta_v, \qquad v \in \mathcal{V} \tag{5.3}$$

Constraints (5.4) force only one route r to be chosen in each time period p. For a chosen route, each subroute c in the route must be served with a service frequency f from the set of potential frequencies $\mathcal{F}_c$. This is ensured by Constraints (5.5), which make sure only one frequency is chosen for each subroute c in the chosen route r through the binary variable z_{prcf}. The same constraints ensure that z_{prcf} is zero for routes not chosen in time period p.

$$\sum_{r\in\mathcal{R}_p} \beta_{pr} = 1, \qquad p \in \mathcal{P} \tag{5.4}$$

$$\sum_{f\in\mathcal{F}} z_{prcf} = \beta_{pr}, \qquad p \in \mathcal{P},\ r \in \mathcal{R}_p,\ c \in \mathcal{C}_r \tag{5.5}$$

Constraints (5.6) restrain the number of vessels used in each time period p to being less than or equal to the number of vessels bought. Constraints (5.7) ensure the frequency in a subroute c to be greater than or equal to the number of vessels used in the subroute. A consequence of excluding these constraints would, for instance be that a frequency of one could be served using two vessels. This is not allowed, as it would result in the vessels only sailing a partial round trip.

$$\sum_{r\in\mathcal{R}_c} \sum_{c\in\mathcal{C}_r} g_{prcv} \leq y_v, \qquad p \in \mathcal{P},\ v \in \mathcal{V} \tag{5.6}$$

$$\sum_{v\in\mathcal{V}} g_{prcv} \leq \sum_{f\in\mathcal{F}} f z_{prcf}, \qquad p \in \mathcal{P},\ r \in \mathcal{R}_p,\ c \in \mathcal{C}_r \tag{5.7}$$

Time constraints

Constraints (5.8) define the round trip time in a subroute c, in route r, in time period p with a vessel of type v and a frequency f. The round trip time is the sum of the sailing time, waiting time and charging time along the subroute. For routes, vessel types and frequencies that are not chosen, the round trip time should be zero. This is ensured by constraints presented later in this section, which ensure that all terms defining the round trip time are zero if the vessel type, route or frequency are not chosen. Further, Constraints (5.9) make sure the frequency multiplied by the round trip time in a subroute c must equal the length of the planning period in period p multiplied by the vessels used in the subroute. Constraints (5.9) are non-linear, due to the multiplication of the round trip time with the binary variable, z_{prcf}. A linearization of these constraints is proposed in Section 5.4.

$$t^{RT}_{prcvf} = \sum_{k\in\mathcal{K}_c} \sum_{s\in\mathcal{S}_v} T_{prckvs} x_{prckvfs} + \sum_{k\in\mathcal{K}_c} \sum_{i\in\mathcal{I}_c} (c_{prcikvf} + w_{prcikvf}), \qquad p \in \mathcal{P},\ r \in \mathcal{R}_p,\ c \in \mathcal{C}_r,\ v \in \mathcal{V},\ f \in \mathcal{F}_c \tag{5.8}$$

$$\sum_{f\in\mathcal{F}_c} \sum_{v\in\mathcal{V}} f z_{prcf} t^{RT}_{prcvf} = \overline{T}_p \sum_{v\in\mathcal{V}} g_{prcv}, \qquad p \in \mathcal{P},\ r \in \mathcal{R}_p,\ c \in \mathcal{C}_r \tag{5.9}$$

The waiting time in a port i must be greater than the minimum waiting time, T_i^w, ensured by Constraints (5.10). Note the use of the binary parameter A_{prcik}, which associates the leg k with the port at its origin i. For vessel types that are not chosen we set the waiting time to zero through Constraints (5.11), while for frequencies and routes not chosen this is assured by Constraints (5.12). It should be noted that Constraints (5.10) contain the product of the two binary variables δ_v and z_{prcf}. A linearization of the product of these two binary variables, is proposed in Section 5.4.

$$w_{prcikvf} \geq \underline{T}_i^w A_{prcik} z_{prcf} \delta_v, \qquad p \in \mathcal{P},\ r \in \mathcal{R}_p,\ c \in \mathcal{C}_r\ v \in \mathcal{V},\ i \in \mathcal{I}_c,\ k \in \mathcal{K}_c,\ f \in \mathcal{F}_c \tag{5.10}$$

$$w_{prcikvf} \leq M_{prc}^2 A_{prcik} \delta_v, \qquad p \in \mathcal{P},\ r \in \mathcal{R}_p,\ c \in \mathcal{C}_r,\ i \in \mathcal{I}_c,\ k \in \mathcal{K}_c,\ v \in \mathcal{V},\ f \in \mathcal{F}_c \tag{5.11}$$

$$w_{prcikvf} \leq M_{prc}^3 A_{prcik} z_{prcf}, \qquad p \in \mathcal{P},\ r \in \mathcal{R}_p,\ c \in \mathcal{C}_r,\ i \in \mathcal{I}_c,\ k \in \mathcal{K}_c,\ v \in \mathcal{V},\ f \in \mathcal{F}_c \tag{5.12}$$

Constraints (5.13) make sure the speed weight variable sums up to one, for each leg k, in each subroute c, for the chosen route r and frequency f, and the chosen vessel type v for each time period p.

$$\sum_{s \in \mathcal{S}_v} x_{prckvfs} = \delta_v z_{prcf}, \qquad p \in \mathcal{P}, r \in \mathcal{R}_p, c \in \mathcal{C}_r,\ k \in \mathcal{K}_c,\ v \in \mathcal{V},\ \ f \in \mathcal{F}_c \tag{5.13}$$

Lastly, Constraints (5.14) and (5.15) define the transit time between the port at the beginning of leg k to the port at the beginning of leg l, in subroute c, in route r, in time period p. It should be noted that the charging and waiting time at the port at the beginning of leg k and leg l is excluded from the transit time between the ports, since it will not affect the passengers' transit time on board.

$$t_{prckl} = \sum_{v \in \mathcal{V}} \sum_{f \in \mathcal{F}_c} \left[\sum_{\hat{k}=k}^{l-1} \sum_{s \in \mathcal{S}_v} T_{prc\hat{k}vs} x_{prc\hat{k}vfs} + \sum_{i \in \mathcal{I}_c} \sum_{\hat{k}=k+1}^{l-1} (c_{prci\hat{k}vf} + w_{prci\hat{k}vf}) \right], \qquad p \in \mathcal{P},\ r \in \mathcal{R}_p,\ c \in \mathcal{C}_r,\ k \in \mathcal{K}_c,\ l \in \mathcal{K}_c \,|\, l > k \tag{5.14}$$

$$\begin{aligned} t_{prckl} = & \sum_{v \in \mathcal{V}} \sum_{f \in \mathcal{F}_c} \left[\sum_{\hat{k}=k}^{|\mathcal{K}_r|} \sum_{s \in \mathcal{S}_v} T_{prc\hat{k}vs} x_{prc\hat{k}vfs} + \sum_{i \in \mathcal{I}_c} \sum_{\tilde{k}}^{|\mathcal{K}_c|} (c_{prci\tilde{k}vf} + w_{prci\tilde{k}vf}) \right. \\ & \left. + \sum_{k'}^{l-1} \left(\sum_{s \in \mathcal{S}_v} T_{prck'vs} x_{prck'vfs} + \sum_{i \in \mathcal{I}_c} (c_{prcik'vf} + w_{prcik'vf}) \right) \right], \\ & p \in \mathcal{P},\ r \in \mathcal{R}_p,\ c \in \mathcal{C}_r,\ k \in \mathcal{K}_c,\ l \in \mathcal{K}_c \,|\, k > l \end{aligned} \tag{5.15}$$

where,

$$\tilde{k} = \min\{|\ \mathcal{K}_c\ |, k+1\}$$
$$k' = \max\{1, l-1\}$$

Battery constraints

Constraints (5.16) and (5.17) define the battery level before sailing a leg k. It is set equal to the battery level before sailing the previous leg, subtracted the energy used on that leg while adding the charged energy at the port before leg k. It should be noted that Constraints (5.17) are included to capture the relationship between the last leg in the set of ports and the first. Thus, ensuring we finish with the same battery level as we started with. Further, Constraints (5.18) and (5.19) make sure the battery level does not exceed its maximum and minimum limits, respectively. Constraints (5.20) ensure that charging is only possible at the ports where charging infrastructure is installed.

Again, we make use of the A_{prcik} parameter to associate each leg k in a subroute c with its port of origin i. Lastly, Constraints (5.21) and (5.22) ensure that the charging variable cannot take values for routes, frequencies and vessel types not chosen.

$$\begin{aligned} b_{prckv} = {} & b_{prc,k-1,v} - \sum_{f \in \mathcal{F}_c} \sum_{s \in \mathcal{S}_v} E_{rc,k-1,vs} x_{prc,k-1,vfs} \\ & + \sum_{i \in \mathcal{I}_r} \sum_{f \in \mathcal{F}_c} A_{prcik} P_i \, c_{prikvf}, \quad p \in \mathcal{P},\ r \in \mathcal{R}_p,\ c \in \mathcal{C}_r,\ k \in \mathcal{K}_c \backslash \{1\},\ v \in \mathcal{V} \end{aligned} \tag{5.16}$$

$$\begin{aligned} b_{prc1v} = {} & b_{prc,|\mathcal{K}_c|,v} - \sum_{f \in \mathcal{F}_c} \sum_{s \in \mathcal{S}_v} E_{prc,|\mathcal{K}_c|,vs} x_{prc,|\mathcal{K}_c|,vfs} \\ & + \sum_{i \in \mathcal{I}_c} \sum_{f \in \mathcal{F}_c} A_{prcik} P_i \, c_{prci,1,vf}, \qquad p \in \mathcal{P},\ r \in \mathcal{R}_p,\ c \in \mathcal{C}_r\ v \in \mathcal{V} \end{aligned} \tag{5.17}$$

$$b_{prckv} \leq \overline{B}_v \delta_v \beta_{pr}, \qquad p \in \mathcal{P},\ r \in \mathcal{R}_p,\ c \in \mathcal{C}_r,\ k \in \mathcal{K}_c,\ v \in \mathcal{V} \tag{5.18}$$

$$\begin{aligned} & b_{prckv} - \sum_{f \in \mathcal{F}_c} \sum_{s \in \mathcal{S}_v} E_{rckvs} x_{prckvfs} \geq \underline{B}_v \delta_v \beta_{pr}, \\ & \qquad\qquad p \in \mathcal{P},\ r \in \mathcal{R}_p,\ c \in \mathcal{C}_r,\ k \in \mathcal{K}_c,\ v \in \mathcal{V} \end{aligned} \tag{5.19}$$

$$c_{prcikvf} \leq M^4_{iv} A_{prcik} \alpha_i, \qquad p \in \mathcal{P},\ r \in \mathcal{R}_p, c \in \mathcal{C}_r,\ i \in \mathcal{I}_c,\ k \in \mathcal{K}_c,\ v \in \mathcal{V},\ f \in \mathcal{F}_c \tag{5.20}$$

$$c_{prcikvf} \leq M^5_{iv} z_{prcf}, \qquad p \in \mathcal{P},\ r \in \mathcal{R}_p, c \in \mathcal{C}_r,\ i \in \mathcal{I}_c,\ k \in \mathcal{K}_c,\ v \in \mathcal{V},\ f \in \mathcal{F}_c \tag{5.21}$$

$$c_{prcikvf} \leq M^6_{iv} \delta_v, \qquad p \in \mathcal{P},\ r \in \mathcal{R}_p, c \in \mathcal{C}_r,\ i \in \mathcal{I}_c,\ k \in \mathcal{K}_c,\ v \in \mathcal{V},\ f \in \mathcal{F}_c \tag{5.22}$$

Passenger flow constraints

We only allow passengers in a subroute to be picked up if a vessel is chosen for the subroute. This is ensured through Constraints (5.23). Further, we restrict the load on a leg k from exceeding the chosen vessel type's capacity, through Constraints (5.24).

$$l_{prcklv} \leq M^7_{prckl} g_{prcv}, \qquad p \in \mathcal{P},\ r \in \mathcal{R}_p,\ c \in \mathcal{C}_r,\ k \in \mathcal{K}_c,\ l \in \mathcal{K}_c,\ v \in \mathcal{V} \tag{5.23}$$

$$\sum_{l \in \mathcal{K}_c} l_{prcklv} \leq Q_v \sum_{f \in \mathcal{F}_c} f \, z_{prcf}, \qquad p \in \mathcal{P},\ r \in \mathcal{R}_p,\ c \in \mathcal{C}_r,\ k \in \mathcal{K}_c,\ v \in \mathcal{V} \tag{5.24}$$

Constraints (5.25) and (5.26) define the passenger balance on a vessel. The constraints make sure that the number of passengers entering the vessel in a port with a specific destination, is the difference between the previous and current passenger load with the same destination. The passengers that potentially could be picked up, are constrained by the number of passengers that wants to use the vessel service at the specific subroute frequency. This is covered by Constraints (5.27). The unmet demand caused by passengers choosing other means of transportation, even when they have the possibility of using the vessel service, is determined by Constraints (5.28). Passengers could also prefer other means of transportation if they consider the frequency to be too low, and Constraints (5.28) are accordingly defined so that the picked up passengers and unmet demand together must equal the total demand, D_{prckl}. Lastly, we define Constraints (5.29) and (5.30) to ensure passengers may only disembark the vessel at their destination.

$$\begin{aligned} & \sum_{f \in \mathcal{F}_c} q_{prcklvf} = l_{prcklv} - l_{prc,k-1,lv}, \qquad p \in \mathcal{P},\ r \in \mathcal{R}_p,\ c \in \mathcal{C}_r, \\ & \qquad\qquad k \in \mathcal{K}_c \backslash \{1\},\ l \in \mathcal{K}_c \,|\, l \neq k,\ v \in \mathcal{V} \end{aligned} \tag{5.25}$$

$$\sum_{f \in \mathcal{F}_c} q_{prc,1,lvf} = l_{prc,1,lv} - l_{prc|\mathcal{K}_c|,lv}, \quad p \in \mathcal{P},\ r \in \mathcal{R}_p,\ c \in \mathcal{C}_r,\ l \in \mathcal{K}_c \backslash \{1\},\ v \in \mathcal{V} \tag{5.26}$$

$$q_{prcklvf} \leq D_{prcklf}\, z_{prcf}, \quad p \in \mathcal{P},\ r \in \mathcal{R}_p,\ c \in \mathcal{C}_r,\ k \in \mathcal{K}_c,\ l \in \mathcal{K}_c,\ f \in \mathcal{F}_c \tag{5.27}$$

$$\sum_{v \in \mathcal{V}} \sum_{f \in \mathcal{F}_c} q_{prcklvf} + u_{prckl} = D_{prckl}\beta_{pr}, \quad p \in \mathcal{P},\ r \in \mathcal{R}_p,\ c \in \mathcal{C}_r,\ k \in \mathcal{K}_c,\ l \in \mathcal{K}_c \tag{5.28}$$

$$l_{prc,k-1,l} \leq l_{prcklv}, \quad p \in \mathcal{P},\ r \in \mathcal{R}_p,\ c \in \mathcal{C}_r,\ k \in \mathcal{K}_c \backslash \{1\},\ l \in \mathcal{K}_c \,|\, l \neq k,\ v \in \mathcal{V} \tag{5.29}$$

$$l_{prc,|\mathcal{K}_c|,lv} \leq l_{prc,1,lv}, \quad p \in \mathcal{P},\ r \in \mathcal{R}_p,\ c \in \mathcal{C}_r,\ l \in \mathcal{K}_c \backslash \{1\},\ v \in \mathcal{V} \tag{5.30}$$

Non-negativity, binary, and integer requirements

This mathematical formulation contains four types of binary variables, the location of charging infrastructure, the selected vessel type, the route selection and the frequency selection. Binary requirements are placed on these variables in Constraints (5.31), (5.32), (5.33) and (5.34), respectively.

$$\alpha_i \in \{0,1\}, \quad i \in \mathcal{I} \tag{5.31}$$

$$\delta_v \in \{0,1\}, \quad v \in \mathcal{V} \tag{5.32}$$

$$\beta_{pr} \in \{0,1\}, \quad p \in \mathcal{P},\ r \in \mathcal{R}_p \tag{5.33}$$

$$z_{prcf} \in \{0,1\}, \quad p \in \mathcal{P},\ r \in \mathcal{R}_p,\ c \in \mathcal{C}_r,\ f \in \mathcal{F}_c \tag{5.34}$$

Furthermore, the mathematical formulation contains two types of decision variables with integrality requirements. These variables are the total fleet size and the number of vessels assigned to a specific subroute. These integralities are enforced by Constraints (5.35) and (5.36).

$$y_v \in \mathbb{Z}^+, \quad v \in \mathcal{V} \tag{5.35}$$

$$g_{prcv} \in \mathbb{Z}^+, \quad p \in \mathcal{P},\ r \in \mathcal{R}_p,\ c \in \mathcal{C}_r,\ v \in \mathcal{V} \tag{5.36}$$

The remaining variables are allowed to take fractional values, and do hence only have non-negativity requirements. Note that the three decision variables concerning passenger flow, l_{prcklv}, $q_{prcklvf}$ and u_{prckl}, are also allowed to have fractional values. This stems from the fact that the total demand is calculated on an average basis, resulting in a fractional total demand. The process of preparing the demand data is further explained in Chapter 7.

$$x_{prckvfs} \in \mathbb{R}^+, \quad p \in \mathcal{P},\ r \in \mathcal{R}_p,\ c \in \mathcal{C}_r,\ k \in \mathcal{K}_c,\ v \in \mathcal{V},\ f \in \mathcal{F}_c,\ s \in \mathcal{S} \tag{5.37}$$

$$l_{prcklv} \in \mathbb{R}^+, \quad p \in \mathcal{P},\ r \in \mathcal{R}_p,\ c \in \mathcal{C}_r,\ k \in \mathcal{K}_c,\ l \in \mathcal{K}_c,\ v \in \mathcal{V} \tag{5.38}$$

$$q_{prcklvf} \in \mathbb{R}^+, \qquad p \in \mathcal{P},\ r \in \mathcal{R}_p,\ c \in \mathcal{C}_r,\ k \in \mathcal{K}_c,\ l \in \mathcal{K}_c,\ v \in \mathcal{V},\ f \in \mathcal{F}_c \tag{5.39}$$

$$u_{prckl} \in \mathbb{R}^+, \qquad p \in \mathcal{P},\ r \in \mathcal{R}_p,\ c \in \mathcal{C}_r,\ k \in \mathcal{K}_c,\ l \in \mathcal{K}_c \tag{5.40}$$

$$t^{RT}_{prcvf} \in \mathbb{R}^+, \qquad p \in \mathcal{P},\ r \in \mathcal{R}_p,\ c \in \mathcal{C}_r,\ v \in \mathcal{V},\ f \in \mathcal{F}_c \tag{5.41}$$

$$c_{prcikvf} \in \mathbb{R}^+, \qquad p \in \mathcal{P},\ r \in \mathcal{R}_p,\ c \in \mathcal{C}_r,\ i \in \mathcal{I}_c,\ k \in \mathcal{K}_c,\ v \in \mathcal{V},\ f \in \mathcal{F}_c \tag{5.42}$$

$$w_{prcikvf} \in \mathbb{R}^+, \qquad p \in \mathcal{P},\ r \in \mathcal{R}_p,\ c \in \mathcal{C}_r,\ i \in \mathcal{I}_c,\ k \in \mathcal{K}_c,\ v \in \mathcal{V},\ f \in \mathcal{F}_c \tag{5.43}$$

$$t_{prckl} \in \mathbb{R}^+, \qquad p \in \mathcal{P},\ r \in \mathcal{R}_p,\ c \in \mathcal{C}_r,\ k \in \mathcal{K}_c,\ l \in \mathcal{K}_c \tag{5.44}$$

$$b_{prckv} \in \mathbb{R}^+, \qquad p \in \mathcal{P},\ r \in \mathcal{R}_p,\ c \in \mathcal{C}_r,\ k \in \mathcal{K}_c,\ v \in \mathcal{V} \tag{5.45}$$

5.4 Linearizations

The mathematical model proposed in Section 5.3 includes non-linear terms, both in the objective function and in several constraints. These terms are linearized, in order to solve the model using a commercial MILP-solver. In this section linearizations of the non-linear terms are presented, by introducing additional variables and constraints. A linearization of similar terms was also done in the ZEVRPP presented by Havre et al. (2021). This section follows and extends their approach.

Linearization of terms in the objective function

The third term in the objective function (5.1) is non-linear, since the charging time, $c_{prcikvf}$ is multiplied with the binary variable z_{prcf}. To linearize this expression we introduce the auxiliary variable v_{prcf}. Further, we introduce Constraints (5.47) and (5.48). In Constraints (5.47), we make sure that v_{prcf} is greater than or equal to the cost of electricity times the available power times the charging time, if z_{prcf} is equal to one. In Constraints (5.48), v_{prcf} is set to zero if z_{prcf} is zero.

$$v_{prcf} \in \mathbb{R}^+, \qquad p \in \mathcal{P},\ r \in \mathcal{R}_p,\ c \in \mathcal{C}_r,\ f \in \mathcal{F}_c \tag{5.46}$$

$$v_{prcf} \geq \sum_{i \in \mathcal{I}_c} \sum_{k \in \mathcal{K}_c} \sum_{v \in \mathcal{V}} C^{VC}_{pi} P_i c_{prcikvf} - M^8_{prc}(1 - z_{prcf}), \qquad p \in \mathcal{P},\ r \in \mathcal{R}_p,\ c \in \mathcal{C}_r,\ f \in \mathcal{F}_c \tag{5.47}$$

$$v_{prcf} \leq M^8_{prc} z_{prcf}, \qquad p \in \mathcal{P},\ r \in \mathcal{R}_p,\ c \in \mathcal{C}_r,\ f \in \mathcal{F}_c \tag{5.48}$$

Subsequently, the third term of the objective function could be replaced by (5.49).

$$\sum_{p \in \mathcal{P}} \sum_{r \in \mathcal{R}_p} \sum_{c \in \mathcal{C}_r} \sum_{f \in \mathcal{F}_c} f\ v_{prcf} \tag{5.49}$$

The seventh term in the objective function (5.1) is also non-linear, due to the number of passengers picked up, $q_{prcklvf}$, being multiplied with the binary variable z_{prcf}. Accordingly, the same approach as for the third term is used for the seventh term, by introducing another auxiliary variable p_{prcf}. Further, Constraints (5.51) and (5.52) are presented to let p_{prcf} be equal to the sum of all passengers picked up in a subroute c, if z_{prcf} is equal to one.

$$p_{prcf} \in \mathbb{R}^{+}, \qquad p \in \mathcal{P},\ r \in \mathcal{R}_p,\ c \in \mathcal{C}_r,\ f \in \mathcal{F}_c \tag{5.50}$$

$$p_{prcf} \geq \sum_{k \in \mathcal{K}_c} \sum_{l \in \mathcal{K}_c} \sum_{v \in \mathcal{V}} q_{prcklvf} - M^{9}_{prcf}(1 - z_{prcf}), \quad p \in \mathcal{P},\ r \in \mathcal{R}_p,\ c \in \mathcal{C}_r,\ f \in \mathcal{F}_c \tag{5.51}$$

$$p_{prcf} \leq M^{9}_{prcf} z_{prcf}, \qquad p \in \mathcal{P},\ r \in \mathcal{R}_p,\ c \in \mathcal{C}_r,\ f \in \mathcal{F}_c \tag{5.52}$$

The seventh term of the objective function (5.1) could then be replaced by (5.53).

$$C^{PW} \sum_{p \in \mathcal{P}} \sum_{r \in \mathcal{R}_p} \sum_{c \in \mathcal{C}_r} \sum_{f \in \mathcal{F}_c} W_{prcf} p_{prcf} \tag{5.53}$$

Lastly, the eighth term of the objective function (5.1) is non-linear as the transit time between two ports, t_{prckl}, is multiplied with the binary variable z_{prcf}. We follow the same approach as for the two previous terms, by introducing a third auxiliary variable, o_{prcf}. Constraints (5.55) and (5.56) are introduced. They ensure that o_{prcf} equals the difference between the actual transit time and the benchmark transit time, multiplied with the demand within the port pair, summed over all port pairs in subroute c, if z_{prcf} is equal to one.

$$o_{prcf} \in \mathbb{R}^{+}, \qquad p \in \mathcal{P},\ r \in \mathcal{R}_p,\ c \in \mathcal{C}_r,\ f \in \mathcal{F}_c \tag{5.54}$$

$$o_{prcf} \geq \sum_{k \in \mathcal{K}_c} \sum_{l \in \mathcal{K}_c} (t_{prckl} - T^{U}_{prckl}) D_{prcklf} - M^{10}_{prcf}(1 - z_{prcf}), \qquad p \in \mathcal{P},\ r \in \mathcal{R}_p,\ c \in \mathcal{C}_r,\ f \in \mathcal{F}_c \tag{5.55}$$

$$o_{prcf} \leq M^{10}_{prcf} z_{prcf}, \qquad p \in \mathcal{P},\ r \in \mathcal{R}_p,\ c \in \mathcal{C}_r,\ f \in \mathcal{F}_c \tag{5.56}$$

The eighth term of the objective function (5.1) could then be replaced by (5.57).

$$C^{SW} \sum_{p \in \mathcal{P}} \sum_{r \in \mathcal{R}_p} \sum_{c \in \mathcal{C}_r} \sum_{f \in \mathcal{F}_c} o_{prcf} \tag{5.57}$$

Linearization of the non-linear constraints

In Constraints (5.10) and (5.13), the two binary variables δ_v and z_{prcf} are multiplied with each other. While in Constraints (5.18) and (5.19) the two binary variables δ_v and β_{pr} are multiplied, causing a non-linearity. We therefore introduce two extra binary variables, ϕ_{prcvf} and γ_{prv}, to solve the issues.

$$\phi_{pcrvf} \in \{0, 1\}, \qquad p \in \mathcal{P},\ r \in \mathcal{R}_p,\ c \in \mathcal{C}_r,\ v \in \mathcal{V}, f \in \mathcal{F}_c \tag{5.58}$$

$$\gamma_{prv} \in \{0, 1\}, \qquad p \in \mathcal{P},\ r \in \mathcal{R}_p,\ v \in \mathcal{V} \tag{5.59}$$

Further, γ_{prv} should equal zero if either β_{pr} or δ_v is equal to zero, and one if both are equal to one. The same applies from ϕ_{prcvf} and the relationship between z_{prcf} and δ_v. Accordingly, Constraints (5.60)-(5.65) are introduced.

$$\gamma_{prv} \geq \beta_{pr} + \delta_v - 1, \qquad p \in \mathcal{P},\ r \in \mathcal{R}_p,\ v \in \mathcal{V} \tag{5.60}$$

$$\gamma_{prv} \leq \beta_{pr}, \qquad p \in \mathcal{P},\ r \in \mathcal{R}_p,\ v \in \mathcal{V} \tag{5.61}$$

$$\gamma_{prv} \leq \delta_v, \qquad p \in \mathcal{P},\ r \in \mathcal{R}_p,\ v \in \mathcal{V} \tag{5.62}$$

$$\phi_{prcvf} \geq z_{prcf} + \delta_v - 1, \qquad p \in \mathcal{P},\ r \in \mathcal{R}_p,\ c \in \mathcal{C}_r,\ v \in \mathcal{V},\ f \in \mathcal{F}_c \tag{5.63}$$

$$\phi_{prcvf} \leq z_{prcf}, \qquad p \in \mathcal{P},\ r \in \mathcal{R}_p,\ c \in \mathcal{C}_r,\ v \in \mathcal{V},\ f \in \mathcal{F}_c \tag{5.64}$$

$$\phi_{prcvf} \leq \delta_v, \qquad p \in \mathcal{P},\ r \in \mathcal{R}_p,\ c \in \mathcal{C}_r,\ v \in \mathcal{V},\ f \in \mathcal{F}_c \tag{5.65}$$

ϕ_{prcvf} could then replace the product of δ_v and z_{prcf} in Constraints (5.10) and (5.13), while γ_{prv} replace the product of β_{pr} and δ_v in (5.18) and (5.19) to achieve a linear model.

The last non-linear Constraints are (5.9), due to the round trip time, t^{RT}_{prcvf} being multiplied with the binary variable z_{prcf}. To overcome this, yet another auxiliary variable, s_{prcf}, is introduced to the model. Further, Constraints (5.67) and (5.68) ensure that s_{prcf} is greater than or equal to the round trip time, when z_{prcf} is equal to one, and zero otherwise.

$$s_{prcf} \in \mathbb{R}^+, \qquad p \in \mathcal{P},\ r \in \mathcal{R}_p,\ c \in \mathcal{C}_r,\ f \in \mathcal{F}_c \tag{5.66}$$

$$s_{prcf} \geq \sum_{v \in \mathcal{V}} t^{RT}_{prcvf} - M(1 - z_{prcf}), \qquad p \in \mathcal{P},\ r \in \mathcal{R}_p,\ c \in \mathcal{C}_r,\ f \in \mathcal{F}_c \tag{5.67}$$

$$s_{prcf} \leq M z_{prcf}, \qquad p \in \mathcal{P},\ r \in \mathcal{R}_p,\ c \in \mathcal{C}_r,\ f \in \mathcal{F}_c \tag{5.68}$$

Subsequently, Constraints (5.9) could be replaced with (5.69) to obtain a linear model.

$$\sum_{f \in \mathcal{F}_c} f s_{prcf} = \overline{T}_p \sum_{v \in \mathcal{V}} g_{prcv}, \qquad p \in \mathcal{P},\ r \in \mathcal{R}_p,\ c \in \mathcal{C}_r \tag{5.69}$$

By introducing s_{prcf} in Constraints (5.69), and excluding the original Constraints (5.9), a problem with the calculation of round trip time, t^{RT}_{prcvf}, occurs. While s_{prcf} takes a value to fulfil Constraints (5.69), t^{RT}_{prcvf} does not necessarily take the same value, when z_{prcf} is equal to one. This is caused by the fact that Constraints (5.67) and (5.68) alone cannot guarantee that t^{RT}_{prcvf} equals s_{prcf}, thus not satisfying the original Constraints (5.9).

Note that all the terms defining t^{RT}_{prcvf} in Constraints (5.8) are indirectly minimized in the objective function (5.1), as they define the transit time between ports, t_{prckl} through Constraints (5.14) and (5.15). This causes the waiting time in each port, $w_{prcikvf}$, to be set equal to the minimum requirement, T^W_i, resulting in $t_{prckl} \leq s_{prcf}$. This is not desirable. Instead we want t^{RT}_{prcvf} to exactly represent the round trip time, as we seek to distribute the port waiting time in an economically efficient manner. To alleviate the issue, we reformulate the definition of the transit times, t_{prckl}, in Constraints (5.70) and (5.71), replacing Constraints (5.14) and (5.15).

$$\begin{aligned} t_{prckl} = \sum_{f \in \mathcal{F}_c} s_{prcf} - \sum_{v \in \mathcal{V}} \sum_{f \in \mathcal{F}_c} \Bigg[\sum_{\hat{k}=l}^{|\mathcal{K}_c|} \Big(\sum_{s \in \mathcal{S}_v} T_{prc\hat{k}vs} x_{prc\hat{k}vfs} + \sum_{i \in \mathcal{I}_c} (c_{prci\hat{k}vf} + \\ w_{prci\hat{k}vf}) \Big) + \sum_{k''} \sum_{s \in \mathcal{S}_v} T_{prck''vs} x_{prck''vfs} + \sum_{i \in \mathcal{I}_c} \sum_{\hat{k}=1}^{k} (c_{prci\hat{k}vf} + w_{prci\hat{k}vf}) \Bigg], \\ p \in \mathcal{P},\ r \in \mathcal{R}_p,\ c \in \mathcal{C}_r,\ k \in \mathcal{K}_c,\ l \in \mathcal{K}_c \,|\, l > k \end{aligned} \tag{5.70}$$

where,

$$k'' = \min\{1, k-1\}$$

$$t_{prckl} = \sum_{f \in \mathcal{F}_c} s_{prcf} - \sum_{v \in \mathcal{V}} \sum_{f \in \mathcal{F}_c} \Bigg[\sum_{\hat{k}=l}^{k-1} \sum_{s \in \mathcal{S}_v} T_{prc\hat{k}vs} x_{prc\hat{k}vfs} + \sum_{i \in \mathcal{I}_c} \sum_{\hat{k}=l}^{k} (c_{prci\hat{k}vf} + w_{prci\hat{k}vf}) \Bigg], \quad p \in \mathcal{P},\ r \in \mathcal{R}_p,\ c \in \mathcal{C}_r,\ k \in \mathcal{K}_c,\ l \in \mathcal{K}_c \,|\, k > l \tag{5.71}$$

5.5 Conventional Model

In this section we present a similar mathematical model to the one presented in Section 5.3, but with the use of conventional vessels. A comparable model was also presented by Havre et al. (2021) for the ZEVRPP. The changes in the mathematical model of the ZEVSNDP to account for conventional vessels are similar to that of the ZEVRPP, and this section is thus based on their approach. The motivation behind presenting an altered model is to benchmark the costs of a Zero-Emission (ZE) service for the instances presented in Chapter 7. In general, the conventional model shares many similarities with the original problem presented in Section 5.3. In the following subsections we therefore focus on the differences between the conventional and the ZE model. Subsection 5.5.1 covers the additional notation required, before Subsection 5.5.2 presents the differences in the mathematical formulation.

5.5.1 Additional notation

The sets remain the same as in Section 5.2, except for the vessel types in $\mathcal{V}$, which all use fossil fuels. Most of the parameters remain the same as in Section 5.2, except some that become redundant.

There is no longer a need for charging infrastructure, which means that the investment cost parameter, C_i^{INF} becomes redundant alongside the available power in port, $\underline{P_i}$. It is also unnecessary to keep track of the battery level between each port in the route. Hence, $\overline{B}_v$ and $\underline{B}_v$ are redundant. We assume that a conventional vessel always has enough fuel to finish as many round trips as required throughout the planning horizon. Consequently, the model will not allocate time for refueling in ports.

The change of energy carrier will also call for modifications to the parameter C_{pi}^{VC}. This parameter previously represented the charging cost at a port i, and is now adjusted to represent the energy cost of fuel, which is assumed equal in all ports. Accordingly, C_{pi}^{VC} is replaced with C^{VC}. It is also assumed that this price do not change through the day, hence a p-index is unnecessary.

Three of the variables from Section 5.2 will be redundant in the model for conventional vessels. As the installation of charging infrastructure is no longer a part of the problem, α_i becomes redundant. The battery level and the time spent charging in port i are additionally no longer considered in the problem, meaning that b_{prckv} and c_{prckvf} become redundant.

The conventional model has one new variable compared to the original model. The variable e_{prcv}^{RT} is included in the problem, and represents the fuel consumption on one round trip of subroute c in route r for a vessel of type v in period p. This variable depends on the sailing speed. The variables that previously regarded the battery and charging decisions are removed from the model, i.e., b_{prckv}, α_i and c_{prckv}.

e_{prcv}^{RT}	Fuel consumption for a round trip for a vessel of type v

5.5.2 Mathematical model

The objective function consists mostly of the same terms as the objective function (5.1) presented in Section 5.3. The fixed cost of investing in a vessel of type v remains, along with the crew cost. The passenger costs remain the same for the conventional model, meaning that all the four last terms in Equation 5.1 are unchanged. Since charging infrastructure is no longer considered, the investment cost related to infrastructure is removed. Charging is naturally not a part of the problem anymore, implying that the variable cost term now sum up the fuel consumption multiplied with the cost of fuel, C^{VC}. The objective for the conventional model becomes:

$$\begin{aligned}\min z = & \sum_{v\in\mathcal{V}} C_v^{FC} y_v + \sum_{p\in\mathcal{P}} \sum_{r\in\mathcal{R}_p} \sum_{c\in\mathcal{C}_r} \sum_{v\in\mathcal{V}} \sum_{f\in\mathcal{F}_c} C^{VC} e_{prcv} f z_{prcf} \\ & + \sum_{p\in\mathcal{P}} \sum_{r\in\mathcal{R}_p} \sum_{c\in\mathcal{C}_r} \sum_{v\in\mathcal{V}} C_v^{CREW} \overline{T}_p g_{prcv} + \sum_{p\in\mathcal{P}} \sum_{r\in\mathcal{R}_p} C_{pr}^{ALT1} \beta_{pr} \\ & + \sum_{p\in\mathcal{P}} \sum_{r\in\mathcal{R}_p} \sum_{c\in\mathcal{C}_r} \sum_{k\in\mathcal{K}_c} \sum_{l\in\mathcal{K}_c} C_{prckl}^{ALT2} u_{prckl} \\ & + C^{PW} \sum_{p\in\mathcal{P}} \sum_{r\in\mathcal{R}_p} \sum_{c\in\mathcal{C}_r} \sum_{f\in\mathcal{F}_c} W_{prcf} z_{prcf} \Big(\sum_{k\in\mathcal{K}_c} \sum_{l\in\mathcal{K}_c} q_{prcklvf} \Big) \\ & + C^{SW} \sum_{p\in\mathcal{P}} \sum_{r\in\mathcal{R}_p} \sum_{c\in\mathcal{C}_r} \sum_{k\in\mathcal{K}_c} \sum_{l\in\mathcal{K}_c} \sum_{f\in\mathcal{F}_c} (t_{prckl} - T_{prckl}^{U}) D_{prcklf} z_{prcf}\end{aligned} \tag{5.72}$$

The model still considers time, meaning that the round trip time, t_{prcvf}^{RT} must be defined. This variable is, however, now defined without the charging time variable c_{prckvf}. Thus, Constraints (5.73) replaces Constraints (5.8). For the same reason Constraints (5.14) and (5.15) are replaced by Constraints (5.74) and (5.75), respectively.

$$t_{prcvf}^{RT} = \sum_{k\in\mathcal{K}_c} \sum_{s\in\mathcal{S}_v} T_{prckvs} x_{prckvfs} + \sum_{k\in\mathcal{K}_c} \sum_{i\in\mathcal{I}_c} w_{prcikvf}, \quad p\in\mathcal{P},\ r\in\mathcal{R}_p,\ c\in\mathcal{C}_r,\ v\in\mathcal{V},\ f\in\mathcal{F}_c \tag{5.73}$$

$$t_{prckl} = \sum_{v\in\mathcal{V}} \sum_{f\in\mathcal{F}_c} \left[\sum_{\hat{k}=k}^{l-1} \sum_{s\in\mathcal{S}_v} T_{prc\hat{k}vs} x_{prc\hat{k}vfs} + \sum_{i\in\mathcal{I}_c} \sum_{\hat{k}=k+1}^{l-1} w_{prci\hat{k}vf} \right], \quad p\in\mathcal{P},\ r\in\mathcal{R}_p,\ c\in\mathcal{C}_r,\ k\in\mathcal{K}_c,\ l\in\mathcal{K}_c \,|\, l>k \tag{5.74}$$

$$\begin{aligned} t_{prckl} = & \sum_{v\in\mathcal{V}} \sum_{f\in\mathcal{F}_c} \Bigg[\sum_{\hat{k}=k}^{|\mathcal{K}_r|} \sum_{s\in\mathcal{S}_v} T_{prc\hat{k}vs} x_{prc\hat{k}vfs} + \sum_{i\in\mathcal{I}_c} \sum_{\tilde{k}}^{|\mathcal{K}_c|} w_{prci\tilde{k}vf} + \\ & \sum_{k'}^{l-1} \Big(\sum_{s\in\mathcal{S}_v} T_{prck'vs} x_{prck'vfs} + \sum_{i\in\mathcal{I}_c} w_{prcik'vf} \Big) \Bigg], \\ & p\in\mathcal{P},\ r\in\mathcal{R}_p,\ c\in\mathcal{C}_r,\ k\in\mathcal{K}_c,\ l\in\mathcal{K}_c \,|\, k>l \end{aligned} \tag{5.75}$$

where,

$$\tilde{k} = \min\{|\ \mathcal{K}_c\ |, k+1\}$$
$$k' = \max\{1, l-1\}$$

All the constraints related to battery level and charging are redundant, meaning that Constraints (5.16) - (5.20) are removed.

We need to include a new constraint to define the fuel consumption per round trip for each time period p, in a route r in each subroute c for a vessel v, e_{prcv}^{RT}. The fuel consumption depends on the vessels' sailing speeds, as for energy consumption in the original model. Hence, we define the fuel consumption by Constraints (5.76). Lastly, we require non-negativity requirement for the fuel consumption (5.77).

$$e^{RT}_{prcv} = \sum_{k \in \mathcal{K}_c} \sum_{f \in \mathcal{F}_c} \sum_{s \in \mathcal{S}_v} E_{prckvs} x_{prckvfs}, \qquad p \in \mathcal{P},\ r \in \mathcal{R}_p,\ c \in \mathcal{C}_r,\ v \in \mathcal{V} \tag{5.76}$$

$$e^{RT}_{prcv} \in \mathbb{R}^{+}. \qquad p \in \mathcal{P},\ r \in \mathcal{R}_p,\ c \in \mathcal{C}_r,\ v \in \mathcal{V} \tag{5.77}$$

Chapter 6

Decomposition Based Heuristic Solution Method

In this chapter, we present the decomposition based heuristic (DB heuristic), a solution method for the ZEVSNDP, mathematically formulated in Chapter 5. Solving the model to optimality is practically impossible for realistic instances, and a solution method based on a heuristic approach is thus necessary to obtain good solutions. The main idea of the DB heuristic is to use the peak period to set the strategic decisions, that is, the infrastructure locations, vessel types and fleet size, and fix the values for these decisions when solving the remaining time periods. The peak period is defined as the time period with the highest total demand. Using the same strategic decisions obtained in the peak period in the remaining periods, is based on the reasoning that if a solution is able to serve the period with the highest demand, it is also able serve the periods with lower throughput satisfactory. The strategic decisions originally make the time periods interdependent. By fixing the values we may solve the other time periods separately with predefined fleet and charging infrastructure layout, thus reducing the solution space and consequently the run time of our model.

The DB heuristic is motivated partly by Aslaksen et al. (2020), and in particular the use of rotations, a concept explained in Section 6.3. Further, the use of a *proxy*, explained in Section 6.4, is motivated by heuristic algorithms in general, which use an evaluation function to quickly evaluate solutions. This chapter presents the DB heuristic by firstly providing a general overview in Section 6.1, before presenting the inherent steps of the solution method in the subsequent sections.

6.1 Overview of the solution method

The overall goal of the DB heuristic is to find good solutions to the Mixed Integer Program (MIP) model presented in Chapter 5, within a limited time frame. In short, we perform several steps that aim to limit the solution space, without discarding promising solutions. As displayed in Figure 6.1, the first step is a heuristic route generation (Section 6.2), with the goal of creating good route structures. These are created by dividing ports in the studied area into groups, and design routes that visit these. The chosen number of groups gives rise to butterfly structures, as introduced in Chapter 3, and a key difference between the routes is their number of butterfly wings. Each of the routes are further used to make *rotations* (Section 6.3). We define a rotation as a composition of the essential integer decisions, as displayed on the next page.

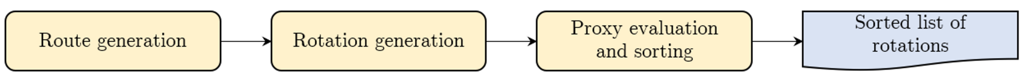

Figure 6.1: First part of the DB heuristic

$$\text{Rotation} = \begin{cases} \beta, & \text{Route structure} \\ z, & \text{Frequency in each subroute} \\ \alpha, & \text{Infrastructure layout} \\ \delta, & \text{Vessel type} \\ y, & \text{Total number of vessels} \\ g, & \text{Number of vessels in each subroute} \end{cases}$$

The key motivation behind using rotations, is the fixing of all integer variables shown above. A rotation may thus serve as input to a Linear Program (LP) based on the MIP presented in Chapter 5, which is significantly simpler to solve than the full MIP-model for the whole ZEVSNDP. Solving an LP for a rotation provides an objective value and the optimal operational decisions, made based on the the strategic and tactical decisions given in the rotation. Even though the LP-models may be solved fast, they still constitute a computational limitation, as the number of rotations could be vast. Hence, we need a method for quickly evaluating the quality of a rotation, without knowing the value of the operational decisions. To do so, we sort the set of rotations, prior to solving them as LPs. An important step here is the use of a *proxy function* to assign a score used in the sorting process (Section 6.4). The proxy function approximates the objective function of the LP-model for a given rotation. Accordingly, the calculation time is shorter, which allows for sorting the whole set of rotations more efficiently than if the LP-model were used directly. Further, the sorted list of rotations is used as input in the next step of the solution method, which is displayed in Figure 6.2.

As shown in Figure 6.2, the LP-version of the MIP-model successively evaluates the most promising rotations in the sorted list (Section 6.5). It is solved for a single period, the peak period, with the highest total demand. Several criteria are checked for each rotation. The first criterion is a fast feasibility check, and rotations are discarded if they are infeasible. Conversely, a feasible rotation is stored for later use, and its true objective function value is compared to the current best. If the objective value is better than the current best, we update the best solution found. There are two stop criteria in the method. Firstly, if a sufficient number of feasible solutions are found without updating the current best solution, the method terminates. Secondly, the method terminates if it runs for a predefined amount of time. After termination, the stored solutions, together with the strategic decisions of the best solution found, are passed to the final step of the solution method.

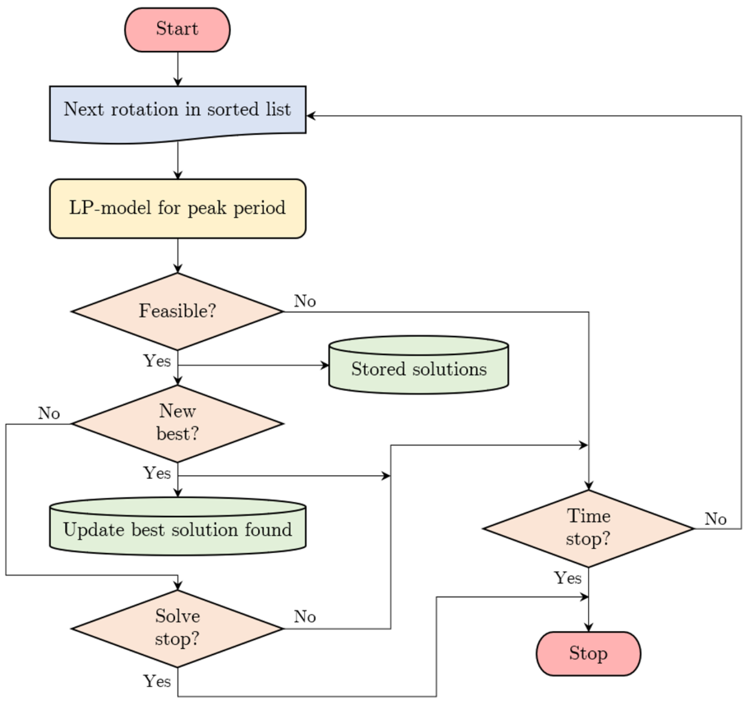

Figure 6.2: Second part of the DB heuristic

The final step in the DB heuristic uses a single period MIP-model to solve each of the remaining time periods to obtain the true objective value for the given strategic decisions (Section 6.6). The model is an alteration of the original MIP-model, presented in Chapter 5. The only difference is the fixation of strategic variables across time periods. These decisions are the infrastructure layout, the vessel type and the total number of vessels. Note that the tactical and operational decisions are allowed to vary between time periods. As the strategic decision variables linking the time periods together are fixed, the single period MIP-model allows for solving the time periods independently.

After the method displayed in Figure 6.2 terminates, the strategic variables from the best solution are sent to the single-period MIP. From the set of stored solutions, a selection of routes forms the basis for the candidate routes in the MIP. Prior to using the routes as input, we perform a processing step. Specifically, we make a copy of each route, and reverse the sailing direction. This is motivated by the assumption that time periods may have an opposite demand pattern. The resulting set of candidate routes is then used as input for the single period MIP-model. This model is solved consecutively for the remaining time periods. The solutions from all periods constitute the solution to the full MIP-model presented in Chapter 5. An illustration of the last part of the DB heuristic is shown in Figure 6.3.

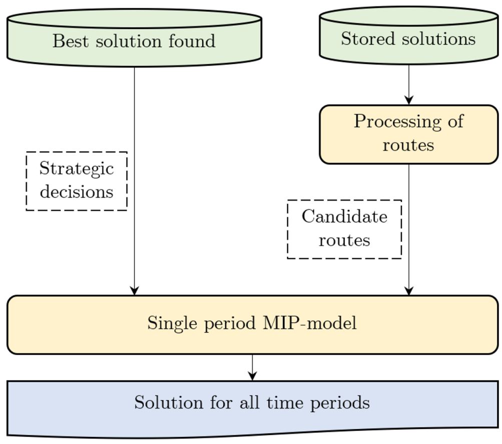

Figure 6.3: Third part of the DB heuristic

6.2 Route Generation

The first step of the DB heuristic is, as mentioned in Section 6.1, a heuristic based route generation. Enumerating all possible combinations of sailing legs in the port network yields a vast amount of routes, of which many are unsuitable and obviously inferior to others. A good process for generating realistic routes is likely to depend on the specific geographical area in consideration. One could imagine this first step of the solution method to be performed in collaboration with operators, policy makers or other stakeholders, as this step touches upon topics which are often unsuited to be determined by mathematical models alone. If a transition from a conventional to a ZE vessel service is the problem at hand, an example of such a topic could be the allowed degree of change from the original service, or if skipping a large number of ports have other negative consequences for the community, not captured by the objective of the ZEVSNDP. As questions regarding route generation are likely to be area dependent, this section presents our approach, somewhat tailored for the service in the Florø area. The specifics of this geographical area are further discussed in Chapter 7.

Following our definition from Chapter 3, a route is a combination of two pieces of information. Firstly, it contains a sequence of port visits, the *main route*. Secondly, every route contains a *subroute* configuration, explaining how the main route is operated in one or more subroutes. The route generation procedure presented in this thesis, constructs the two aforementioned aspects of a route in separate steps. First, a set of main routes are constructed. These routes are only sequences of ports, and contain no specification of subroute structure. In the second step, we use the main routes as input, and subsequently create routes with all possible configurations of subroutes, for each main route. The two separate generation methods are explained in detail in the following subsections.

6.2.1 Generation of main routes

The route generation proposed as a part of the DB heuristic produces butterfly and cyclical routes, with properties as described in Chapter 3. The reasons for developing the route generation around these route structures are plentiful. Firstly, they visit many ports in an effective manner. Secondly, the structures resemble the routes found in the area today, and are thus assumed to be found reasonable for existing passengers and operators. The butterfly routes, in particular, are interesting on account of three characteristics: 1) They result in, on average, shorter travel times to a central hub. This becomes beneficial in the studied demand structure, because many are traveling to and from the port of Florø. 2) Butterfly routes allow for multiple subroute configurations. A different number of vessels and varying frequencies in the different subroutes enable a more customized transport system. 3) Butterfly routes reduce the need for charging infrastructure. By visiting a port several times throughout a route, vessels can utilize the infrastructure (if installed in the hub), more than once through their route, and thus reduce the need for investments in charging capabilities. For simplicity, the cyclical routes generated in this method are referred to as (butterfly) routes with one wing. The main routes are generated in seven steps:

1 Start with all ports considered for the routes.

2 Divide the ports into n natural groups based on adjacent locations. Groups do not need to be of equal size, e.g. may a northern group contain four ports whereas a southern only contain two. All groups of ports should be mutually exclusive, except one port, the central hub, that should appear in all of them.

3 Based on the groups from the previous step, create butterfly routes with $1..n$ wings. For a butterfly route with n wings, each port group becomes a separate wing. However, for butterfly routes with a lower amount of wings, groups must be combined to create the correct wings. The way to combine the groups is a predefined input to the generation method, and should be based on geographical positioning of the different groups. To demonstrate, consider four distinct port groups called *S*, *E*, *W* and *NW*, indicating a southern, eastern, western and north-western port group. When creating a butterfly route with four wings, each group is placed in a separate wing. For a route with three wings, *S* and *E* are placed in their own wings, while *N* and *NW* are combined for the third wing. This procedure continues in the described pattern until a route with one wing, the cyclical route, is generated with all four groups in the same wing. Note that the division into n port groups, yields a set of routes with $1..n$ butterfly wings. This is motivated by the possibility of comparing routes with a different number of butterfly wings directly.

4 Within each wing, we solve a Traveling Salesman Problem (TSP), and organize the ports in order to minimize total travel distance in the wing. The TSP is solved using a Miller-Tucker-Zemlin formulation, as described by Miller et al. (1960).

5 The routes created this far have not considered the different directions a wing may be sailed, i.e, clockwise and counterclockwise. To account for this, the generation method endeavors to create all possible combinations of routes where each wing is sailed either in clockwise or counterclockwise direction.

6 The next step of the route generation is removal of ports. Up to this point, all routes contain all ports, combined in a unique fashion. The process, performed on every route, proceeds as follows: Make a copy of the route, and remove the port with the lowest alternative cost induced by not visiting it. This cost is the product of demand and the alternative cost of transportation per passenger demanding travel to or from the port. Continue this process until a predefined number of ports remain.

7 The resulting set of routes is the finished set, and is ready for separation into subroutes, as described in Subsection 6.2.2.

6.2.2 Configuration of subroutes

The division of routes into subroutes is straightforward. For each generated butterfly route, all possible divisions into subroutes are generated. To illustrate the process, consider a butterfly route consisting of three wings as illustrated in Figure 6.4a. For a butterfly route with three wings there exists five possible configurations of subroutes. One option is to let all wings be the same subroute, as illustrated in Figure 6.4b, denoted [ABC]. Further, there are three ways of separating three wings into two subroutes, [AB][C], [AC][B] and [BC][A], shown in Figure 6.4c-e. The last subroute configuration available, is a configuration where all wings are placed in different subroutes, [A][B][C], as presented in Figure 6.4f.

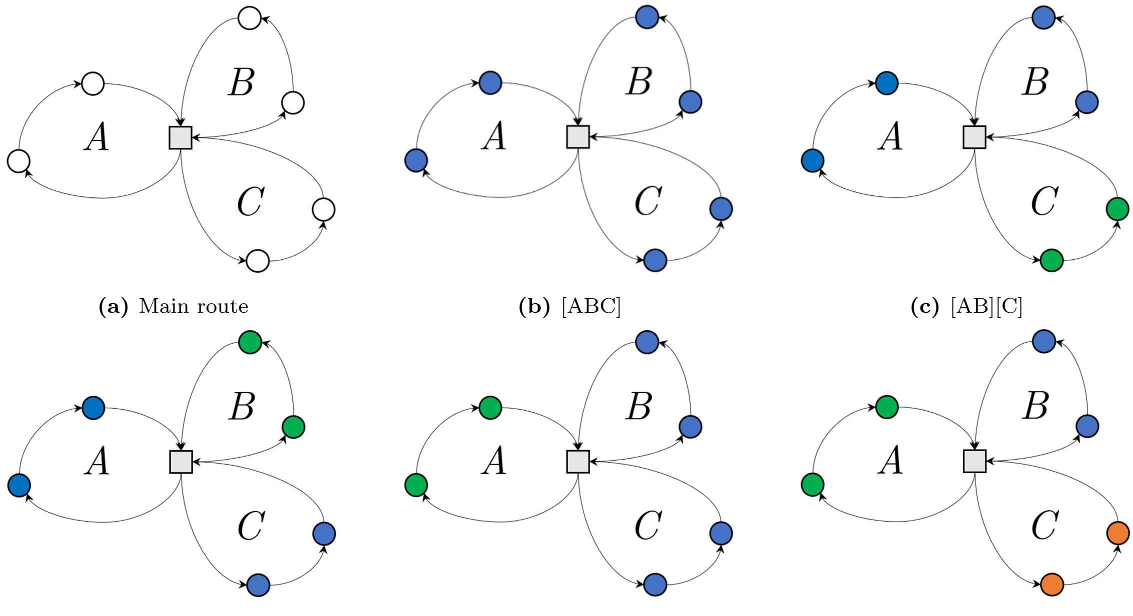

(a) Main route **(b)** [ABC] **(c)** [AB][C]

(d) [AC][B] **(e)** [BC][A] **(f)** [A][B][C]

Figure 6.4: Main butterfly route and its possible subroute configurations

One could argue that a configuration such as [CB][A] is different from [BC][A] due to sailing order, and that such a configuration also should be included in the end result. That is, however, not the case. Any passenger traveling from one subroute to another will exit the vessel in the central hub and wait for their corresponding vessel service. The waiting time in the hub is, as explained in Chapter 5, dependent on the service frequency in the subroute they are entering, thus making the sailing order of wings within a subroute irrelevant. This is a direct result of the modeling choice of letting passengers disembark the vessel in the central hub, if their final destination is not in the next butterfly wing.

The generation of all subroute configurations is performed for every main route. After this process, a route is distinguished from another not only by its sequence of ports, but also by its underlying subroute configuration. The set of routes is now complete, containing a diverse set of cyclical and butterfly routes, with a broad specter of subroute configurations. These routes are subsequently passed on to the next step of the DB heuristic, the generation of rotations.

6.3 Rotation Generation

The use of rotations is common in the modeling of liner shipping problems, and the concept is discussed in Section 4.3 in Chapter 4. In this report, we bring the concept to HSVs, and we use the rotation structure defined in Section 6.1. The rotations used in this problem are first and foremost a combinatorial construct. The set of possible rotations is immense, and we accordingly need to limit the number we create. Measures and procedures to decrease this number at construction are presented for each of the attributes. Note that when we limit the solution space of the rotation attributes, the upper bounds are contingent on practical rules in accordance with the studied area, and not based on theoretical solution possibilities. As already stated, the rotations contain more information than previous literature on the subject, and we describe the procedure of determining appropriate values in the following.

Firstly, feasible and promising routes are constructed as described in Section 6.2. These routes are split into subroutes, and the main route, along with its subroute configuration, serves as input to the rotation generation. Each route is coupled with an associated vessel type, a number of vessels per subroute, a service frequency per subroute. Further, a rotation contains a plan for infrastructure, i.e., information regarding where such is built. Note that the values of these attributes are based on the peak period, in other words, the period with the most demand. We assume that a feasible solution for the peak period remains attainable for periods with lower demand. We now describe the rationale behind the value range for each of these attributes.

When generating rotations, we allow for frequencies up to a predefined upper bound. We try to set this upper bound high enough such that we are most likely to include the optimal frequencies within the generated rotations. The value of the upper bound is set with the assumption that it is sufficiently high when rotations with the upper frequency bound is not chosen in subsequent optimization solutions. The frequencies are set on a subroute basis. This entails that each subroute is an independent system when regarding frequency. To exemplify, a rotation containing three subroutes may consequently be operated with frequencies of 1, 2 and 3, respectively. All frequency combinations of the subroutes are generated in the rotations.

Following the requirements from the model in Chapter 5, we allow the total system to choose only one vessel type, meaning that the same vessel type must be used across all subroutes. Additionally, the maximum frequency described earlier serves as an upper bound to the number of vessels that operate each subroute. Further, the infrastructure layout is designed based on the peak period, and in particular on the observed demand. We sort the ports in decreasing order based on total demand during the peak period. Different layouts of infrastructure solutions are then generated. These may contain charging facilities in a varying number of ports. Specifically, the number of facilities vary from one to a maximum value, given as input to the DB heuristic. The locations are selected from the ports with the highest demand. This selection stems from the fact that a high number of passengers entering and exiting a vessel in a port, decreases the total passenger costs in terms of incurred inconvenience from waiting on board while charging. The central hub of a butterfly route is a mandatory charging location, due to its repeated visits.

A schematic representation of the main procedure behind the rotation generation is shown in Figure 6.5. The sections of the procedure marked in blue are input from the route generation process. The figure shows the generation of rotations for a route with two subroutes, both with potential service frequencies from one to three. The process yields six different solutions for each subroute. Assuming three different vessel types and ten different configurations of infrastructure layout, a total of $3 \cdot 10 \cdot 6 \cdot 6 = 1080$ rotations are constructed. Many of these rotations do however yield infeasible models when used as input to the LP-model, presented in Section 6.5. To avoid using computational power on infeasible rotations, measures are taken to remove these during construction.

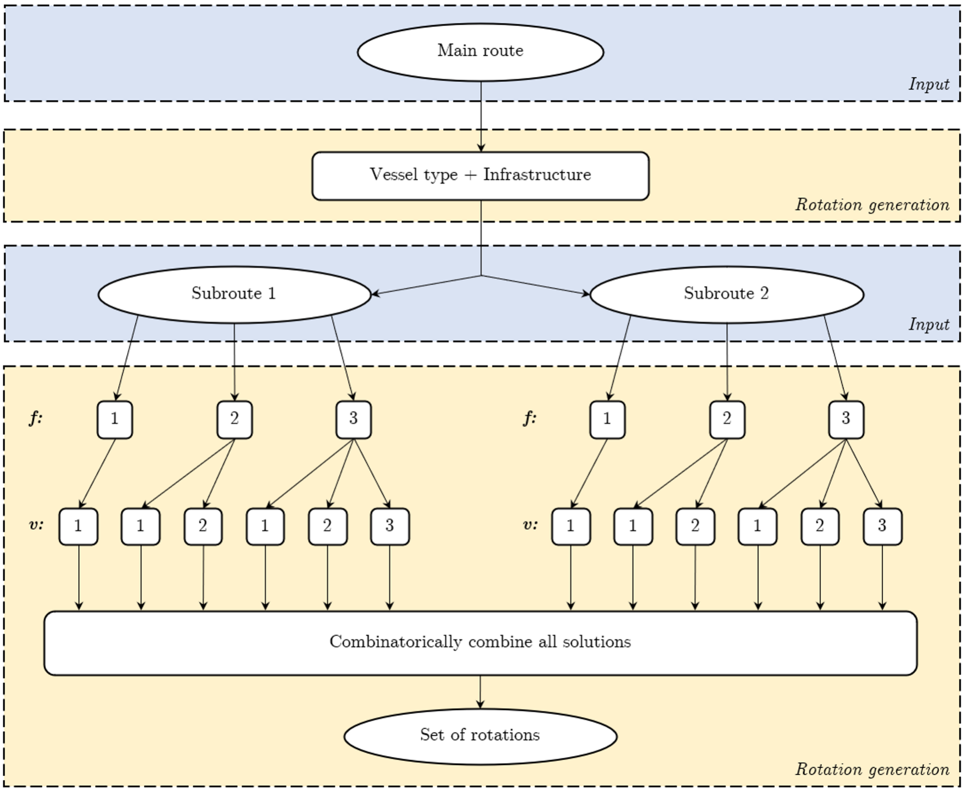

Figure 6.5: Schematic representation of the rotation generation procedure. f and v indicate the service frequency and the number of vessels used in the subroute, respectively.

During the generation procedure a removal of infeasible rotations is performed. One key check is based on the energy requirements of the vessels. If a vessel cannot complete a subroute within the time period at its lowest speed level, when taking into account charging and waiting time, the rotation is discarded. The observant reader would object that one may be able to complete the route faster by increasing the sailing speed. The answer to that is that due to the convex behavior of energy consumption and linear relationship between time and charging, a faster speed leads to a prolonged round trip time. The vessels require a greater than linear amount of energy for increasing speed levels. The charging time, is, however, linearly dependent on time, resulting in a shorter reach for higher speed levels. As a result, the lowest speed serves as an upper bound on the vessel's range. In our rotation generation procedure, a large number of rotations is discarded by this feasibility check.

6.4 Proxy Evaluation and Sorting of Rotations

Every rotation generated in the procedure described above, is ready to be used as input in the LP-model, as described in Section 6.1. However, we introduce an intermediate step in order to compare the rotations more efficiently. The goal of this step is to avoid solving all the rotations in the LP-model. Although a single LP-model is solved very quickly, solving a model for all rotations can be time consuming. We try to mitigate the latter by sorting the rotations and solving them in order. This approach enables us to evaluate the best solutions first. The sorting is based on a proxy function, approximating the value of the proper objective function the rotation would obtain, if solved in the LP-model. Each rotation is assigned a proxy score indicating whether it is promising or not. The rotations are subsequently sorted from best to worst based on this score, enabling the LP-model to solve them exactly from most promising to least promising. In this way, we may assume that when the procedure in Figure 6.2 terminates, even if it is before all rotations are solved, we have solved a sufficient number in order to obtain a good solution overall. This section presents the proxy evaluation method and the assumptions related to it.

Each term in the objective function is approximated separately. Recall from Chapter 5 that the eight terms of the objective function are vessel investments, crew costs, infrastructure investments, energy costs, unmet demand due to unvisited ports, unmet demand due to capacity and frequency, waiting time in port and the cost of excess sailing time. The value of the eight terms are estimated as follows.

Vessel and infrastructure investments

The first two terms are estimated in a straightforward manner. As their values rely solely on strategic decisions, that is, vessel type, vessel amount and number of ports containing infrastructure, these may be calculated exactly already in the proxy evaluation.

Cost of energy

An input parameter is necessary for the next term, the cost of energy. As the rotation contains no information regarding sailing speed (which is decided in the LP-model), an assumed average speed is introduced. Based on this assumed speed, the total sailing distance of the route and associated frequencies, an energy consumption may be calculated. Accordingly, a cost related to the energy usage of the vessel service is approximated.

Crew costs

The remaining operator costs, crew costs, are directly linked to the capacity of the vessel type. We assume, similarly to the mathematical formulation in Section 5.3, that there are different staffing requirements associated with the different vessels, and use these values directly. Consequently, the crew costs are also calculated exactly in the proxy evaluation. This term concludes the estimation of the operator costs.

Unmet demand

The passenger alternative cost caused by not visiting a port, is calculated exactly. An exact calculation is achievable due to the fact that all port visits are available in the rotation, which enables a summation of the passengers' alternative travel costs caused by unvisited ports. The next term, the alternative travel cost caused by insufficient vessel capacity, is estimated by using an assumed level of service. This level is a function of the rotation's service frequencies and the passenger capacity of the vessel type, because these two variables together stipulate the service's ability to serve demand. We calculate a constructed level of service per subroute, indicating the proportion of total demand in the visited ports being served. The function defining the service level in our approximation is presented below, where f_c is the frequency in subroute c, ΣD the sum of the demand and Q, the vessel capacity. We observe that the service level is one if all demand is served, whereas it deteriorates once the vessels cannot serve all passengers.

$$\text{Service Level} = \begin{cases} 1, & \text{if } f_c \cdot Q > \Sigma D \\ \dfrac{\Sigma D}{f_c \cdot Q}, & \text{otherwise} \end{cases}$$

Passenger waiting time

The next passenger inconvenience cost term in the proxy is passenger waiting time. This is the sum of the costs incurred by passengers waiting for a vessel to pick them up in their origin port, or in the hub if they are in transit. The cost is approximated by multiplying the passengers going from a specific destination to a specific port, with the passenger value of time, and an assumed percentage of the served demand. In order to efficiently calculate the value of this term, we do not use the actual values for the demand. We rather assume that a given percentage of demand is fulfilled in general, and hence use this number to estimate the cost. Finally, we divide the aforementioned terms with two times the service frequency, as described in Section 5.1 in Chapter 5.

Cost of excess sailing time

The last term we add to the the proxy expression, is the costs incurred by the inconvenience experienced by the passenger due to the time spent aboard. These costs are estimated by multiplying all the passenger's excess time aboard the vessels with "passengers value of time", a constant encompassing the monetary value of one hour of excess travel time. We calculate the abundant travel time by computing the difference between a proxy for actual travel times and the fastest possible travel time, serving as a benchmark. The total travel time from one port to another, is the sum of sailing time, charging time and waiting time along the route. We proceed by first calculating a proxy for the actual travel time, before a benchmark travel time is calculated exactly.

To approximate the total travel time, we first calculate the sailing distance of each sailing leg within the subroutes. The distances are divided by an assumed average speed, and the result serves as a proxy sailing time along each leg. To estimate the value(s) for the charging time(s) along the subroute, the total energy consumption when sailing at the average speed, is used. Further, we obtain the charging power from the port with the highest installed charging capacity. This power level is used to approximate the total charging time throughout the subroute. To limit computational complexity, the calculated charging time is distributed equally on all ports with installed charging infrastructure in the rotation. For an approximation of the waiting time along the subroute, the minimum required waiting in each visited port is added. Finally, the remaining of the time period after subtracting the sailing, waiting and charging times is added as additional waiting time in the central hub. A summation across all subroutes in a route, for all the aforementioned terms of the travel time, yields the final proxy for actual travel time.

After the proxy travel time is computed, we calculate the benchmark travel time, i.e., the fastest possible travel time within each port pair. This, together with the minimum requirement for waiting time in each port, is used to calculate the benchmark. If a passenger travels aboard a vessel that completes a round trip at benchmark time, no inconvenience cost is incurred. Charging time is omitted for the benchmark. The final proxy score of excess sailing time becomes the sum of the difference between the proxy travel time and the fastest possible travel time for each port pair, multiplied with the number of passengers and their cost of sailing time.

6.5 LP-model for Peak Period

After the rotations are created, evaluated and sorted, following the procedures in Section 6.3 and Section 6.4, they are individually used as input to an LP-model (Linear Programming). This model is a rewritten version of the original mathematical formulation presented in Chapter 5. The main difference between the two versions is the fixation of all binary and integer variables. This procedure reduces the solution time of the model drastically, thus allowing for solving many instances of the model consecutively. The value of the original binary and integer variables, representing the strategic and tactical decisions of the ZEVSNDP, are all part of the rotation used as input to the model. The following section provides an overview of the main changes from the original model proposed in Chapter 5, to the LP-model. The complete LP-model is found in Appendix C.

Starting with the objective function, (6.1), some immediate changes become apparent. Firstly, the costs related to infrastructure investments, vessel investments and crew are all fixed terms. These costs are calculated directly from the parameters, based on the strategic and tactical decisions stored in the rotation. This is also the case for the fifth term, the alternative travel cost incurred by not visiting ports. The remaining terms are also simplified, due to the fixed strategic and tactical decisions. The variables and parameters do now only depend on the subroute and sailing leg, as the problem is solved for a fixed period, route, vessel type, fleet size and service frequency.

$$\begin{aligned}\min z = {} & C^{FC} + C^{INF} + C^{CREW} \\ & + \sum_{c \in \mathcal{C}} \sum_{k \in \mathcal{K}_c} C^{VC}_{ck} \overline{P}_{ck} F_c c_{ck} + C^{ALT1} + \sum_{c \in \mathcal{C}} \sum_{k \in \mathcal{K}_c} \sum_{l \in \mathcal{K}_c} C^{ALT2}_{ckl} u_{ckl} \\ & + C^{PW} \sum_{c \in \mathcal{C}} W_c \Big(\sum_{k \in \mathcal{K}_c} \sum_{l \in \mathcal{K}_c} q_{ckl} \Big) + C^{SW} \sum_{c \in \mathcal{C}} \sum_{k \in \mathcal{K}_c} \sum_{l \in \mathcal{K}_c} (t_{ckl} - T^{U}_{ckl}) D_{ckl}\end{aligned} \tag{6.1}$$

All strategic and tactical constraints become redundant in the LP-model, as these decisions are already made in the rotation generation process. The other constraints remain, but are rewritten to take into account that decisions are only made within subroutes. In the objective function, $\overline{P}_{ck}$ is introduced for storing the infrastructure investments from the rotation. This parameter is 0 if no infrastructure is installed in the port at beginning of leg k, and takes the value of the installed charging power, if an investment was made. This is possible, as the relation between port and sailing leg is now one to one, as the model only considers a single route, as opposed to the full model presented in Section 5.3.

As mentioned in Section 6.1, the rotations are passed to the LP-model and solved until a stop criterion is met. If a rotation yields a better objective value in the LP-model than any previous rotations, its solution is saved as the current best. In addition, all the feasible rotations are stored for later use, sorted after their objective value in the LP-model. The first stop criterion is the number of feasible solutions found since the last time a new best solution was found. If a total of m feasible solutions are found, without updating the best solution, the LP-model terminates. The other stop criterion is solution time. If the repeated solving of LP-model instances lasts for t seconds without reaching the first criterion, the solving of rotations terminates. These two input parameters, m and t, are important for the quality of the final solution, and the determination of appropriate parameter values is further discussed in Chapter 8. Two types of output is obtained by solving the LP-model successively. Firstly, the value of all strategic decision variables are gathered from the best solution found. This includes vessel type, total fleet size and infrastructure locations. Secondly, a set of rotations containing promising routes from feasible LP-model runs are saved. The use of these outputs is further explained in the final step of the DB heuristic below.

6.6 Single Period MIP-model

The final step of this proposed solution method is a single period Mixed Integer Programming model. As explained above, all strategic decisions are fixed based on the results from the successive solving of the LP-model. These decisions are used as input for the model, along with the set of promising routes. Because the original formulation of the problem, presented in Chapter 5 exhibits a structure where only a limited number of constraints and variables (related to the strategic decisions) connect the time periods, we exploit the reduced complexity obtained by fixing these variables. The MIP-model consequently becomes a collection of independent subsystems, which may be solved for each time period separately. The complete rewritten model formulation is presented in Section C.2 in Appendix C. This model corresponds to that in Chapter 5, but with fixed strategic decisions.

Apart from the strategic decisions, all tactical and operational decisions are made in the single period MIP-model. In addition to the strategic decisions, the model is given a set of promising routes from the LP-model solutions. This set is large, and an integral part of obtaining good solutions from the single period MIP-model is thus the selection of good, unique and diverse routes from this set. This is accomplished by a route processing that returns a set of r candidate routes. The processing is performed as follows. Every route is split into its respective subroutes, while duplicates are removed. From these routes, new routes that cover all directional combinations of the subroutes are constructed. This means that each subroute is included both with its original and opposite sailing direction. This is similar to the approach used in the initial main route generation, described in Section 6.2. This approach accounts for the chance of demand mainly flowing in the opposite direction at other times of the day in the routes passed on to the single period MIP-model. One could imagine that a beneficial route for serving demand in the morning, would be more suitable in the afternoon, if one or more subroutes were reversed. The resulting set of r unique routes is as input for the single period MIP-model.

After solving the single period MIP-model for all remaining time periods, that is, all except the peak period, a complete solution for the entire ZEVSNDP is obtained. The strategic decisions, as well as the tactical and operational decisions for the peak period are derived from the successive solution of rotations in the LP-model, while the remaining decisions are obtained from solving the single period MIP-model for the other time periods. An integral part of the solution method is the transferal of promising routes from the peak period solved in the LP-model to the other periods solved in the MIP-model. This process relies on several parameters, which values are further discussed in Chapter 8. This concludes the chapter on the procedures in the proposed DB heuristic.

Chapter 7

Data Collection and Test Instances

This chapter presents the process and results of the data collection and the generation of test instances. The data collection is based on Havre et al. (2021), with updates to values and parameters that have changed, or are used differently. A key difference is that we in this thesis study a substantially larger geographical area than Havre et al. (2021), which has made the data collection more extensive. The relevant data collection, and its results, are found in Section 7.1. Further, seven test instances are presented in Section 7.2. We split the instances into performance-testing instances and instances used to provide managerial insights. The former are used to tune important solution method parameters, whereas the latter are used for insights, discussed in subsequent chapters.

7.1 Input Data

In this section, we describe the process of finding data and making it suitable as input to the model described in Chapter 5. Specifically, Subsection 7.1.1 describes the data from the Florø Basin, the geographical area in consideration. Further, Subsection 7.1.3 explains the data regarding the Zero-Emission (ZE) vessels, whereas Subsection 7.1.4 describes the data used for the conventional vessels. Finally, the cost parameters are reported in Subsection 7.1.5.

7.1.1 Geographical area, ports and distances

The Florø Basin consists of 20 ports, as displayed in Figure 7.1. The figure shows the ports divided into three groups, *North*, *West* and *South*, based on how the area is served today. Note that the port of Florø is excluded from the groups, as this is the central hub with recurring visits from all three port groups. This division into port groups based on geographical location, is an important motivation for both modeling choices and our proposed solution method.

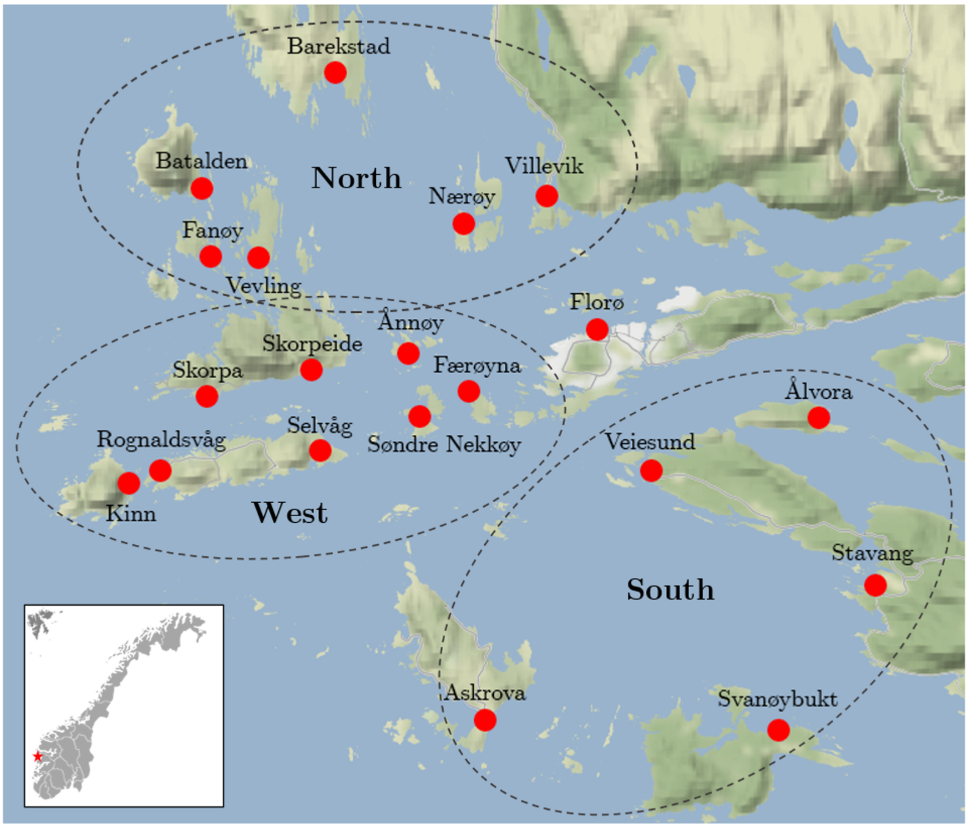

Figure 7.1: Map of the ports in the Florø basin, and the current division into port groups

There are different schedules planned for the port groups. The schedules and routes vary during the day and there are typically distinct morning and afternoon routes. Figure 7.2a and Figure 7.2b show examples of this. In Figure 7.2b, the North and West areas are served by two routes, while the same areas are served by one route in Figure 7.2b. Furthermore, note that the sailing direction differs between the two examples. The vessels that operate the service also vary in both size and specifications, further discussed in Subsection 7.1.3 and Subsection 7.1.4.

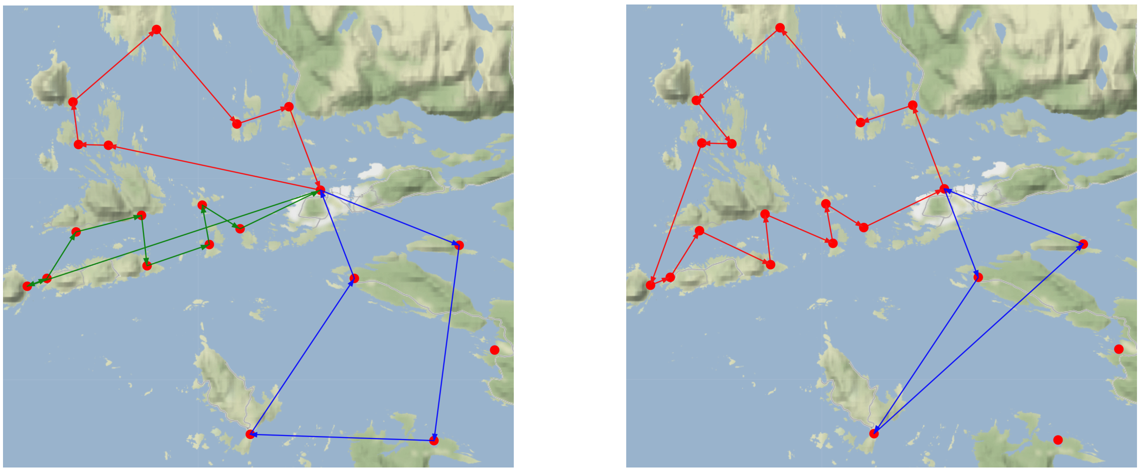

(a) Example 1 **(b)** Example 2

Figure 7.2: Examples of how the area currently is served with different route structures throughout the day

Information about the ports in the area was obtained from Skyss AS, with corresponding geospatial locations. The lengths of the legs between the ports were calculated using Google Maps, tracing the actual sailing paths. The resulting distances are not used as explicit parameters in the model, but to calculate other key parameters, e.g., sailing time and energy consumption, and may be found in Table D.2 in Appendix D.

All ports are further assigned an available charging power, P, of 3 000 kW. If this value was differentiated, reflecting the actual charging power in each port, the resulting infrastructure setup in the solution would be more precise. However, such data was not easily available, justifying the choice of an equal value for all ports. We next assigned the T^W parameter a value, which represents the minimum waiting time for on and off-boarding of passengers. One could argue that this parameter should be a function of the traffic in the port in consideration, for example making busy ports require a longer waiting time for on and off-boarding. Our model does not encapsulate this effect, and the minimum waiting time is thus assigned a value of three minutes, or 0.05 hours, in all ports. This number is based on the Norwegian mean time per harbor stop, as found in Sundvor et al. (2021).

7.1.2 Demand data, time periods and frequency levels

The demand data used to create test instances for the ZEVSNDP is based on ticket sales obtained from the operator, Skyss AS. The original data set contained ticket sales for the entire year of 2019. Based on pre-pandemic travel habits, the data set is assumed to provide a reasonable estimate of the demand for transportation in the area. We further split the data set, and focus on the ticket sale for three months, February, March, and April. These months were chosen in order to make the periods comparable to each other, as these are months with few holidays and abnormalities to the schedules. We further extracted weekends from the demand data, because the weekend routes and schedules diverge greatly from the remaining days. We then split each day into four time periods, each with a duration of four hours. These time periods represent the real world demand from 5:00 AM - 9:00 AM, 9:00 AM - 1:00 PM, 1:00 PM - 5:00 PM and 5:00 PM - 9:00 PM. This split was performed to allow for a more granular solution and, consequently, more applicable results for decision support.

We do not present the final demand matrix, as it is too extensive. A tabular overview of the peak period (1:00 PM - 5:00 PM) may however be found in Table D.3 in Appendix D. An important step after processing the demand data, is making it frequency-dependent. As explained in Chapter 3, we assume that the demand is endogenous to the service. This means that a better-perceived service from a passenger's point of view will raise the prospects of this passenger choosing this mode of transport. In order to account for this aspect, we scale the total demand linearly with increasing frequencies. The observed demand, based on the data set acquired from Skyss, is denoted $D_{observed}$, and corresponds to an observed service frequency, denoted $\hat{f}$. Using a scaling coefficient, K, the frequency-dependent demand for a given service frequency, $f \in \mathcal{F}$, is calculated following the equation below.

$$D_f = K^{(f-\hat{f})} \cdot D_{observed}$$

Note that this procedure indicates $D_f = D_{observed}$ for $f = \hat{f}$. A frequency higher than the observed frequency yields a higher demand than observed, while the opposite effect is seen for lower frequencies. For the Florø area, and thus all the test instances presented in Section 7.2, the available service frequencies are $\mathcal{F} = \{1,\ 2,\ 3\}$. The observed demand, upon which the observed demand data is based, is 1. With a scaling coefficient, K, equal to 1.2, this yields a frequency-dependent demand parameters of ($D_{observed}$), ($1.2 \cdot D_{observed}$) and ($1.44 \cdot D_{observed}$) for frequency levels of 1, 2 and 3, respectively. Note that the equation for extrapolating an observed demand, based on one specific service frequency, to other frequencies, may easily be changed. An option could be to include a function incorporating the frequency elasticity of demand based on empirical studies. An example of the use of such an elasticity may be found in Totten (2016).

7.1.3 Zero-Emission vessel type data

We received data on different vessel types from Paradis Nautica AS, a maritime consulting agency in Bergen, Norway. They provided a model that computes several vital battery-electric vessel parameters under varying circumstances. As input, the model takes battery capacity in kWh, the dead weight percentage, i.e., the proportion of the maximum dead weight on board, the weight of the battery per kWh, and finally, the battery price in NOK/kWh. Additionally, the vessel types have features such as length, passenger capacity, weight, total displacement and investment cost. The model includes seven different combinations of length and passenger capacities, as displayed in Table 7.1. These seven combinations are coupled with a set of candidate battery capacities to construct realistic vessel types. To remain within the scope of realistic vessel types, Paradis Nautica advises an upper limit of 3200 kWh and 5600 kWh for the battery levels of the 30 and 40-meter vessel types, respectively. These limits are based on their perception of the technological boundaries of today, and may be subject to changes in the future.

	1	**2**	**3**	**4**	**5**	**6**	**7**
Length (m)	30	30	30	30	40	40	40
PAX	50	100	150	200	200	250	300

Table 7.1: Combinations of lengths and passenger capacities (PAX) used for generating vessel types

We generate 21 different vessel types using this approach combined with three adjustments of the battery capacity. The 30-meter vessel types are generated with capacities of 1000, 2000 and 3000 kWh, while the 40-meter vessel types are generated with battery capacities of 2000, 3500 and 5000 kWh. All the ZE vessel types are shown in Table 7.2. Note the conventions for naming the vessel types. The names of the candidate vessels consist of a number and a letter. The numbers are decided by the length and passenger capacity, and a low number corresponds to small dimensions, whereas a higher number corresponds to larger dimensions. The letters divide the vessels with the same numbers, with respect to battery size. S, M and L correspond to Small, Medium and Large batteries, respectively. To ensure that the battery is used in a way that preserves its lifetime, an upper and lower limit is set for the operational charge and discharge allowed. All vessel types are assigned the same limits in percentage of their full battery capacity, that is, a lower limit of 40% and an upper limit of 90%. To illustrate, a vessel with a total battery capacity of 1000 kWh would have a lower charge limit of 400 kWh and an upper limit of 900 kWh.

A set of candidate speed levels is associated with each of the 21 vessel types. In our test instances, all 21 vessel types are associated with the same five speed levels, $\mathcal{S}$, seen below in knots.

$$\mathcal{S} = \{10,\ 15,\ 20,\ 25,\ 30\}$$

Every vessel is further associated with a power demand per speed level. Although the vessels have the same set of speed levels, the power demand will vary between them as the size and weight, and thereby the displacement, of the vessels vary significantly with passenger and battery capacities. Power demands for maintaining different speed levels are displayed below in Figure 7.3 and Figure 7.4 for a 30 meter vessel, with a passenger capacity of 50 in Figure 7.3 and a battery capacity of 1000 kWh in Figure 7.4.

VT	Length (m)	PAX	Cost (mill.)	Battery (kWh)	Speed levels (nm)	Power demand (kW)
1S	30	50	92.9	1000	(10, 15, 20, 25, 30)	(115, 405, 703, 1079, 1637)
1M	30	50	99.8	2000	(10, 15, 20, 25, 30)	(116, 447, 766, 1159, 1737)
1L	30	50	106.7	3000	(10, 15, 20, 25, 30)	(121, 490, 833, 1239, 1841)
2S	30	100	93.9	1000	(10, 15, 20, 25, 30)	(119, 472, 805, 1205, 1798)
2M	30	100	100.8	2000	(10, 15, 20, 25, 30)	(125, 517, 873, 1287, 1904)
2L	30	100	107.7	3000	(10, 15, 20, 25, 30)	(133, 564, 946, 1369, 2013)
3S	30	150	94.9	1000	(10, 15, 20, 25, 30)	(129, 544, 915, 1335, 1967)
3M	30	150	101.8	2000	(10, 15, 20, 25, 30)	(140, 593, 990, 1418, 2078)
3L	30	150	108.7	3000	(10, 15, 20, 25, 30)	(153, 644, 1068, 1503, 2193)
4S	30	200	95.9	1000	(10, 15, 20, 25, 30)	(147, 622, 1035, 1467, 2145)
4M	30	200	102.8	2000	(10, 15, 20, 25, 30)	(162, 674, 1115, 1553, 2261)
4L	30	200	109.7	3000	(10, 15, 20, 25, 30)	(179, 729, 1199, 1640, 2381)
5S	40	200	117.8	2000	(10, 15, 20, 25, 30)	(104, 347, 954, 1416, 2225)
5M	40	200	128.2	3500	(10, 15, 20, 25, 30)	(114, 374, 1019, 1513, 2350)
5L	40	200	138.5	5000	(10, 15, 20, 25, 30)	(124, 404, 1087, 1613, 2477)
6S	40	250	118.8	2000	(10, 15, 20, 25, 30)	(114, 376, 1023, 1518, 2357)
6M	40	250	129.2	3500	(10, 15, 20, 25, 30)	(124, 406, 1091, 1618, 2484)
6L	40	250	139.5	5000	(10, 15, 20, 25, 30)	(135, 438, 1163, 1721, 2614)
7S	40	300	119.8	2000	(10, 15, 20, 25, 30)	(125, 408, 1095, 1624, 2491)
7M	40	300	130.2	3500	(10, 15, 20, 25, 30)	(135, 440, 1167, 1727, 2621)
7L	40	300	140.5	5000	(10, 15, 20, 25, 30)	(147, 474, 1241, 1833, 2752)

Table 7.2: Zero-Emission vessel types (VT) used for the test instances

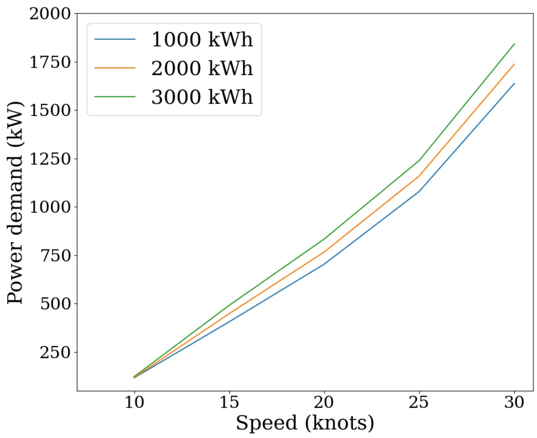

Figure 7.3: Power demand for different battery sizes (kWh)

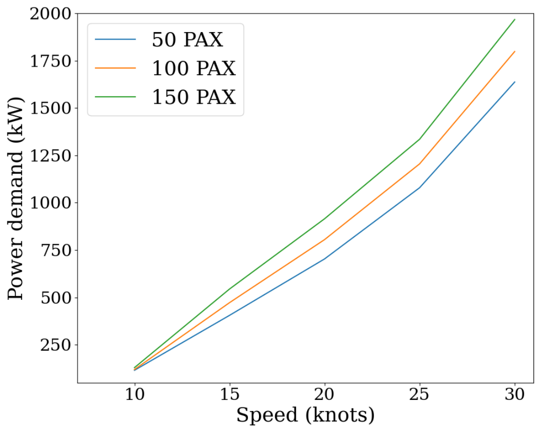

Figure 7.4: Power demand for different passenger capacities (PAX)

Based on the data presented above, two functions are implemented to calculate the T_{prckvs} and E_{prckvs} parameters. These represent, as explained in Section 5.3, in Chapter 5, the sailing time and the energy consumption in period p, on route r in cluster c, on leg k with a vessel of type v sailing at a speed level s. These functions combine the leg distance given as input above with the power demand per time unit, and calculate the sailing times and energy usages. The values of the T_{prckvs} parameter, are further used to calculate the values of the T^U_{prckl} parameter, used as a benchmark for the transit time between the ports at the beginning of leg k and the beginning of leg l (in subroute c in route r in time period p).

7.1.4 Conventional vessel type data

A set of conventional vessel types is defined to support the comparison between the cost of ZE vessels and that of conventional vessels. Here, we made the simplifying assumption that conventional vessels share the properties of the ZE vessels. This reduces the amount of conventional vessels to seven, as there is no differentiation by battery capacity. We assume that each conventional vessel requires the same amount of power as the corresponding ZE vessel with the same dimensions and medium battery size. Further, we assume that the costs also correspond to the costs of the ZE vessel with same dimensions and medium battery. The conventional vessel types are shown in Table 7.3. Note the connection to Table 7.2. For example, a conventional vessel of type 4C corresponds to the ZE alternative 4M.

VT	Length (m)	PAX	Cost (mill.)	Speed levels (knots)	Power demand (kW)
1C	30	50	99.8	(10, 15, 20, 25, 30)	(116, 447, 766, 1159, 1737)
2C	30	100	100.8	(10, 15, 20, 25, 30)	(125, 517, 873, 1287, 1904)
3C	30	150	101.8	(10, 15, 20, 25, 30)	(140, 593, 990, 1418, 2078)
4C	30	200	102.8	(10, 15, 20, 25, 30)	(162, 674, 1115, 1553, 2261)
5C	40	200	128.2	(10, 15, 20, 25, 30)	(114, 374, 1019, 1513, 2350)
6C	40	250	129.2	(10, 15, 20, 25, 30)	(124, 406, 1091, 1618, 2484)
7C	40	300	130.2	(10, 15, 20, 25, 30)	(135, 440, 1167, 1727, 2621)

Table 7.3: Conventional vessel types (VT) used for the test instances

7.1.5 Cost parameters

The model takes several cost parameters as input. The first cost in the objective function is the fixed cost of acquiring a vessel of type v, C_v^{FC}. We assume that this cost only differs among the vessel types with respect to the investment cost. We thus simplify the parameter such that only the investment cost is included, scaled to the length of one day. We base the capital costs on Straume and Bertelsen (2015), who propose the following formula:

$$\text{Cost of capital} = r \cdot \left(\frac{K}{1 - e^{-rn}}\right)$$

r is the yearly interest rate, and K is the investment cost of acquiring a new HSV. n is the assumed lifetime of an HSV. As an example, we calculate the fixed costs below, assuming a yearly interest rate of 5%, a lifetime of 20 years and an investment cost of 100 mNOK. Further, the costs are scaled to one day.

$$C^{FC} = 5\% \cdot \left(\frac{100 \text{ mNOK}}{1 - e^{-5\% \cdot 20}} \cdot \frac{1}{365}\right) = 21\,671 \text{ NOK}$$

The cost of installing charging infrastructure in a port i, C_i^{INF}, is calculated following the same procedure as above. In the test instances, all ports are treated as equal and are assigned an infrastructure investment cost of 12 mNOK. The cost level is based on data obtained from Statkraft AS. We assume the same yearly rate and usage per day as for the vessels. The third cost parameter, C_{pi}^{VC}, is energy cost per kWh of charged energy in a port i, in period p. This parameter value is also based on the data obtained from Statkraft, and is found in Table 7.4. The cost is for simplicity assumed to be equal along the route.

OPEX energy	0.3 NOK/kWh
OPEX grid	2.5 NOK/kWh
OPEX other	0.3 NOK/kWh
C_{pi}^{VC}	3.1 NOK/kWh

Table 7.4: A breakdown of the charging cost

The value assigned to C_{pi}^{VC} in Table 7.4 only applies to the ZE vessel types. The energy cost per outputted kWh is estimated to be 3.0 NOK for the conventional vessel set. Here we assume an MGO (marine gas oil) price of 1 100 USD/ton, a conversion rate of 9.74 NOK/USD, an MGO heating value of 42.7 kJ/g and a thermodynamic efficiency of 30%. The heating value and efficiency are inspired by the report from Dr. Ing. Yves Wild Ingenieurbüro GmbH (2005), whereas the MGO price is based on the price level in Bergen per 22.05.2022 (Bergen Bunkers AS, 2022).

One of the most challenging cost parameters to assign a value to is the alternative cost of transportation between a pair of ports. This parameter should be paid close attention to, as it is important in the prioritization of passengers based on their alternative options. One could immerse into great detail on the topic, but this report assumes that this cost takes one of two values. We consider a pair of ports and assign a high value to the parameter if the high-speed passenger vessel service is the only realistic public transportation option, and a lower one if alternatives exist, such as a bus or car ferry connection. These values are 100 000 NOK and 500 NOK per passenger, respectively.

The next cost parameter is the value of passenger time. We distinguish between passenger time spent waiting in port, and waiting time spent on board. Firstly, we consider the value of time spent on board. For numerical values, we rely on the data estimated by Flügel et al. (2020) for high-speed vessels. The value for trips less than 70 km is 112 NOK/hour, and we thereby assign this value to the parameter C^{SW}. Secondly, for the value of time spent waiting for a departure, Wardman et al. (2016) find that the waiting cost in a system with high frequency should be 1.5 times higher than the cost of time spent on board. In our test instances, however, the frequency is set substantially lower than in Wardman et al. (2016). Own observations have shown that in systems with lower frequencies, the travelers plan ahead and arrive with a distribution skewed towards the departure time. We thus assume that the cost of waiting in port is reduced compared to the cost of time spent aboard. Specifically, we assume that this cost is 0.5 times the cost of time spent aboard. C^{PW} thus becomes 56 NOK/hour.

The final cost parameters are the crew costs. These are calculated based on Tveter et al. (2020), for each vessel type. Their study finds the cost of an eight-hour shift to be 4 098 NOK and 2 727 NOK, for senior and junior crew, respectively. An estimation of the number of crew members for each vessel type, was performed based on the number of crew members on conventional vessels, currently in operation. Across a set of current vessels, passenger capacity was found to be the best explanatory variable for crew size. An overview of the crew sizes for the passenger capacities apparent in the set of vessel types is provided in Table 7.5. In addition, the table presents the hourly crew cost for vessel types of varying passenger capacity.

Passenger capacity	50	100	150	200	250	300
Senior crew (#)	1	1	2	2	3	3
Junior crew (#)	2	2	1	2	1	2
Cost per hour (NOK)	1 194	1 194	1 365	1 706	1 878	2 219

Table 7.5: Number of senior and junior crew for different passenger capacities

7.2 Test Instances

In this section, we present the test instances that are applied in the computational study in Chapter 8. We separate the test instances into two parts. In the first category, presented in Subsection 7.2.1, we introduce the six *managerial test instances* used for managerial decision support later on. Furthermore, we present four additional test instances, the *performance test instances*, used for demonstrating the parameter value tuning in the DB heuristic.

7.2.1 Managerial test instances

To ensure a high-quality analysis of our results, we generate six different test instances by varying the included ports in the problem, and the energy carrier of the vessels. This is done by creating three test instances coupled with Zero-Emission and conventional vessels, respectively. The first test instance, considers all 20 ports in the Florø Basin. The second test instance only includes a set of ports in close proximity to the central hub, Florø. The third test instance only considers ports with a relatively high demand for transportation to and from Florø. As previously stated, the three test instances are created for both ZE and conventional vessels, yielding a total of six managerial instances. This enables a comparison between Zero-Emission and conventional operations for a broad range of scenarios. In addition to the instance including all ports, we choose to focus on test instances where distances and demand vary because we are interested in how these parameters influence abatement costs and route choices. The proposed test instances may contribute to a better understanding of the effect from these input parameters in general.

Main test instance: All Ports (AP)

In the first test instance, the selection of ports is made as similar to the existing service as possible. In other words, we include all ports to imitate the real-world service in the Florø Basin. This test instance acts as the main instance in subsequent analyses (Chapter 8), due to its comparability to the existing vessel service. A map of the area, with indications of port locations, is found in Figure 7.5. As explained in Subsection 7.1.2, the available service frequencies in the test case are $\{1, 2, 3\}$, not straying far from the current service, which operates at frequencies of 1 and 2 in the different time periods. We now introduce the naming conventions used for the subsequent test instances. `AP` refers to the All Ports test instance in general, whereas `AP-ZE` and `AP-C` distinguishes between the Zero-Emission and Conventional versions, respectively.

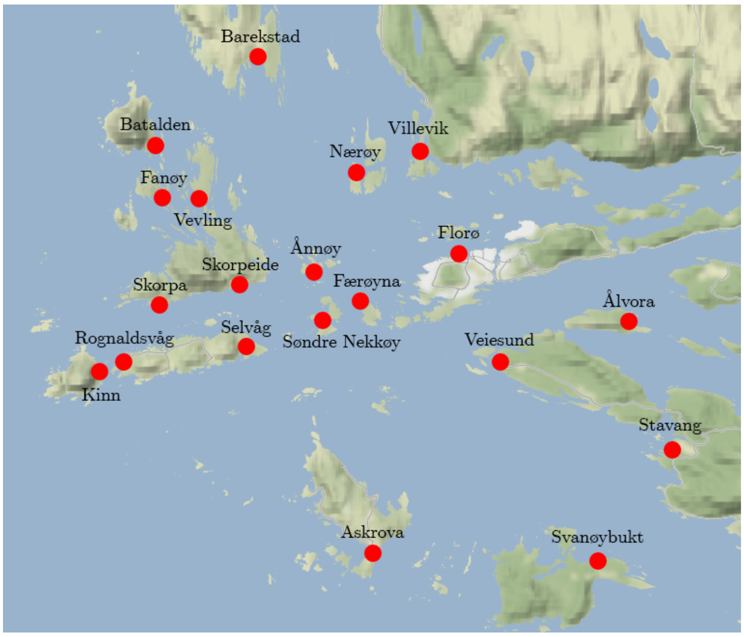

Figure 7.5: Ports considered in the `AP` test instance

As mentioned in Chapter 6, an important step of the route generation procedure in the DB heuristic, is the separation of ports into port groups. The number of port groups is linked to the number of butterfly wings, and n port groups allow for up to n butterfly wings in the generated routes. The specific grouping of ports used in the Florø case is shown in Figure 7.6. Recall from Chapter 6 that the set of candidate routes includes routes with $1..n$ butterfly wings. This allows for a direct comparison between routes with a varying number of wings. For the `AP` test instance, we want the possibility of comparing routes with up to four butterfly wings, necessitating a split into four port groups, that is $n = 4$. The groups are named N, NW, W and S, representing their cardinal direction from Florø, the central hub. An overview of the specific ports included in each group, is presented in Table 7.6.

Group	Hub	Additional ports
N	Florø	Barekstad, Nærøy, Villevik
NW	Florø	Batalden, Fanøy, Vevling
W	Florø	Ånnøy, Færøyna, Kinn, Rognaldsvåg, S. Nekkøy, Selvåg, Skorpa, Skorpeide
S	Florø	Ålvora, Askrova, Stavang, Svanøybukt, Veiesund

Table 7.6: Overview of included ports in the four initial port groups in the `AP` test instance

To construct the routes with fewer butterfly wings than $n = 4$, we combine the four initial groups to obtain fewer, but larger groupings. The combination patterns when creating fewer groups, is an important input to the DB heuristic. After creating all routes containing four butterfly wings, groups N and NW are merged, resulting in three remaining groups. Based on these, all routes with three butterfly wings are generated. Subsequently, group N, NW and W are combined to yield a total of two groups. On this basis, all routes containing two butterfly wings are created. Finally, the simple cycle routes, containing only one butterfly wing, are created by placing all the initial port groups in the same group. This procedure is illustrated in Figure 7.6.

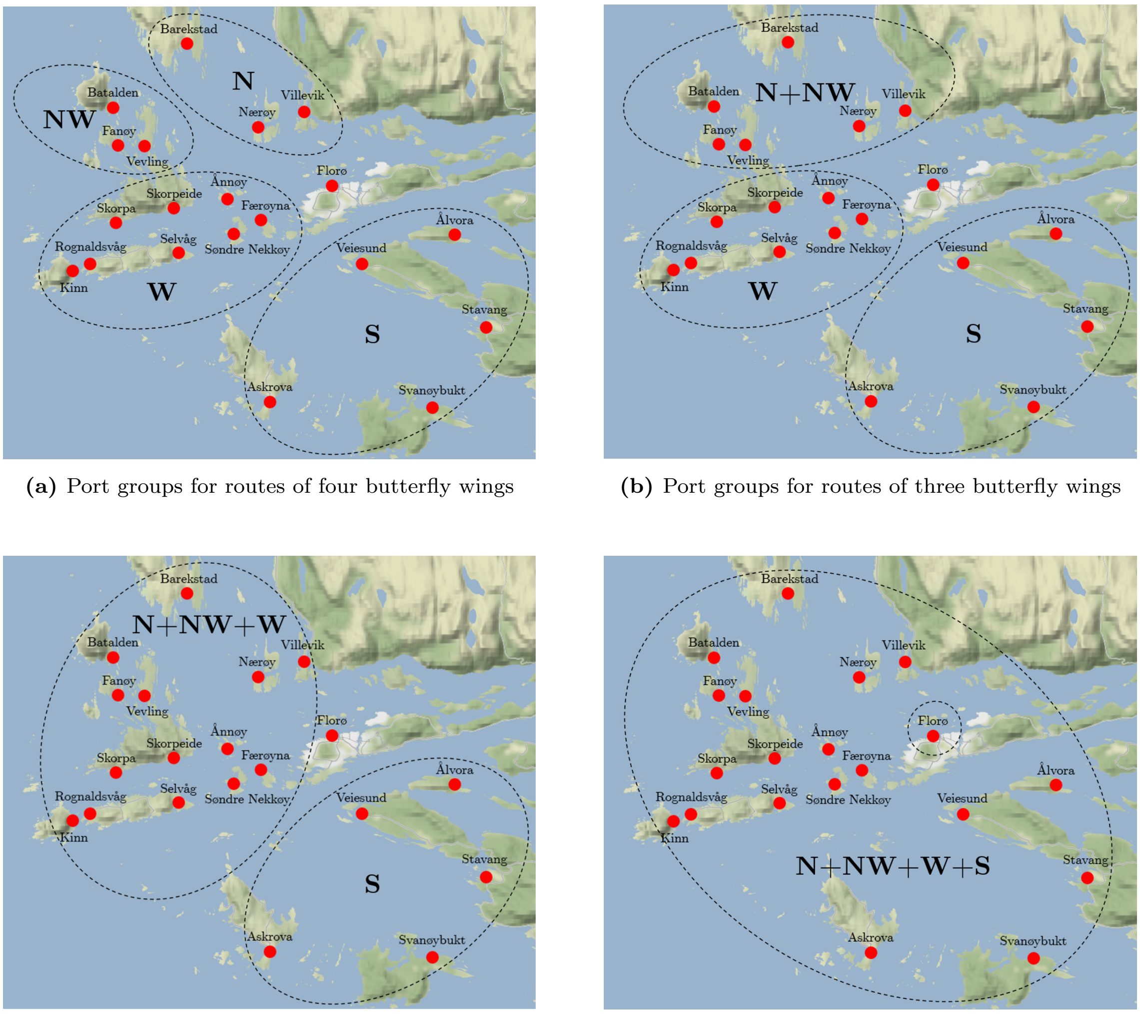

(a) Port groups for routes of four butterfly wings

(b) Port groups for routes of three butterfly wings

(c) Port groups for routes of two butterfly wings

(d) Port group for routes of one butterfly wing

Figure 7.6: Separation into port groups for varying number of wings in the butterfly routes

Second test instance: Near Ports (NP)

In the second test case, NP, we seek to construct a test case with shorter sailing distances. As the route generation procedure, elaborated on in Chapter 6, is focused around butterfly routes with Florø as a central hub, the ports are selected based on their distance from Florø. The values in Table D.2, in Appendix D, are used to find the mean port distance from Florø, 5.8 nautical miles. The test instance includes all ports within this sailing distance from Florø. The procedure forms a test instance with nine ports, including Florø, shown in Figure 7.7, and the frequency options are equal as in the AP test instance. The motivation for solving this instance is to analyze a service where a lower travel distance is covered, and see if, and eventually how the solution changes. Another important aspect of the solution is the comparison of abatement costs to the conventional model. Specifically, we want to observe how distance affects these costs. Following the naming convention from the AP test instance, NP refers to the Near Ports test instance in general, whereas NP-ZE and NP-C distinguishes between the Zero-Emission and Conventional versions, respectively.

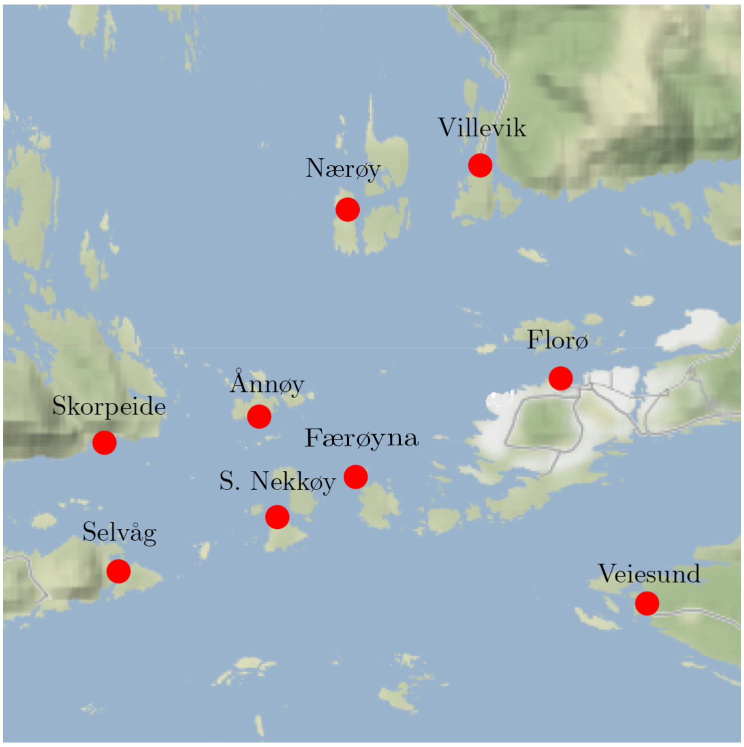

Figure 7.7: Ports considered in the NP test instance

Similarly to the AP test instance, the ports are divided into groups. The division into groups is based on the same principles as above, but none of the ports from the NW group are included, as these are too remotely located. This yields a total of three groups, such that $n = 3$. An overview of the three port groups in the NP test instance is provided in Table 7.7. A merging process of the groups to create butterfly routes with $1..n$ wings, is performed accordingly, following the steps from the AP instance. Due to the NP instance already containing few ports, we exclude the step of skipping ports from the route generation in the DB heuristic.

Group	Hub	Additional ports
N	Florø	Nærøy, Villevik
W	Florø	Ånnøy, Færøyna, S. Nekkøy, Selvåg, Skorpeide
S	Florø	Veiesund

Table 7.7: Overview of included ports in the three initial port groups in the NP test instance

Third test instance: High Demand (HD)

The third managerial test instance is the high-demand instance, labeled the `HD` instance. In this case, we only include the ports that have demand higher than the average value of demand to and from Florø. This constraint leaves eight ports, including Florø, as illustrated in Figure 7.8. In addition to providing insight into the effect of serving ports with higher demand, the ports in the `HD` test instance are, unintentionally, spread far apart geographically. The test instance may thus illustrate the influence of longer distances in the served area, acting as an opposite version of the `NP` test instance. The aim of solving this instance is to show the effects of a service where most of the demand is covered, and see if, and eventually, how the solution changes. Yet again, it is of great interest to compare the abatement costs to the conventional model. In particular, we want to observe how high demand and longer distances affect these costs. Again we follow the naming convention from the `AP` test instance. `HD` refers to the High Demand test instance in general, whereas `HD-ZE` and `HD-C` distinguishes between the Zero-Emission and Conventional versions, respectively.

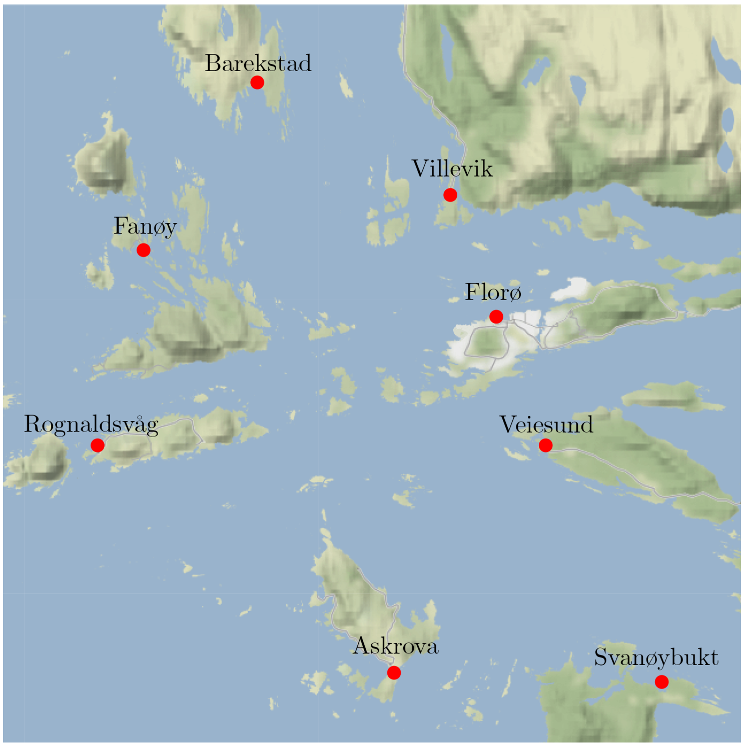

Figure 7.8: Ports considered in the `HD` test instance

Similarly to the `AP` and `NP` test instances, the ports are divided into groups. The division into groups is based on the same principles as above, yielding a total of four groups, implying that $n = 4$. An overview of the four port groups in the `HD` test instance is provided in Table 7.8. Again, a merging process of the groups to create butterfly routes with $1..n$ wings is performed. The procedure follows the steps from the `AP` instance. Following the same reasoning as for the `NP` instance, port skipping is omitted in the DB heuristic for the `HD` instance.

Group	Hub	Additional ports
N	Florø	Barekstad, Villevik
NW	Florø	Fanøy
W	Florø	Rognaldsvåg
S	Florø	Askrova, Svanøybukt, Veiesund

Table 7.8: Overview of included ports in the four initial port groups in the `HD` test instance

Summary of the managerial test instances

As mentioned in the presentation of the three test instances, the average distance to Florø, and the demand to/from Florø varies. For a direct comparison of these metrics for the three instances, consider Table 7.9. Note the number of ports is substantially higher in the `AP` instance. Further, the average distance to Florø is notably lower in the `NP` case than in the remaining instances. Lastly, the average daily demand is highest in the ports contained in the `HD` instance.

Instance	Number of ports	Average distance to Florø	Average daily demand t/f Florø
`AP`	20	5.8 nm	17.9
`NP`	9	3.7 nm	8.5
`HD`	8	6.4 nm	42.6

Table 7.9: Overview of important parameters for the different test instances

7.2.2 Performance test instances

In order to fully utilize the power of our proposed solution method, some important parameter values need to be set. More specifically, we would like to investigate the relationship between the maximum number of butterfly wings, n, the stopping criteria defined by m and t, and the routes passed from the LP-model to the single period MIP-model, r. The process of tuning these parameters to adequate values for each test instance is presented in Chapter 8. The demonstration of the process is based on the `AP-ZE` test instance, and to provide a thorough explanation we utilize four *performance test instances*. These instances, named `P1`, `P2`, `P3` and `P4`, are alterations of the previously defined `AP-ZE`, including all ports in the Florø Basin. Each instance is initialized with a value for n corresponding to the number in its name. This implies that we vary the maximum number of butterfly wings in the route generation procedure in the DB heuristic. To clarify, `P1` only generates routes with one butterfly wing, in other words, simple cyclical routes. `P3`, on the other hand, generates all routes with one butterfly wing, all routes with two butterfly wings, up to its maximum of three butterfly wings, as indicated in its name. The different groups used to generate the different butterfly routes are equal to that of `AP`. Note that this means that `P4` is equal to the `AP-ZE` instance, presented in the previous subsection. The wing structure of the different instances is shown in Table 7.10 below.

Test instance	n	Number of wings in included butterfly routes
`P1`	1	1
`P2`	2	1, 2
`P3`	3	1, 2, 3
`P4`	4	1, 2, 3, 4

Table 7.10: Overview of number of butterfly wings in included routes for the four performance test instances

Chapter 8

Computational Study

In this chapter, we firstly find adequate parameter values for the Decomposition Based heuristic (DB heuristic, presented in Chapter 6), for each of the three instances presented in Section 7.2. The process of finding adequate values for these parameters is thoroughly explained for the `ZE-AP` instance in Section 8.1, utilizing the *performance test instances*, from Subsection 7.2.2. Further, an overview of the parameters for the remaining instances is presented. In Section 8.2, the performances of both the original formulation for the ZEVSNDP presented in Chapter 5 and the DB heuristic, are discussed. The results from solving the instances for Zero-Emission (ZE) and conventional vessels are presented in Section 8.3 and Section 8.4. Section 8.3 presents cost breakdowns for each instance, alongside their strategic decisions, while Section 8.4 focuses on the route structures and service frequencies. After presenting the results, we center the discussion around three focal aspects of the solutions. In Section 8.5 we describe how replanning vessel services leads to a cheaper adaption of ZE operations. Further, in Section 8.6, we perform sensitivity analyses on two important parameters, the electricity price and passenger cost of sailing. Finally, Section 8.7 discusses the implications of changes in the future carbon taxation levels, and the effects of an increased carbon tax on abatement costs for the studied instances.

We performed the executions on local computers provided by the Department of Industrial Economics and Technology Management at NTNU (Norwegian University of Science and Technology). The model runs were conducted on identical computers with the same software and processing power. The applied software and hardware are described in further detail in Table 8.1.

Computer	Dell OptiPlex 7780 AIO
Processor	Intel Core i7-10700 @ 2.90GHz
RAM	16 GB
Operating System	Windows 10 Education
Gurobi Licence Type	Academic
Gurobi Version	9.1.2
Python Version	3.8.8

Table 8.1: Description of hardware and software used for the computational study

8.1 Adequate Parameter values for the DB heuristic

In this section we seek the optimal parameter values for the DB heuristic for the test instances introduced in Chapter 7. Throughout the search, we look for the best trade-off between runtime and a good objective function value. In the DB heuristic, multiple parameters affect the runtime. Firstly, the parameter n that decides the maximal number of butterfly wings in the routes, affects the created number of rotations. A higher value of n increases the necessary amount of rotations, and, consequently the computational time of the DB heuristic. Note that $n = 1, 2, 3$ and 4 corresponds to performance test instances `P1, P2, P3` and `P4`, respectively, as described in Subsection 7.2.2. Next, the number of rotations that are evaluated in the LP-model (Section 6.5), affects the overall computational time of the DB heuristic. As previously described, this step has two stop criteria. It terminates if 1) the number of feasible rotations evaluated without updating the current best equals the predefined parameter, m, or 2), if it reaches the predefined time limit in this step, t. Lastly, the number of routes, r, sent from the route processing to the single period MIP (Section 6.6), affects the computational time of the DB heuristic. As seen later, more successive runs of the LP-model increase the likelihood of finding good solutions for the peak period. Including more routes in the MIP-model after the strategic decisions are made for the peak period, may yield better solutions overall, due to a greater solution space for the other time periods. An overview of the parameters is provided in Figure 8.1. The section is organized as follows. In Subsection 8.1.1, we seek input parameter values that yield the best objective in the peak period, i.e., values for parameters n, m and t, for the `AP-ZE` instance. Note that we only provide a thorough explanation of our approach for the `AP-ZE` instance, but similar steps are taken for the other instances. Further, Subsection 8.1.2 presents the process of finding an appropriate size of the set of routes, r, that serves as input to the MIP-model for the remaining time periods. Lastly, we summarize the adequate parameter values for all instances in Subsection 8.1.3.

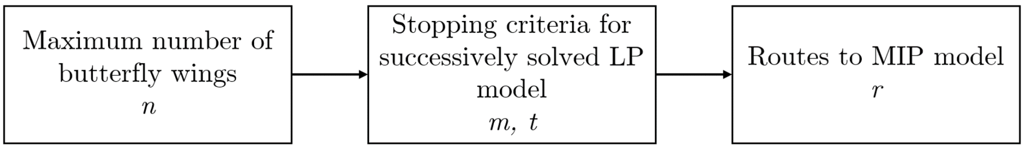

Figure 8.1: Overview of parameters in the DB heuristic

8.1.1 Adequate parameter values for the successive solution of LP-models

In this subsection, we seek the parameter values for the DB heuristic that return the best objective value in the peak period, yielding as short solution times as possible without compromising the objective value. As mentioned above, these parameters are n, m and t. To test for different values for n, we use the performance test instances `P1`, `P2`, `P3` and `P4`, corresponding to $n = 1, 2, 3, 4$. Recall that when $n = 3$, for example, all butterfly routes with one and two wings are included in addition to the routes with three wings. Accordingly, increasing the n parameter increases the computational time of the rotation generation (Section 6.3), as the number of routes grows rapidly. This also applies to the evaluation and sorting of rotations based on proxy scores (Section 6.4). The motivation for testing for a range of n values is to determine if computational time may be saved, which would be the case if it is proven that the objective value for the peak period of a lower value of n, yields the same result as for greater values. Further, we let the parameter that decides the maximum number of iterations without a new best solution from the LP-model, m, vary. At the same time, we set the time criterion, t, sufficiently high to make the former criterion redundant. This enables us to record the time from the start of successive LP-model runs until m solutions without a new best are found.

In the course of solving the test instances, `P1` and `P4` emerged problematic to solve. In `P1`, which allows for only one port group, i.e., $n = 1$, we obtain zero feasible rotations. This is caused by the feasibility check described in Section 6.3, meaning that none of the ZE vessels are able to serve the whole set of ports in one round trip within the time period. In `P4`, when n is set to 4, the DB heuristic was unable to generate routes and rotations, and evaluate and sort proxy scores, within acceptable time (12 hours). The combinatorial generation of all rotations proves to be a weakness towards the scalability of the DB heuristic, and a more advanced algorithm may be considered, as discussed in Chapter 10.

Test instances `P1` and `P4`, are left out of the subsequent analyses, due to the traits discussed above. We accordingly shift focus towards the remaining instances and firstly consider test instance `P2`. Recall from Subsection 7.2.2 that the ports are separated in two groups in `P2`, corresponding to

$n = 2$. In this instance, 18 900 rotations are created and the time used for the first part of the DB heuristic, i.e., route generation, rotation generation and proxy evaluation and sorting, is 80 seconds. Further, we successively solve the LP-model, while varying the values of m. Table 8.2 illustrates the objective value in the peak period for different values of this stopping criterion. It also presents the time used in the successively solved LP-model and the number of times the current best solution is updated.

m	10	50	100	500	1000	10 000
Objective value in peak period	1 537 648	61 531	57 026	57 026	57 026	57 026
Time (s)	0.8	6.7	31	83	145	1 091
New best found	1	2	3	3	3	3

Table 8.2: Objective values in peak period and computational time for different values of m for performance test instance `P2`

Table 8.2 showcases that when $m = 100$, we obtain the same objective value as for all higher values of m tested. The computational time in the successively solved LP-model, when $m = 100$ was 31 seconds. Accordingly, we may assume that a good solution for the peak period could be found within $80 + 31 = 111$ seconds. The same procedure is conducted for instance `P3`. When $n = 3$, a total of 212 058 rotations are generated. One reason for the rapid increase in the number of rotations derive from the fact that more configurations of subroutes (Subsection 6.2.2) are possible when three butterfly wings are allowed. In addition, all the rotations based on butterfly routes with two wings are included. The computational time of route and rotation generation, and proxy evaluation and sorting, increases to 880 seconds ($\sim$ 15 minutes) in the `AP-ZE` instance. The results from instance `P3` are displayed in Table 8.3.

m	10	50	500	5 000	10 000	100 000
Objective value in peak period	55 508	55 508	**55 140**	**55 140**	**55 140**	**55 140**
Time (s)	0.7	3.6	64	638	1 251	20 350
New best found	1	2	2	2	2	2

Table 8.3: Objective values in peak period and computational time for different values of m for performance test instance `P3`, with the best values marked in bold

We observe in Table 8.3 that when m is set to 500, the same objective is returned for the peak period as for $m = 100\ 000$. An m of 500 yields a computational time of 64 seconds. Thus, a good solution for the peak period is found within a total computational time of 944 seconds (64 seconds + the 880 seconds from the previous step). By comparing Table 8.2 and Table 8.3, we observe that the objective value in the peak period is better for groups of three. As a result, routes consisting of three wings are better for the peak period, and we set $n = 3$ in the subsequent discussion. We observe from both Table 8.2 and Table 8.3 that the best solution for the peak period is found early in the process. This implies that the proxy evaluation and sorting are well functioning and decrease the required number of LP-runs, and thus the overall computational time.

In the DB heuristic, the strategic decisions are determined with the aim of optimizing the objective value in the peak period. Accordingly, as discussed above, the parameter m must be set greater than or equal to 500, and we must allow for routes consisting of three wings, i.e., $n = 3$. Even though we want to minimize computational time, we also want the number of stored solutions to be of an appropriate size, increasing the probability of including routes better suited for the other time periods. Accordingly, we set $m = 5000$, although the best solution is found when $m = 500$. This increases the computational time to 1 518 seconds (880 seconds for proxy evaluating and sorting, and 638 seconds in the LP step), but at the same time, we increase the probability of finding good solutions for all periods in the MIP-model, presented in the next subsection.

8.1.2 Adequate parameter values for MIP-model

In this subsection, we describe the process of finding an adequate value for the input parameter r, for the MIP-model constituting the final step of the DB heuristic (Section 6.6). The r parameter determines the size of the set of available routes in each remaining time period. In Subsection 8.1.1, we found the appropriate parameters to achieve a good solution for the peak period. We fix the strategic decisions from this solution in the MIP-model. The successively solved LP-model also provides a set of stored rotations, sorted after their objective value for the peak period. As explained in Section 6.5, we extract a set of unique routes from the stored rotations, which are also sorted after how promising they were in the peak period. We then let the size of the number of routes used as input in the MIP-model vary, denoted by the parameter r. We record the objective function for all periods, along with the computational time in the MIP. The results are illustrated in Table 8.4.

r	5	10	20	40	80	160	320
Objective value	164 921	163 921	163 716	155 676	155 631	153 212	**153 202**
Time (s)	4.1	7.7	18.1	42	118	797	960

Table 8.4: Objective value and computational time for different sizes of the set of candidate routes, r. The best objective value is indicated in bold.

In Table 8.4 the objective values for the entire planning period are listed for each value of r. The table showcases that the computational time depends on the size of the set of candidate routes. Further, note that a higher number of routes yields better objective function values, meaning that a good route in the peak period is not necessarily a suitable route for the other time periods. It should also be noted that the computational time for $r = 320$ is smaller than expected, when inspecting the computational time for $r = 160$. This is caused by the fact that m bounds the value of r. Increasing m (most likely) leads to an increase in the number of routes, because more rotations, and consequently more routes are included in the stored solutions sent to the MIP-model. In this case, the number of unique routes sent to the MIP-model is cut off at a number lower than 320. This shows that setting m higher than the bare minimum in Subsection 8.1.1 at the expense of solution time was beneficial towards obtaining a better objective function value overall. A lower number for m would most likely result in fewer unique routes in the stored solutions, and the best route might not have been included. We choose to move on with setting $r = 320$, which yields an objective value of 153 202 for all time periods. The total computational time of the DB heuristic then accumulates to 2 478 seconds. The runtime is calculated by adding the solution time of the MIP-model (960 seconds), to the 1 518 seconds used to generate and evaluate the rotations for the peak period.

8.1.3 Adequate parameter values for the `NP` and `HD` test instances

The same procedure as described in Subsection 8.1.1 and Subsection 8.1.2 is used to find adequate parameter values for the `NP` and `HD` test instances. Table 8.5 provides an overview of the different instances' best parameter values, their objective value and the total time of the solution method.

	n	m	r	Total time (s)	Objective value
AP-ZE	3	5 000	320	2 478	153 202
AP-C	3	1 000	80	682	119 474
NP-ZE	3	500	20	44	63 729
NP-C	3	500	50	27	61 757
HD-ZE	3	500	50	60	149 659
HD-C	3	500	60	27	111 922

Table 8.5: Overview of optimal parameters, total runtime and objective value for all instances

The conventional instances are generally solved faster than the ZE instances, as fewer rotations are created due to a smaller set of potential vessel types and no charging infrastructure. Further, for the `NP` and `HD` instances, the m-parameter is set lower than for the `AP` instances. This is also motivated by fewer rotations being created, since we do not allow for the creation of routes where ports are cut off in these instances. It should be noted that the objective values of the different instances vary, a result further discussed in Section 8.3.

8.2 DB Heuristic Performance

In this section we discuss the performance of the DB heuristic. It should be noted that the DB heuristic is unable to guarantee optimality of a solution to the ZEVSNDP, due to its heuristic nature. It does, however, succeed at providing good solutions quickly. To assess the quality and solution times of the DB heuristic, we use the original mathematical formulation as a benchmark for its results. To do so we first implement the exact mathematical formulation proposed in Chapter 5, and attempt to solve the model to optimality using a commercial solver.

Although the exact formulation of the ZEVSNDP in theory may prove optimality of a solution, this would require all possible routes to be generated in advance and used as input. This is not a viable option, and thus a heuristic route generation is still performed prior to solving the exact formulation of the ZEVSNDP. The solution space containing all possible combinations of routes is vast, and it is far too extensive to derive all combinations. Accordingly, even though we solve the full implementation of the ZEVSNDP, we cannot verify if the solution is optimal, due to the heuristic generation of routes. We thus use the set of promising candidate routes found for performance instance `P3` in the DB heuristic, with $m = 5000$ as a basis. Similar to the last step of the DB heuristic, we use the r best routes of this basis as input to the exact formulation. The motivation for using the best routes from `P3` as a basis for the set of candidate routes, is that they have been proven feasible and promising for the peak period, already. As the process of generating a set of promising candidate routes is not included in the solution time of the exact formulation, a comparison of solution times should be made between the final MIP-model in the DB heuristic (Table 8.4), rather than considering all steps. In Table 8.6, we showcase the upper bounds and optimality gaps, when solving the exact formulation for different time limits and input sizes. The tests are performed on the `AP-ZE` test instance.

Routes	5		10		20	
Time	UB	Opt. gap	UB	Opt. gap	UB	Opt. gap
10 min	166 114	48.8 %	159 022	46.5 %	-	-
20 min	166 114	48.8 %	159 022	46.5 %	171 257	50.3 %
30 min	153 516	44.1 %	159 022	46.5 %	163 507	48.0 %
1 hour	153 516	44.1 %	159 022	46.5 %	161 749	47.4 %
2 hours	153 516	0.0 %	163 848	46.5 %	161 749	47.4 %

Table 8.6: Optimality gap and upper bound (UB) for different length of the set of potential routes and different time limits for the test instance `AP-ZE` solved with the exact mathematical formulation

We observe in Table 8.6 that the full model is sensitive to the number of routes used as input. When testing for a set of 30 routes, the solver ran out of memory before commencing the solution process. Additionally, when 10 and 20 routes are used as input, the optimality gap is still above 46 % after two hours. The MIP-model in the DB heuristic, on the other hand, solves a set of 320 routes within reasonable time (960 seconds, Table 8.4). Thus, the DB heuristic is better suited to evaluate larger sets of candidate routes for all time periods.

The different time periods have varying demand patterns. By only using a few routes that are promising for the peak period as input, we obtain poorer results when solving both the exact formulation and the MIP-model in the DB heuristic, since the inputted routes are not necessarily good for the other time periods. The DB heuristic handles a larger set of potential routes in the MIP-model, which proves advantageous, as better solutions are found than for the exact formulation. To illustrate, the best objective value found by the DB heuristic is 153 202 for the `AP-ZE` instance (Section 8.1), which is better than any of the solutions in Table 8.6. The best objective value found by the DB heuristic required 320 routes as input to the MIP-model. Solving for the same amount of routes in the exact model would be impossible.

A disadvantage of the exact formulation is that only a small number of routes can be considered. On the other hand, it makes the strategic decisions based on all periods, instead of only considering the peak period, as is the case in the DB heuristic. In Table 8.6, it may be observed that the ZEVSNDP is solved to optimality within two hours when the set of routes has a size of five, yielding an objective value of 153 516. These five routes are the same five routes that are sent to the MIP-model in the DB-heuristic for r equal to five, which yielded an objective function value of 164 921, observed in Table 8.4. This indicates that deriving the strategic decisions from the peak period not necessarily yields the best solution.

To conclude, the DB heuristic has the disadvantage of not taking all periods into account when setting the strategic decisions. On the other hand, it handles a more extensive set of routes as input in the final MIP-model. This yields a better objective value than attempting to solve the full model to optimality. In addition, the DB heuristic is faster, finding good solutions using shorter solution times.

8.3 System Cost Breakdown and Strategic Decisions

In this section, we present the system cost breakdown of the three studied instances in addition to their respective strategic decisions. In Subsection 8.3.1, we focus on the `AP` instance, which considers all the ports in the Florø Basin. Further, Subsection 8.3.2 concerns the near ports instance (`NP`) whereas Subsection 8.3.3 covers the high demand instance (`HD`).

8.3.1 Cost breakdown of the `AP` test instance

The cost breakdown of the `AP` test instance, where all ports may be a part of the final route structure in the solution, is presented in Table 8.7. The ZE solution is denoted as `AP-ZE`, and the conventional solution denoted as `AP-C`. Firstly, we observe that `AP-ZE` is around 30 % costlier than `AP-C`. The most substantial costs in both cases are the vessel investment, the crew cost and the cost of waiting in port, whereas the energy cost is a dominating factor in the conventional case.

We further break the results into the terms in the objective function. Firstly, the vessel investment costs in the ZE case are double those in the conventional case. This is caused by the acquisition of two vessels in the ZE case, as opposed to one in the conventional case. Note that the same vessel type is chosen. Recall from Chapter 7 that for conventional vessels, the vessel type corresponds to the ZE alternative with the same dimensions, and medium energy storage. Further, the infrastructure investment is, naturally, only applicable to the ZE case. These impose only a fraction of the total costs in `AP-ZE`. Infrastructure is only installed in Florø, leading to a low percentage of the total costs. The energy costs are substantially lower in the ZE case. This is closely linked with the operating speeds of the respective services. The ZE vessels operate at lower speeds along the sailing legs than the conventional vessels. The latter consequently consumes more energy, and the costs are higher as the unit cost of energy is almost the same for both technologies, as described in Chapter 7. The crew costs are also doubled in the ZE solution, which follows naturally from doubling the number of vessels. Moving on to the cost of alternative transport, this is lower in `AP-ZE`. Recall that this term represents the cost of unmet demand, i.e., the inconvenience cost of those wanting to travel but are not served by the system due to full capacity. This is a result of the two subroutes served by one vessel each in `AP-ZE` compared to the single subroute in the conventional solution. Hence, more passengers are transported by the ZE service than the conventional service. This also leads to a higher cost of waiting in port in `AP-C`. On average, the passengers in the conventional service wait longer in the ports than in the ZE service. The cost of unvisited ports is negligible, because the demand is very low from and to the single excluded port, Stavang. The same port is excluded in both cases. Finally, the transit cost is almost triple in size in the ZE solution. This may be caused by the low sailing speed. The transit time of the ZE-vessels lies well above the benchmark time, meaning that a cost is incurred for the passengers. This cost is far less in the conventional case, where the transit speeds are higher.

	AP-ZE		AP-C		
Cost Term	Value (NOK)	% of total	Value (NOK)	% of total	% of ZE
Vessel investment	39 722	25.9 %	19 861	16.6 %	50.0 %
Infrastructure investment	2 388	1.6 %	*NA*	*NA*	*NA*
Energy cost	20 720	13.5 %	26 984	22.6 %	130 %
Crew cost	38 208	24.9 %	19 104	16.0 %	50.0 %
Cost of alt. transport	7 821	5.1 %	10 318	8.6 %	132 %
Cost of unvisited ports	16	0.0 %	16	0.0 %	100 %
Cost of waiting at port	32 776	21.4 %	38 278	32.0 %	117 %
Transit cost	11 549	7.5 %	4 912	4.1 %	42.5 %
Total system cost	153 202	100.0 %	119 474	100.0 %	78.0 %

Table 8.7: Cost breakdown of the AP instance

Decision	AP-ZE	AP-C
Vessel type	1M	1C
Total number of vessels	2	1
Infrastructure	Florø	-

Table 8.8: Strategic decisions in the AP instance

8.3.2 Cost breakdown of the NP test instance

The results from the NP-ZE and NP-C test instances, are presented in Table 8.9 and Table 8.10.

	NP-ZE		NP-C		
Cost term	Value (NOK)	% of total	Value (NOK)	% of total	% of ZE
Vessel investment	18 488	28.9 %	19 861	32.2 %	107 %
Infrastructure investment	2 388	3.7 %	*NA*	*NA*	*NA*
Energy Cost	3 690	6.3 %	9 258	15.0 %	251 %
Crew cost	19 104	29.9 %	19 104	30.9 %	100 %
Cost of alt. transport	10 315	16.1 %	5 979	9.7 %	58.0 %
Cost of waiting in port	7 660	12.0 %	4 616	7.5 %	60.3 %
Transit cost	2 084	3.1 %	2 939	4.8 %	141 %
Total system cost	63 729	100 %	61 757	100 %	96.9 %

Table 8.9: Cost breakdown of the NP instance

Decision	NP-ZE	NP-C
Vessel type	1S	1C
Total number of vessels	1	1
Infrastructure	Florø	-

Table 8.10: Strategic decisions in the NP instance

The NP-ZE and NP-C test instances consider the ports with a sailing distance to Florø below average of the initial 20 ports. In these instances, the most substantial costs are the vessel investments, and the crew costs, accounting for approximately 60% of the total costs in both cases. We observe that only one vessel is chosen in both solutions, but different vessel types. The vessel types have the same dimensions, but their energy capacities differ. The crew costs are consequently the same in absolute terms in both solutions. Further, the energy costs are far higher in the conventional case, caused by the speed differences also seen in the AP instances. Moving on to the following cost parameter, the cost of alternative transport, this is higher in the NP-ZE. This may be caused by a higher service frequency in the NP-C. The service frequency here is two, as opposed to one in NP-ZE. As a result, more people need to find alternative transport in the latter. The choice of frequency also affects the cost of waiting in port. This term is substantially lower in the conventional case. In the final term, the transit cost is lower in the NP-ZE, because there are fewer people picked up, yielding a higher sum of the inconveniences in NP-C. An interesting result from this instance, is that the total cost of the conventional solution is 97% of the ZE solution, as opposed to a higher percentage in the AP instance. The most apparent difference between this and the two other instances is the acquisition of only one vessel, which, along with the associated crew costs, are the main drivers of the proportional objective function values.

8.3.3 Cost breakdown of the HD test instance

In the high-demand instances, the total costs are yet again higher in HD-ZE. Here, two vessels are acquired, whereas one is acquired in the conventional case, similarly to in the AP case. In HD-ZE, the route is split into two subroutes, necessitating two vessels, whereas the route is served in a single subroute by one vessel in HD-C. The energy costs are higher in the conventional case, and even though the high demand prompts higher speeds in HD-ZE than in the other instances, this speed is still limited by the frequent charging. The conventional vessel may consequently sail faster, consuming more energy. There is only a 5% difference in the costs for alternative transport, meaning that almost the same number of people are served. This also applies to the cost of waiting in port. The transit cost, however, is substantially higher in HD-ZE. This may be caused by high inconvenience costs incurred by the large number of passengers.

	HD-ZE		HD-C		
Cost term	Value (NOK)	% of total	Value (NOK)	% of total	% of ZE
Vessel investment	39 722	25.7 %	20 060	17.9 %	50.5 %
Infrastructure investment	2 388	1.5 %	*NA*	*NA*	*NA*
Energy cost	23 324	12.8 %	32 214	28.8 %	138 %
Crew cost	38 208	24.7 %	19 104	17.1 %	50.0 %
Cost of alt. transport	14 880	10.9 %	14 877	13.3 %	95 %
Cost of waiting in port	20 260	13.6 %	20 254	18.1 %	100 %
Transit cost	10 877	6.1 %	5 414	4.8 %	57.8 %
Total system cost	149 659	100 %	111 922	100 %	81.4 %

Table 8.11: Cost breakdown of the HD instance

Decision	HD-ZE	HD-C
Vessel type	1M	2C
Total number of vessels	2	1
Infrastructure	Florø	-

Table 8.12: Strategic decisions in the HD instance

8.3.4 Summary of abatement costs for all instances

We calculate the abatement costs of transitioning to a ZE service for all instances. The results are displayed in Table 8.16. We present the daily abatement cost for all instances in the fourth column, the costs on a yearly basis in the fifth column and the costs for the lifetime of a vessel (20 years) in the sixth column. Note that the abatement costs for one year is far higher for the `AP` and `HD` instances, than for the `NP` instance, as discussed in Subsection 8.3.2. An interesting metric is the abatement cost per passenger. We make this calculation for the `AP` instance. The observed demand adds up to approximately 342 passengers per day. Thus, the daily abatement costs for a trip becomes $33\,728/342 \approx 100$ NOK/passenger.

Instance	ZE cost	Conventional cost	1 day	1 year	20 years
`AP`	153 202	119 474	33 728	12.3 mill.	246 mill.
`NP`	63 729	61 757	1 972	0.72 mill.	14.4 mill.
`HD`	149 659	111 922	37 737	13.8 mill.	276 mill.

Table 8.13: Abatement cost of the different instances

8.4 Route and Frequency Decisions

Route and frequency decisions are essential for enabling ZE vessel services. By investigating the differences across test instances and time periods, insight regarding these decisions may be obtained. This section covers a selection of interesting observations from the route and frequency decisions for each instance. A complete overview of the routes and frequencies for each instance, is provided in Appendix E.

8.4.1 Subroute configurations for ZE operations

A general restriction for ZE passenger vessels, is their limited energy storage. One could be tempted to assume that multiple subroutes are caused only by this limited capacity. In most instances, this is not the case. More precisely, the limited battery capacity inhibits routes where one vessel visits all the ports without charging. However, it is the requirement of covering a subroute within the time horizon that calls for additional subroutes and vessels. The ZE vessels must charge their battery to the initial level within each time period, and the extra time spent charging decreases their reach. The alternative is to split the routes into several subroutes. This enables the service to visit the required ports, but also induces the acquisition of extra vessels and associated crew costs. Using the conventional solution as a baseline for solutions without charging requirements, we observe that the route adjustment comes at a cost. This cost is not sufficiently counteracted by the cost reductions of offering the passengers a better service, making the ZE-solutions the costlier alternative.

In order to elaborate on the differences between the subroutes, Figure 8.2 illustrates the best route structures of `AP-C` and `AP-ZE`, for time period 3. Apart from an opposite sailing direction in the southern butterfly wing and a different service frequency in the northern wing, the only difference is a separation into two subroutes for the ZE vessel service. This is a consequence of the limitation mentioned abovem, i.e., that the ZE vessels are unable to complete the entire butterfly route in a single subroute. The use of two subroutes is seen across all time periods for the `AP-ZE` and `HD-ZE` test instances, due to their long sailing distances. `NP-ZE` is however possible to operate using only a single subroute, naturally explained by its near ports, and thus shorter sailing distances.

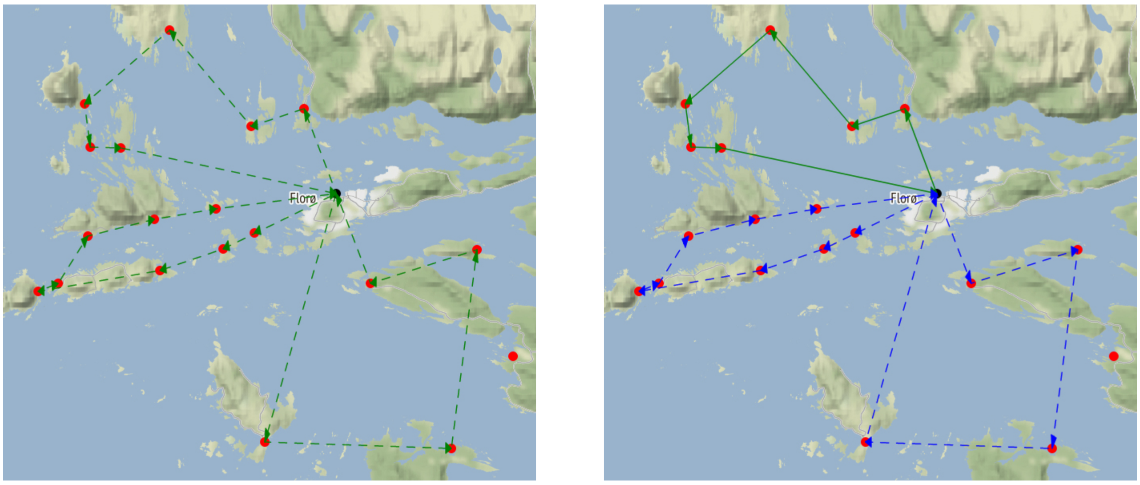

(a) `AP-C`: Time period 3 **(b)** `AP-ZE`: Time period 3

Figure 8.2: Route structures in time period 3 for conventional (a) and Zero-Emission (b) vessels. Different colored lines indicate separate subroutes. Dashed lines indicate a frequency of 1, whereas solid lines indicate a frequency of 2.

Although coming at an extra cost, using two subroutes rather than one enables increased frequency levels in subroutes where this outweighs the additional energy costs. This possibility is a consequence of a shorter sailing distance in the subroute, enabling a roundtrip of sailing, charging and waiting to make up a fractional value (for instance a half, for a frequency of two) of the time period duration. The ability to increase service frequency when splitting the route into multiple subroutes, is also a property of the best solution in time period 3 for `AP-ZE` (Figure 8.2). The possibility of increasing the frequency level for some ports, when splitting the route into two subroutes, decreases the aforementioned extra cost of acquiring two vessels to serve two subroutes.

8.4.2 Demand dependency

Comparing route structures across time periods provides insights into the effect of demand on the optimal route choices. Demand is the only parameter that changes values across time periods in the three test instances, and one may hence place all motivation for changing route structure, from one time period to another, on differences in demand patterns. To provide a background for the different route structures observed, consider Table 8.14, providing an overview of total demand for the different time periods in each test instance.

Time period	`AP`	`NP`	`HD`
1	124.4	29.1	108.6
2	10.3	1.5	8.6
3	169.4	33.9	148.8
4	37.7	3.9	33.6

Table 8.14: Total demand for transportation per time period for each instance

Focusing on the `AP` instance, we observe that the total demand is significantly higher in time periods 1 and 3, where the latter is defined as the peak period. These time periods correspond to morning and afternoon, respectively, and could thus be considered time periods dominated by commuters. The significant differences in total demand are also visible from the optimal route decisions. If we compare the best route structures for time period 1 and 4 in the `AP-ZE` test instance, illustrated in Figure 8.3, some major differences become apparent. Firstly, the ports are served by a butterfly route with three wings in time period 1, whereas the route in time period 4 only has two wings. In general, a higher total demand leads to more wings for ZE vessels. This result is also observed in the NP-ZE instance, whereas the HD-ZE shows less variation in route structure between time periods. Secondly, the sailing direction of the southern butterfly wing varies between time periods 1 and 4. The direction is a result of minimizing the passenger costs by reducing average transit times in the subroute. The service frequency however, is a trade-off between the additional energy cost of sailing twice as long within the same time period, and the decreased passenger costs of waiting in port and the need for alternative transportation. This trade-off has resulted in different outcomes for the two time periods. While the reduced passenger costs of providing a service frequency of two outweighed the increased energy costs in time period 1, the opposite result proved cheaper overall for time period 4. The reason behind the different outcomes in the two time periods, is the difference in demand.

In addition to influencing route structure between time periods with large differences in total demand, e.g., time periods 1 and 4, the varying demand patterns also form a basis for the different route choices in time periods 1 (Figure 8.3a) and 3 (Figure 8.2b). Despite both possessing high levels of total demand (Table 8.14), two important features arise when comparing the best routes for each time period. Firstly, the butterfly wing operated as a separate subroute, with a service frequency of 2, is different. For time period 1 this is the southern wing, whereas it is the northern wing for time period 3. The reasoning behind this, could be that the subroute configuration is chosen such that the butterfly wing with the highest total demand, and thus yielding the largest decrease in passenger costs when operated with a frequency of 2, is placed in a separate subroute. Secondly, an important observation is that all butterfly wings are sailed in opposite directions in the two time periods. This strengthens the initial assumption made in the DB heuristic, stating that different time periods may have an average total demand flowing in opposite directions between time periods, thus benefiting from reversed routes. As time periods 1 and 3 are considered time periods with a high degree of commuter travel, this result is not unexpected.

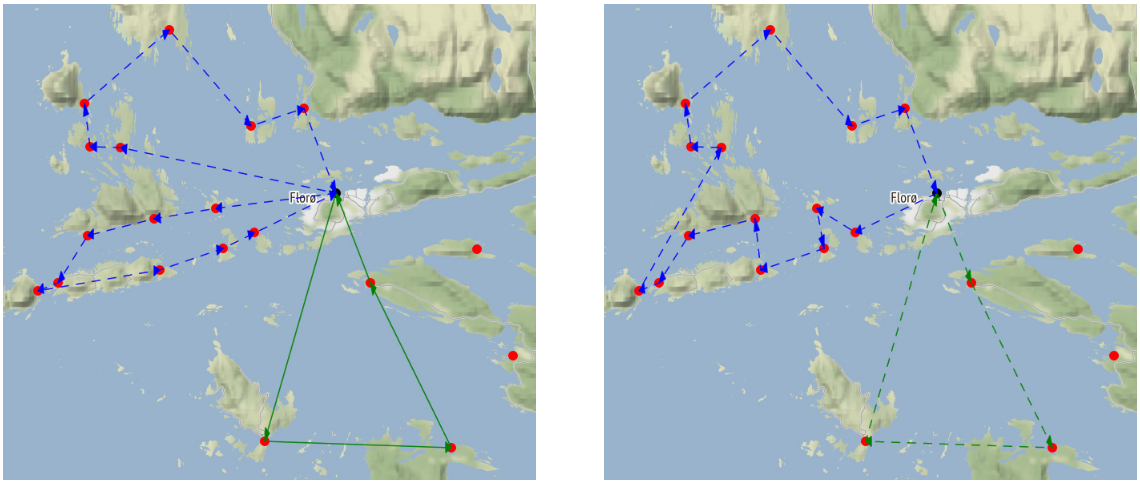

(a) `AP-ZE`: Time period 1 **(b)** `AP-ZE`: Time period 4

Figure 8.3: Route structures in AP-ZE for time period 1 and 4. Different colored lines indicate separate subroutes. Dashed lines indicate a frequency of 1, whereas solid lines indicate a frequency of 2.

8.4.3 Ability to skip ports

So far, skipping of ports has not been discussed thoroughly. The DB heuristic generates many possible solutions where ports are left unvisited in the AP instance. However, we can observe from Figure 8.2 that Stavang is the only port that is not visited in time period 3, the peak period. Further, it is observed from Table 8.7, that skipping Stavang incurs a cost of just 16 NOK per day, implying that it costs more than 16 NOK to sail by Stavang. Stavang is considered a mainland port, meaning that the cost of alternative modes of transportation is 500 NOK per passenger. For the island ports, there are no other options than to make use of the vessel service, and the cost of alternative modes of transportation was set to 100 000 NOK per passenger in Section 7.1. As a result, the island ports are only bypassed in periods when the demand at the island is zero, which could be observed in Figure 8.3, where Alvora is skipped. Following from the fact that the Florø area is an island community, very few ports are skipped in the test instances. By detaching from the real scenario and rather defining all ports as mainland ports, we can vary the cost of alternative transportation and inspect at which cost the different ports are visited. The number of rotations created increases greatly when we allow for routes where only a few ports are visited. We set a lower bound of at least seven ports being visited to limit the created number of rotations. In Figure 8.4, we demonstrate the relation between the number of visited ports and the cost of alternative transportation in the peak period. The visited ports may be seen in Table 8.15. In the table, an abbreviation for the port name is used. An overview explaining each abbreviation is found in Table D.1 in Appendix D.

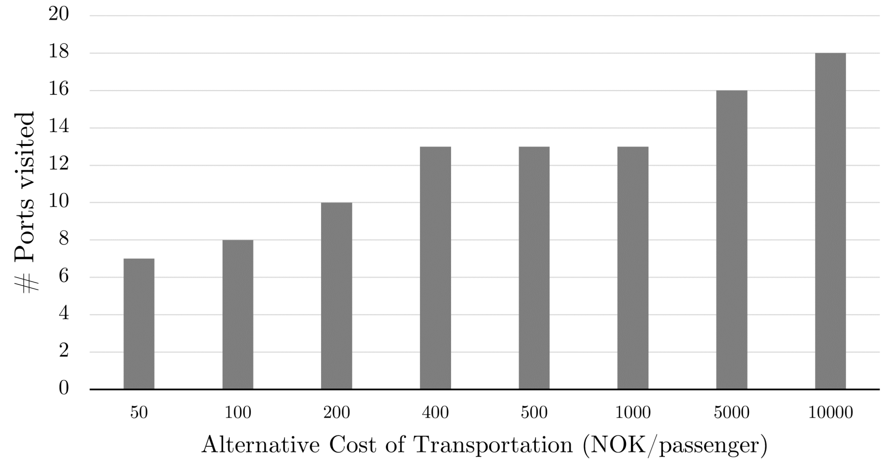

Figure 8.4: Ports visited for different values of the alternative cost of transportation, C^{ALT}, in the third period

C^{ALT}	*Ports visited*
50	Flo, Sva, Ask, Vil, Bar, Fan, Rog
100	Flo, Sva, Ask, Vil, Bar, Fan, Rog, Vei
200	Flo, Sva, Ask, Vil, Bar, Fan, Rog, Vei, Ska, Kin
400	Flo, Sva, Ask, Vil, Bar, Fan, Rog, Vei, Ska, Kin, Ner, Ann, Fer
500	Flo, Sva, Ask, Vil, Bar, Fan, Rog, Vei, Ska, Kin, Ner, Ann, Fer
1 000	Flo, Sva, Ask, Vil, Bar, Fan, Rog, Vei, Ska, Kin, Ner, Ann, Fer
5 000	Flo, Sva, Ask, Vil, Bar, Fan, Rog, Vei, Ska, Kin, Ner, Ann, Fer, Son, Vev, Bat
10 000	Flo, Sva, Ask, Vil, Bar, Fan, Rog, Vei, Ska, Kin, Ner, Ann, Fer, Son, Vev, Bat, Ske, Sel

Table 8.15: Ports visited for different values of C^{ALT}

In order to visit a port, the cost of sailing and picking up the passengers must be less than the cost of alternative transportation. In other words, the costs of the detour must be lower than the costs incurred by not visiting the port. The reasoning behind the order when adding ports to the solution as the cost parameter increases is complex. One could presume that the ports with the highest demand would be included first. This is to some extent true, but it also depends on the distance from the already included ports. To exemplify, the inclusion of a port would in some cases only be feasible if a bigger vessel or an extra port with infrastructure is invested in. Additionally, the inclusion of a port would also yield higher energy consumption.

By studying Figure 8.4 and Table 8.15, we can derive what it costs per passenger to visit the different ports. Ten ports are visited when the cost of alternative transportation is 200 NOK per passenger. When the cost increases to 400, the vessel service also visits *Nærøy*, *Annøy* and *Ferøyna*. Thus, to visit the three extra ports could be understood to cost less than 400 per passenger. When the alternative cost of transportation is 10 000, Stavang and Alvora are the only ports not visited out of the 20 ports in the area. Accordingly, the inclusion of these two ports will cost more than 10 000 per passenger.

8.5 Value of Optimizing Route Structure and Frequency Levels

To further analyze the value of optimizing route structures and service frequency levels of ZE vessel services, we investigate ZE solutions where the route and frequency levels are fixed to those in the best conventional solutions. We perform this analysis to estimate the economic gain of reconsidering routes and frequencies, when switching from conventional to ZE technologies, for real world passenger vessel services. To make the results comparable, we create three additional test instances, `AP-ZE-F`, `NP-ZE-F` and `HD-ZE-F`, where the route structures and frequency levels are fixed, prior to solving, to their values in the best solutions found for `AP-C`, `NP-C` and `HD-C`, respectively. Technically, this is done through an alteration of the rotation generation procedure in the DB heuristic (Section 6.3), only allowing the generation of rotations with the fixed route and frequency choices to be generated.

An immediate observation is the fact that `AP-ZE-F` and `HD-ZE-F` yield no solutions, due to infeasibility. Transferring the route and frequency decisions from conventional vessels directly to ZE vessels is not possible. These two instances have longer sailing distances than the `NP` instance. To complete long routes within the four hour time periods, the conventional vessels maintain a high speed. High speed levels are, however, problematic for ZE vessels. Higher speed implies a higher energy usage, again forcing longer charging times. As energy usage is a convex non-linear function with respect to sailing speed, and charging speed is linear with respect to time, higher sailing speed increases the total roundtrip time, when including the added charging times. The instances are infeasible as completing the required frequency is impossible within the time period duration of four hours. In the `AP-ZE` and `HD-ZE` test instances, this is solved by splitting the routes in two subroutes for each time period. This is however not an option in the `AP-ZE-F` and `HD-ZE-F` instances, as the single-subroute structures from the `AP-C` and `HD-C` instances are fixed. The result that conventional services require replanning to be operated by ZE vessels, is in line with Sundvor et al. (2021), finding only 15% of Norwegian high-speed vessels suitable for battery-electric propulsion in their current operation.

As the `AP-ZE-F` and `HD-ZE-F` are infeasible, they fail to provide a numerical estimate of the value of replanning the route and service frequencies for ZE operations. We may however analyze the results from `NP-ZE-F` to gain further insights. As the total sailing distances in the `NP` instance are shorter, ZE vessels are able to follow the route and frequency levels from the best conventional solution, keeping the model feasible. The fact that `NP-ZE-F` is feasible, is also expected, as the routes in the best solution to the `NP-ZE` only contain one subroute, in opposition to `AP-ZE` and `HD-ZE`. A breakdown of the cost terms in the best solution to the `NP-ZE-F` instance, is provided in Table 8.16.

	NP-ZE-F		
Cost term	Value (NOK)	% Change from NP-ZE	% Change from NP-C
Vessel investment	19 861	7.4 %	0.0 %
Infrastructure investment	2 388	0.0 %	*NA*
Energy cost	11 310	206 %	22.2 %
Crew cost	19 104	0.0 %	0.0 %
Cost of alt. transport	5 978	-42.0 %	0.0 %
Cost of waiting in port	4 616	-39.7 %	0.0 %
Transit cost	1 993	-4.4 %	-32.2 %
Total system cost	65 250	2.4 %	5.7 %

Table 8.16: Cost breakdown of the NP-ZE-F test instance

The fixation of the routes and frequency levels from the best conventional solution, increases two cost terms, when comparing NP-ZE-F to NP-ZE. The vessel investments are higher, as a different vessel type is acquired. Where vessel type 1S, with a battery capacity of 1 000 kWh is sufficient in NP-ZE, a 2 000 kWh battery is required to operate the fixed routes and frequency in NP-ZE-F. This corresponds to a vessel of type 1M, yielding a somewhat higher investment cost, but an equal crew cost. In addition to a different vessel type, service frequencies fixed to higher levels than for NP-ZE, result in a need for increased sailing speeds. Higher sailing speeds require more energy, thus increasing the energy cost substantially. The increased frequency levels in the NP-ZE-F compared to the NP-ZE, also contribute to reductions in the cost of alternative transportation and passenger cost from waiting in port. The increased speed levels needed to achieve the higher frequency levels also contribute to slightly lower transit costs, as the fixed route structures in NP-ZE-F include fewer stops in Florø, where a large portion of the passengers have their final destination. For illustrations of the differences in route structures, consider Appendix E.

The best solution found, yields an objective value of 65 250 NOK per day for the NP-ZE-F instance. This value is 2.4% higher than the best objective value found for the NP-ZE instance, giving an indication of the gain of replanning routes and frequencies. If we compare the best objective value for the NP-ZE-F to the conventional instance, NP-C, the abatement cost is 3 493 NOK per day, 5.7% of the NP-C objective value. The abatement cost when not fixing the route and frequency from the conventional instance, is only 1 972 NOK per day, or 3.2% of the NP-C objective value. A total of 1 521 NOK are saved every day when allowing the model to choose different routes and frequencies in the ZE test instance, totaling 555 165 NOK over a year, or 11.1 mNOK over the 20 years assumed life span of the vessels. An illustration of the relation between objective values for the three instances discussed in this paragraph, is provided in Table 8.16.

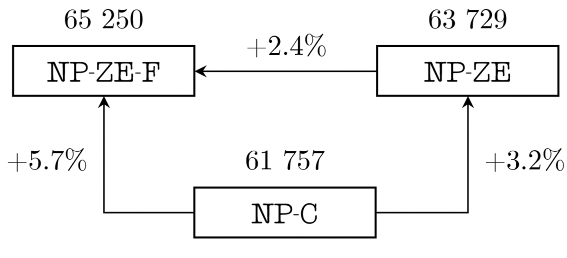

Figure 8.5: Overview of relation between total system costs for the NP-C, NP-ZE and NP-ZE-F test instances

8.6 Sensitivity Analyses

In this section we perform a sensitivity analysis of the electricity price and the passenger value of sailing time in Subsection 8.6.1 and Subsection 8.6.2, respectively. The analysis is performed on all instances i.e., `AP`, `NP` and `HD`. We use the DB heuristic with the same adequate parameters found in Section 8.1 in the analysis. It is time-consuming to run the DB heuristic multiple times, and in order to reduce the total run time, we perform the analysis by halving, doubling, and tripling the original value of the C^{VC} parameter.

8.6.1 Electricity price

In this subsection we perform a sensitivity analysis of the electricity price, C^{VC}_{pi}. The conventional instances are left out of the analysis due to apparent reasons. Originally, the electricity price summed to 3.1 NOK/kWh in all ports and in all periods (Section 7.1). Further, we execute the DB heuristic three times for each instance to perform the analysis. Once where the original electricity price is halved, once where it is doubled, and once where it is tripled. The relationship between objective value and electricity price is illustrated in Figure 8.6.

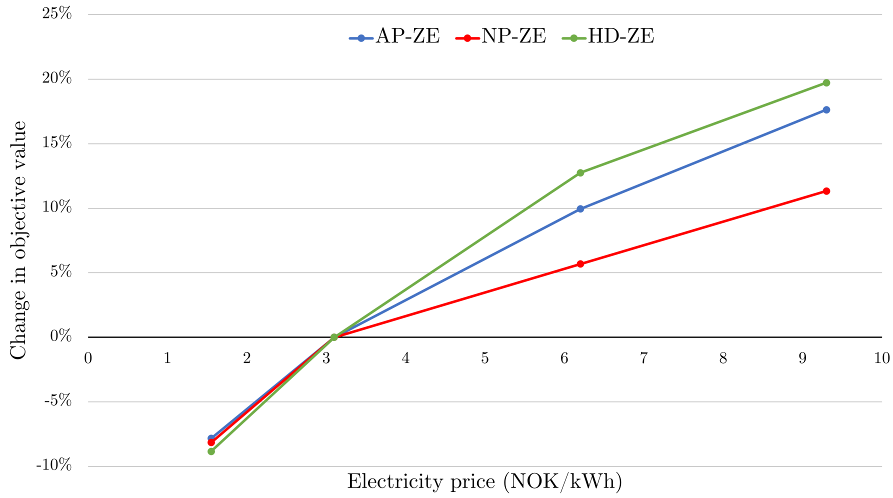

Figure 8.6: Objective value change as a function of the electricity price

We observe from Figure 8.6 that all instances have a lower objective value if the electricity price is halved. Further, only the `NP-ZE` instance becomes cheaper than its conventional counterpart. Recall from Section 8.3 that the difference in total costs between the ZE solution and conventional solution was the lowest for this instance. For the two other instances, a halving of the electricity price does not decrease the costs sufficiently to make the ZE solution cheaper than the conventional. We also observe from Figure 8.6 that the `HD-ZE` instance is the most sensitive to changes in the electricity price. This is caused by a higher overall sailing speed than in the other instances. The best solutions with an increased electricity price, is when sailing speed is reduced to lower the electric power consumption. In the best solution based on the original electricity price in the `HD-ZE` instance, periods 1 and 3 have a route consisting of two subroutes, both served with a frequency of two. Each subroute was served by one vessel only. When the electricity price is tripled, the solution includes the same route and subroute structure but the frequency is reduced to one in both periods. This enables the vessels to reduce their sailing speeds, and limit energy usage. Thus, the service is worsened for the passengers when the electricity price increases. This is displayed in Table 8.17.

	Value (NOK)	Increase from original cost
Operator cost	105 739	2.0 %
Passenger cost	73 455	59.6 %

Table 8.17: Operator and passenger cost in the `HD-ZE` instance with tripled electricity price

In Table 8.17, the operator and passenger costs for the `HD-ZE` instance, when the electricity price is tripled, is observed, along with the increase from the original electricity price. Even though the electricity price directly affects the operator, the indirect cost increase for the passengers is significantly higher.

8.6.2 Passenger cost of sailing

In this subsection, we conduct a sensitivity analysis of the value of passenger time while sailing, C^{SW}. This parameter is the coefficient in the eight term of the objective function (5.1). The analysis is performed on all instances, since the parameter is included in both the conventional and ZE models. In Section 7.1, the C^{SW} parameter was found to be 112 NOK/hour. We run the DB heuristic on all instances again to perform the analysis, when the parameter is halved, doubled, and tripled. The results are shown in Figure 8.7.

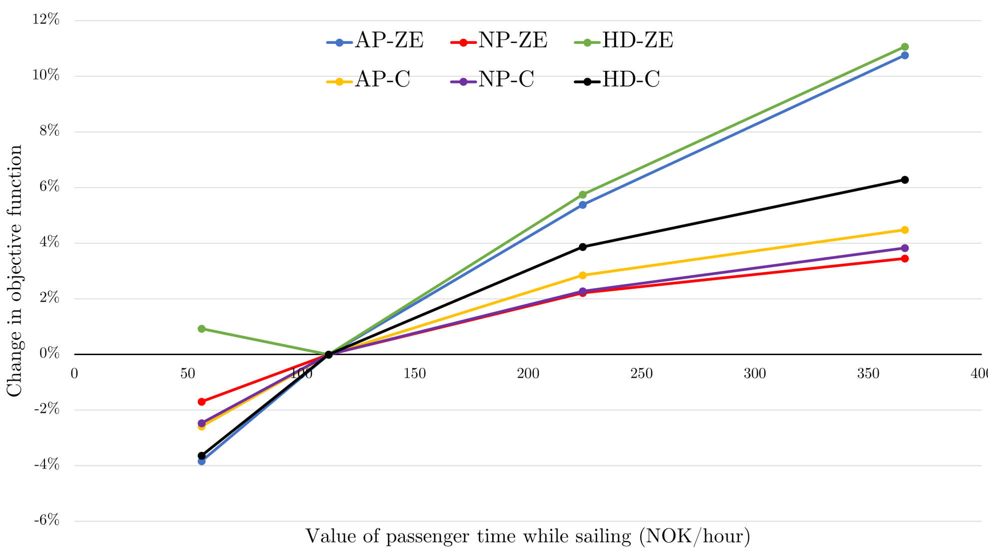

Figure 8.7: Change in objective function value for different value of passenger time while sailing

From Figure 8.7, one may observe that the ZE solutions are more sensitive to changes in the cost of sailing parameter, except for the `NP` instances. The difference between the `NP` instance and the other instances, is that the transit cost constitute a larger part of the objective value for `NP-C` than for `NP-ZE`. In both the `AP` and `HD` instances, the transit cost affects the objective value more in the ZE solutions. The transit costs' relative share of the objective values is shown in Table 8.7, Table 8.9 and Table 8.11 in Section 8.3.

In Figure 8.7, the graph, representing the increase in the objective value increase, has breakpoints for all instances. The increase in the coefficient of the transit cost causes the model to make different decisions to reduce the effects of the increased value of passenger time. An important consequence of the coefficient increase is that the vessels choose to sail faster to reduce the impact of the transit cost term. Increased sailing speeds increase the energy usage, and thus the energy cost. Hence, even though the transit cost is considered a passenger cost, it indirectly affects the operator costs.

When the cost parameter is reduced, the vessels in all instances sail slower since the coefficient in the transit cost term decreases. This causes a frequency reduction in most instances. The reduced frequency yields a worse service for the passenger and the unmet demand increases. In the peak period, the model seeks to uphold the frequency to reduce the amount of unmet demand. As the strategic decisions are based on the peak period, this could lead to worse solutions overall when the cost parameter is reduced, as observed for the HD-ZE instance. For the HD-ZE instance, a route structure consisting of two subroutes is chosen, where both subroutes are served with a frequency of two, at the original value of the cost parameter. When the cost parameter is reduced, so is the frequency in one of the subroutes, while a frequency of two is maintained in the other. In the subroute with a frequency of one, the vessel may reduce its speed, and hence a vessel with reduced battery capacity is chosen. Since the same vessel type must be used in all subroutes, infrastructure is installed in an extra port in the subroute with a service frequency of two, to maintain the required speed level. The extra infrastructure is not needed in the other time periods, since the vessels simply reduce their speed levels when the demand is lower. Thus, regardless of the reduction in the cost parameter, we obtain worse objective values overall in this instance. This exemplifies the possible disadvantage of the DB heuristic, basing the strategic decisions on the peak period.

8.7 Implications of Carbon Pricing

One important aspect of the choice between ZE and conventional energy carriers, is the environmental benefit of reduced CO_2-emissions. The taxation of CO_2-emissions has become a political instrument, intending to reduce emissions (The World Bank, 2014). This aspect is not accounted for in the ZEVSNDP. We thus present an analysis of the emissions from the different test instances and the implications of a carbon taxation scheme for these instances.

We calculate the CO_2-emissions based on the fuel consumption in the instances, and use a conversion rate of one kilogram fuel to 3.2 kilograms of CO_2 (Statistics Norway, 2017). Table 8.18 shows the daily fuel consumption and corresponding CO_2 emissions for each of the conventional test instances.

Instance	Fuel consumption (kg)	CO_2-emissions (kg)
AP-C	758.3	2426.6
NP-C	260.2	832.6
HD-C	905.3	2897.0

Table 8.18: Overview of daily CO_2-emissions in the different instances

From Table 8.18, we observe that the fuel consumption, and consequently the CO_2-emission are far higher for instances AP-C and HD-C, than for NP-C. In the former instances, longer distances are covered, naturally yielding a higher consumption. Furthermore, HD-C is operated at higher speeds than AP-C, which accounts for the difference between these instances.

When moving on to further analyses, a measure of particular interest is the abatement costs of transitioning to a ZE service. The abatement costs in this section describe the extra costs associated with transitioning from the best conventional service to the best ZE service, found by the DB heuristic. We further show the implications of different levels of CO_2-taxes. The relationship between tax levels and abatement costs for instances AP-C, HD-C and NP-C are shown in Figure 8.8 and Figure 8.9. NP-C is presented on its own, as the abatement costs are far lower than for the other two instances.

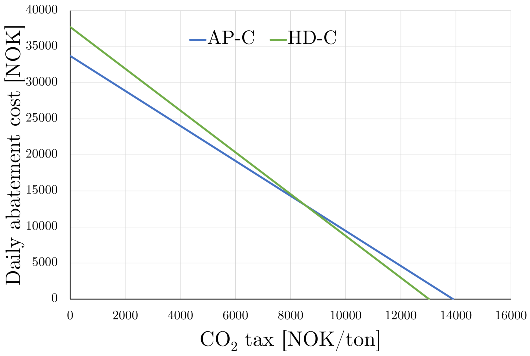

Figure 8.8: Abatement cost for the `AP` and `HD` instance

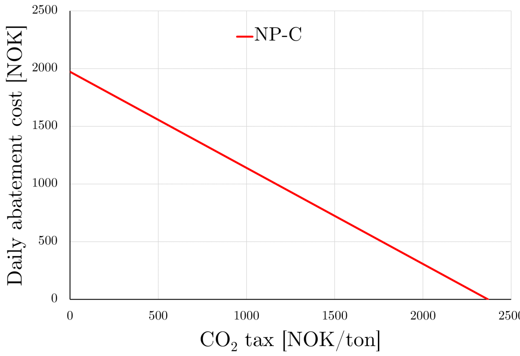

Figure 8.9: Abatement cost for the `NP` instance

Note that `HD-C` has a steeper reduction in the abatement costs than the `AP-C` when the tax increases. This is caused by higher emissions in this instance, making it more sensitive to changes in tax levels. The cost of the `NP-C` instance breaks even at a tax of 2 369 NOK/ton CO_2. Politicians and experts have expressed a goal of an emission taxation level of 2 000 NOK/ton by 2030 (Energi og Klima, 2021b), and the break-even cost is thus not far from this goal in the `NP` instance. It is thus a highly interesting test instance when transitioning to ZE operations in the Florø Basin. Table 8.19 shows the break-even CO_2-tax level for all instances in the first line. Further, the abatement costs at the tax level of 2 000 NOK/ton are shown in the second line. Finally, the third line presents the abatement costs with a tax level of 2 000 NOK/ton, relative to a zero tax rate. Table 8.19 shows that a tax level of 2000 NOK/ton is insufficient for all instances, and instances `AD` and `HD` in particular. However, if the tax level becomes higher, the `NP` test instance may be viable as a ZE alternative, when exclusively regarding costs.

Instance	`AD`	`NP`	`HD`
Break-even CO_2-tax (NOK/ton)	13 899	2 369	13 026
Abatement cost at 2 000 NOK/ton (NOK)	28 875	307	31 943
% of original abatement cost	85.6 %	15.6 %	84.6 %

Table 8.19: Overview of the effect of a CO_2-tax on the different instances

Chapter 9

Concluding Remarks

In this thesis, we have provided decision support for the implementation of Zero-Emission (ZE) passenger vessel services. In particular, we have focused on overcoming the technical and economic challenges imposed by a ZE transition. Firstly, we introduced the Zero-Emission Passenger Vessel Service Network Design Problem (ZEVSNDP) and presented a mathematical Mixed Integer Programming (MIP) model for solving the ZEVSNDP exact. The ZEVSNDP covers a broad range of decisions related to the implementation and operations of a ZE passenger vessel service. These include strategic decisions, such as investments in a vessel fleet and onshore charging infrastructure, and tactical decisions like route structures and service frequencies. In addition, operational decisions such as speed levels, charging times, waiting times, and passenger flow is included in the problem to provide feedback regarding the quality of the strategic and tactical decisions. The model is solved across multiple time periods, allowing for more granularity in the parameters, hence making it a more realistic and versatile tool for decision support.

The originally formulated MIP-model requires a pre-generated set of candidate routes and proves difficult to solve to optimality even for small instances. This requirement motivates the implementation and use of a Decomposition Based (DB) heuristic to analyze the problem further. The DB heuristic contains multiple steps, assessing pre-generated combinations of strategic and tactical decisions in a Linear Programming (LP) version of the original MIP-model. As discussed in Chapter 8, the DB heuristic is a result of the trade-off between high-quality solutions and short solution times.

Even though the DB heuristic performs better for the ZEVSNDP than the exact formulation, the method has some drawbacks. One of these is the dimensioning of strategic decisions based on the peak period, in instances where the demand pattern is volatile throughout the day. Even though this assumption may hold well when the demand pattern is relatively constant, the most promising routes found in the peak period are not necessarily optimal when there are large differences in demand over the course of a day. Proposed alterations to the DB heuristic are presented as future research in Chapter 10.

We adjusted the ZEVSNDP and the DB heuristic to reflect a conventional service instead of using ZE vessels. This adjusted model and solution method were used to compare the results of the ZEVSNDP, and thus served as a premise for decision support. Both the ZE and conventional versions of the model were solved using three test instances. The test instances are all based on the geographical area of Florø, situated on the west coast of Norway. This area is characterized by multiple islands surrounding the urban hub of Florø, located on the mainland. The test instances were created by varying the considered ports, with `AP` including all ports, `NP` only including the ports in close proximity to Florø, and `HD` only including the ports with the highest total demand to and from Florø. The three test instances allowed for diverse analyses and results.

The conducted analyses show that the ZE solutions have higher total costs than the conventional solutions in all instances. The near ports instance, however, diverged from the two others. In this instance, the costs were comparable to the conventional solution. The main driver of the abatement costs, is the need for an additional vessel, and associated crew costs, in the ZE instances of AP and HD, caused by their longer sailing distances. A general result is thus that transferring to ZE operations is more costly for services covering large geographical areas.

We observed a general divergence in route choices and frequencies between the same test instances in the conventional and ZE solutions. The conventional vessels managed to complete longer routes within a given time period. This is caused by their ability to maintain a higher speed, as this has no implications for charging time. On the contrary, Zero-Emission vessels are not as well suited for longer routes due to their frequent charging requirements. As a result, the feasible (and thus the best) routes, are shorter in the ZE instances. To illustrate the matter further, the optimal routes in the conventional solutions are infeasible for their ZE counterparts in the AP and HD test instances.

The conducted analyses indicated that the route and frequency decisions are highly influenced by demand. Varying demand patterns throughout the day, caused a wide variety of route and frequency decisions across time periods. More specifically, the demand influences the number of butterfly wings in the routes, the operating frequency, and the sailing direction. We observed in the HD case that the number of butterfly wings increased because many passengers travel to or from the central hub. This could be generalized to other geographical areas, containing a centrally placed hub with high levels of demand compared to other ports. Further, high demand yields increased service frequencies, to decrease the passenger cost incurred by waiting and alternative transportation. Finally, the sailing direction follows the average direction of demand, and thus varies between time periods.

In the conclusion of the computational study, we look to the future and the implications of a stipulated increase in CO_2-taxation. Even though all our ZE instances were costlier than the conventional alternative, these conclusions may change with a taxation scheme on CO_2. Governments and experts have expressed a goal of a tax on emissions of 2 000 NOK/ton by 2030. A tax scheme at this level, would make the abatement costs of all instances smaller. The impact is, however, substantially larger for the NP test case, as the best conventional solution is less carbon intense than in the two other test instances, AP and HD. For the two latter instances, CO_2-taxation must be set at a far higher level to even up the abatement costs.

Chapter 10

Future Research

This chapter summarizes suggestions for further research that may be conducted on the basis of this thesis. The main focus of this chapter is placed on the possible improvements to the Decomposition Based heuristic (DB heuristic), proposed in Chapter 6, but there is however, room for general extensions to the problem itself, defined in Chapter 3, and the mathematical formulation, presented in Chapter 5, improving its capabilities as a decision support tool. To structure the proposals for future research, Section 10.1 first covers possible extensions to the ZEVSNDP and its mathematical formulation. Further, Section 10.2 discusses changes and improvements to the DB heuristic.

10.1 Problem and Model Extensions

Considering the modeling of the ZEVSNDP itself, as presented in Chapter 5, many aspects could be added to the problem to extend its reach. We propose four possible extensions: including the possibility of more than one vessel type, introducing additional energy carriers, including crowding costs and allowing for "on-call" port stops.

Multiple vessel types

The version of the ZEVSNPD proposed in Chapter 5 is restricted to choosing one specific vessel type. This is initially assumed to be a practical assumption to limit complexity and to ensure an equal service across different departures. One could however consider adding the possibility for selecting multiple vessel types, instead placing the limit of one vessel type within the subroutes. This would enable subroutes with varying demand and/or service frequency to be operated in a more efficient manner. A scenario where this could be an interesting possibility is if two subroutes in a route exhibits very different demand levels. Having the opportunity of selecting multiple vessel types could provide a solution with a small vessel in the subroute with low demand, and a larger one in the subroute where demand is higher. Allowing for multiple vessel types across subroutes makes the ZEVSNDP applicable to a wider range of real world instances.

Multiple energy carriers

As thoroughly described in Chapter 3, battery-electric vessels is not the only option to a Zero-Emission (ZE) passenger service. The mathematical formulation in Chapter 5 is based upon battery-electric vessels, but alterations could easily be made to allow the model to consider energy carriers such as hydrogen or ammonia. A model where these types of ZE energy carriers are used may be more similar to the conventional vessel model presented in Section 5.5, but additional requirements for onshore infrastructure is needed. Together with the aforementioned extension, one could imagine a vessel service operated optimally as a hybrid between energy carriers, e.g., part battery-electric and part hydrogen. Energy carriers such as hydrogen and ammonia has not yet played a big role in ZE passenger transportation, but if it were to do so in the future, alterations to the model enabling this, would be of great value.

Introducing crowding costs

An interesting topic, not yet introduced to the ZEVSNDP, is the concept of crowding costs. Crowding costs are, within public transportation literature, the experienced passenger disutility of traveling caused by crowding. The more passengers on board, the higher the crowding cost, and vice versa. For a more detailed description of crowding costs and its implications, we refer to Batarce et al. (2016) and de Palma et al. (2017). In the ZEVSNDP, a crowding cost could be introduced by letting the passenger cost of sailing, C^{PW}, be a function of the number of passengers on board, relative to the vessel capacity. This would penalize filling the vessels to their maximum capacity, and incentivize increasing capacity.

"On-call" port visits

A feature of many vessel services observed today, is the concept of "on-call" port stops. Passengers to and from such ports need to notify the operators about their travel plans prior to departing. This concept is useful for ports with low demand, as no stop is required if no passenger is planning to enter or exit the vessel in that location. By visiting ports "on-call" only, operators are able to plan vessel schedules containing more stops than if they had to berth in every single one. Using statistics, and the demand data already collected, probabilities for a passenger wanting to travel to or from a port could be calculated. Based on this an extension incorporating stochastic modeling could be implemented. Introducing a subset of "on-call" ports to the predefined routes would enable longer routes served more efficiently, and could thus be an interesting extension to the ZEVSNDP.

10.2 Improvements to the Decomposition Based heuristic

As discussed in Section 8.2, the DB heuristic from Chapter 6 provides good solutions to the ZEVSNDP for relatively short run times. However, being based on heuristics, there are several areas of improvement to the solution method. In this section we present three specific points of improvement, whereas the first two are concerned with the use of the peak demand period for setting strategic decisions and sorting out promising routes, while the last point covers a more thorough restructuring of the solution method, utilizing a search heuristic.

Individually evaluating promising routes for each time period

A possible change to the DB heuristic is to generate promising routes for each time period. The current solution method uses the peak period to dimension not only the strategic decisions, but also the set of candidate routes, used as input when solving the other time periods. This could, for certain instances, lead to a suboptimal set of candidate routes. In particular, this poses a problem if the peak demand period has very different characteristics from the other time periods. To overcome this challenge, candidate routes could be generated separately for each instance. This would involve generating rotations for each time period, however limiting the generation to the strategic decisions set for the peak period. Further, a separate proxy evaluation and sorting procedure would be necessary, before the sorted list for each time period would be iterated through and evaluated as LPs. Doing this for each time period would mitigate the final single-period MIP-model, as each time period is assigned operational decisions by the best solution to the LP. This procedure could provide even better solutions to the ZEVSNDP, but may also come at a cost. Generating rotations, proxy evaluating and sorting them, prior to revealing their true objective value through successive LP-model runs, is time consuming. Although mitigating the final step of solving a single-period MIP, the total runtime is likely to increase. The uncertainty around total runtime for the DB heuristic was the initial reason for not evaluating promising candidate routes for each time period separately. However, further work on such a procedure could prove it effective, in particular if the number of time periods is low.

Avoid using the peak period to dimension strategic decision

A central assumption of the DB heuristic proposed in Chapter 6, is that using the time period with the highest total demand to dimension the strategic decisions, is preferable. As mentioned in Chapter 8, this is however not always the case. Basing the strategic decisions on the period with the highest total demand could lead to overestimating the vessel size, fleet size or number of charging points required for optimal operations across the entire day. This constitutes an issue in particular if the demand has a volatile profile, varying substantially between time periods. A possible alteration of the DB heuristic is to base the strategic decisions on an average of all time periods, rather than using the peak alone. This would lead to strategic decisions optimized for a lower total demand, increasing the cost stemming from the peak period, but decreasing the overall costs. It is however not given that the total system costs of the entire service decreases, as the relative relationship between the time periods is unknown prior to solving the model.

Using more advanced methods for solving the ZEVSNDP

A final option for further research inspired by this thesis, is a more severe restructuring of the DB heuristic solution method proposed in Chapter 6. Although providing relatively good solutions within an acceptable time frame, the DB heuristic may prove difficult to scale, as number of routes and rotations grow rapidly, e.g., when allowing for butterfly routes with more than four wings. Abandoning the decomposition based method, could pave the way for other heuristic approaches. The opportunities are many, but combining a construction heuristic with an improvement heuristic based on any kind of search algorithm, such as for example an ALNS (Adaptive Large Neighborhood Search) algorithm (Ropke & Pisinger, 2006), could prove promising. This could allow for a solution method spending less run time constructing routes and rotations not improving the solution. Another interesting feature of using a search algorithm is the ability to test a wider range of route structures. The proposed solution method from Chapter 6 is limited to simple cycles and butterfly routes in its current form, and although performing well for the test instances presented in this thesis, this could be drawback when considering other geographical areas. If classes of promising route structures are hard to identify, an approach utilizing a search based heuristic may be better suited to find good solutions.

Bibliography

Agency, I. E. (2019). *The future of hydrogen - seizing today's opportunities.*

Andersson, H., Fagerholt, K. & Hobbesland, K. (2015). Integrated maritime fleet deployment and speed optimization: Case study from roro shipping. *Computers and Operations Research*, *55*, 233–240.

Arbex, R. & da Cunha, C. (2015). Efficient transit network design and frequencies setting multi-objective optimization by alternating objective genetic algorithm. *Transportation Research Part B: Methodological*, *81*, 355–376.

Aslaksen, I., Svanberg, E., Fagerholt, K., Johnsen, L. & Meisel, F. (2020). Ferry service network design for kiel fjord. *Lecture Notes in Computer Science (including subseries Lecture Notes in Artificial Intelligence and Lecture Notes in Bioinformatics)*, *12433 LNCS*, 36–51.

Aslaksen, I., Svanberg, E., Fagerholt, K., Johnsen, L. & Meisel, F. (2021). A combined dial-a-ride and fixed schedule ferry service for coastal cities. *Transportation Research Part A: Policy and Practice*, *153*, 306–325.

Azam Marine. (2022). *Kilimanjaro iv.* Retrieved 21/05/2022, from https://azammarine.com/catamarans/kilimanjaro-iv/

Batarce, M., Muñoz, J. C. & de Dios Ortúzar, J. (2016). Valuing crowding in public transport: Implications for cost-benefit analysis. *Transportation Research Part A: Policy and Practice*, *91*, 358–378.

Bergen Bunkers AS. (2022). *Daily market update.* Retrieved 20/05/2021, from https://www.bergenbunkers.no/wp-content/uploads/2022/05/pdf-markets-11.pdf

Brødrene Aa AS. (2017). *Brødrene aa wins contract for three high speed catamarans.* Retrieved 14/12/2021, from https://www.braa.no/news/brdrene-aa-wins-contract-for-three-high-speed-catamarans

Brouer, B. D., Alvarez, J. F., Plum, C. E. M., Pisinger, D. & Sigurd, M. M. (2014). A base integer programming model and benchmark suite for liner-shipping network design [Cited by: 152; All Open Access, Green Open Access]. *Transportation Science*, *48*(2), 281–312.

Brown, T. (2017). *Arpa-e's vision for carbon neutral liquid fuels.* Retrieved 14/12/2021, from https://www.ammoniaenergy.org/articles/arpa-es-vision-for-carbon-neutral-liquid-fuels/

Buba, A. T. & Lee, L. S. (2019). Hybrid differential evolution-particle swarm optimization algorithm for multiobjective urban transit network design problem with homogeneous buses [Cited by: 8; All Open Access, Gold Open Access, Green Open Access]. *Mathematical Problems in Engineering*, *2019*.

Bunkerspot. (2022). *Asia pacific: Fully electric fast passenger ships set to join auckland's ferry fleet.* Retrieved 21/05/2022, from https://www.bunkerspot.com/asia/56120-asia-pacific-fully-electric-fast-passenger-ships-set-to-join-auckland-s-ferry-fleet

Ceder, A. (2007). *Public transit planning and operation: Theory, modeling and practice.*

Ceder, A. & Wilson, N. H. (1986). Bus network design. *Transportation Research Part B: Methodological*, *20*(4), 331–344.

Chuah, S. P., Wu, H., Lu, Y., Yu, L. & Bressan, S. (2016). Bus routes design and optimization via taxi data analytics. *Proceedings of the 25th ACM International on Conference on Information and Knowledge Management*, 2417–2420.

de Palma, A., Lindsey, R. & Monchambert, G. (2017). The economics of crowding in public transport. *Journal of Urban Economics*, *101*, 106–122.

DNV GL. (2019). *Comparison of alternative marine fuels.*

Dr. Ing. Yves Wild Ingenieurbüro GmbH. (2005). *Determination of energy cost of electrical energy on board sea-going vessels.* Retrieved 11/12/2021, from http://www.effship.com/PartnerArea/MiscPresentations/Dr_Wild_Report.pdf

Elsevier. (2021). *Scopus - your brilliance connected.* Retrieved 15/12/2021, from https://www.elsevier.com/__data/assets/pdf_file/0017/114533/Scopus-fact-sheet-2022-web.pdf

Energi og Klima. (2021a). *Elektriske bilferger i norge.* Retrieved 10/11/2021, from https://energiogklima.no/elektriske-bilferger-i-norge/

Energi og Klima. (2021b). *Klimameldingen: Varsler kraftig økning i co_2-avgiften.* Retrieved 12/12/2021, from https://energiogklima.no/nyhet/dette-vet-vi-om-innholdet-i-regjeringens-klimamelding/

Energi og Klima. (2022). *Utrulling av elbiler.* Retrieved 30/05/2022, from https://energiogklima.no/klimavakten/utrulling-av-elbiler/

Fagerholt, K., Laporte, G. & Norstad, I. (2010). Reducing fuel emissions by optimizing speed on shipping routes. *Journal of the Operational Research Society*, *61*(3), 523–529.

Fjellstrand AS. (2014). *Zerocat tm 120.* Retrieved 14/12/2021, from http://fjellstrand.no/flyers/flyer_1696.pdf

Flügel, S., Halse, A. H., Hulleberg, N., Jordbakke, G. N., Veisten, K., Sundfør, H. B. & Kouwenhoven, M. (2020). *Verdsetting av reisetid og tidsavhengige faktorer. dokumentasjonsrapport til verdsettingsstudien 2018-2019.* Institute of Transport Economics.

Havre, H., Lien, U. & Ness, M. (2021). *Planning for zero emission passenger vessels.* NTNU.

Ianssen, C., Ianssen, E. & Sandblost, T. (2017). *Battery/fuel cell fast ferry.* Retrieved 06/11/2021, from https://www.nho.no/siteassets/nox-fondet/rapporter/2018/nox-report---rev-8.doc-002.pdf

IMO. (2020). *Fourth imo greenhouse gas study.*

International Energy Agency. (2022). *Transport improving the sustainability of passenger and freight transport.* Retrieved 30/05/2022, from https://www.iea.org/topics/transport

Klier, M. & Haase, K. (2015). Urban public transit network optimization with flexible demand. *OR Spectrum*, *37*(1), 195–215.

Klima- og miljødepartementet. (2021). *Norges kyst og havområder.* Retrieved 15/12/2021, from https://www.regjeringen.no/no/tema/klima-og-miljo/naturmangfold/innsiktsartikler-naturmangfold/hag-og-kyst---behov-for-a-sikre-artsmangfold/id2076396/

Klima- og miljødepartementet. (2022). *Klimaplan for 2021–2030.*

Kobayashi, H., Hayakawa, A., Somarathne, K. K. A. & Okafor, E. C. (2019). Science and technology of ammonia combustion. *Proceedings of the Combustion Institute*, *37*(1), 109–133.

Lai, M. & Lo, H. K. (2004). Ferry service network design: Optimal fleet size, routing, and scheduling. *Transportation Research Part A: Policy and Practice*, *38*(4), 305–328.

Li, J.-Q., Borenstein, D. & Mirchandani, P. B. (2008). Truck scheduling for solid waste collection in the city of porto alegre, brazil. *Omega*, *36*(6), 1133–1149.

Liu, Y., Feng, X., Yang, Y., Ruan, Z., Zhang, L. & Li, K. (2022). Solving urban electric transit network problem by integrating pareto artificial fish swarm algorithm and genetic algorithm [Cited by: 2]. *Journal of Intelligent Transportation Systems: Technology, Planning, and Operations*, *26*(3), 253–268.

Marine Link. (2022). *Stockholm electric fast ferry routes announced*. Retrieved 21/05/2022, from https://www.marinelink.com/news/stockholm-electric-fast-ferry-routes-496546

Miller, C. E., Tucker, A. W. & Zemlin, R. A. (1960). Integer programming formulation of traveling salesman problems. *J. ACM*, *7*(4), 326–329.

Norled. (2018). *Nå har den elektriske ferjen mf «ampere» gått 6 x ekvator*. Retrieved 06/11/2021, from https://www.norled.no/nyheter/ampere---6-ganger-rundt-ekvator/

Norwegian Ministry of Foreign Affairs. (1994). *Om sikkerhet og forhold som har betydning for norsk hurtigbåtnæring*. Retrieved 02/12/2021, from https://www.regjeringen.no/contentassets/bee23e85425c4fca84346e100bf745c7/no/pdfa/nou199419940009000dddpdfa.pdf

NRMA. (2022). *5 reasons why the ferry is the best way to commute in sydney*. Retrieved 21/05/2022, from https://www.mynrma.com.au/benefits/my-fast-ferry/5-reasons-why-the-ferry-is-the-only-way-to-commute-in-sydney

Offshore Energy. (2022). *Uber boat building uk's 1st hybrid high-speed passenger ferry*. Retrieved 21/05/2022, from https://www.offshore-energy.biz/uber-boat-building-uks-1st-hybrid-high-speed-passenger-ferry/

Reinhardt, L. & Pisinger, D. (2012). A branch and cut algorithm for the container shipping network design problem. *Flexible Services and Manufacturing Journal - FLEX SERV MANUF J*, *24*.

Rinaldi, M., Parisi, F., Laskaris, G., D'Ariano, A. & Viti, F. (2018). Optimal dispatching of electric and hybrid buses subject to scheduling and charging constraints. *IEEE Conference on Intelligent Transportation Systems, Proceedings, ITSC*, *2018-November*, 41–46.

Ritari, A., Spoof-Tuomi, K., Huotari, J., Niemi, S. & Tammi, K. (2021). Emission abatement technology selection, routing and speed optimization of hybrid ships. *Journal of Marine Science and Engineering*, *9*(9).

Rogaland Fylkeskommune. (2021). *Byggestart for verdens første hurtigbåt med nullutslipp*. Retrieved 06/11/2021, from https://www.rogfk.no/aktuelt/byggestart-for-verdens-forste-hurtigbat-med-nullutslipp.110237.aspx

Rogge, M., van der Hurk, E., Larsen, A. & Sauer, D. U. (2018). Electric bus fleet size and mix problem with optimization of charging infrastructure. *Applied Energy*, *211*, 282–295.

Ropke, S. & Pisinger, D. (2006). An adaptive large neighborhood search heuristic for the pickup and delivery problem with time windows. *Transportation Science*, *40*, 455–472.

Sassi, O. & Oulamara, A. (2014). Electric vehicle scheduling and optimal charging problem: Complexity, exact and heuristic approaches. *International Journal of Production Research*, *55*.

Shang, H., Liu, Y., Huang, H. & Guo, R. (2019). Vehicle scheduling optimization considering the passenger waiting cost. *Journal of Advanced Transportation*, *2019*.

Statistics Norway. (2017). *Emission factors used in the estimations of emissions from combustion*. Retrieved 12/12/2021, from https://www.ssb.no/_attachment/291696/binary/95503?_version=547186

Straume, A. & Bertelsen, D. (2015). *Documentation of calculation modules in effekt 6.6*. Norwegian Public Roads Administration.

Sundvor, I., Thorne, R. J., Danebergs, J., Aarskog, F. & Weber, C. (2021). Estimating the replacement potential of norwegian high-speed passenger vessels with zero-emission solutions. *Transportation Research Part D: Transport and Environment*, *99*, 103019.

Teknisk Ukeblad. (2021). *Grenser flyttes med verdens første hydrogenferge*. Retrieved 15/12/2021, from https://www.tu.no/artikler/grenser-flyttes-med-verdens-forste-hydrogenferge/507556

The World Bank. (2014). *Pricing carbon*. Retrieved 12/12/2021, from https://www.worldbank.org/en/programs/pricing-carbon

Thun, K., Andersson, H. & Christiansen, M. (2017). Analyzing complex service structures in liner shipping network design. *Flexible Services and Manufacturing Journal*, *29*(3), 535–552.

Totten, J. L. (2016). Cross-elasticities in frequencies and ridership for urban local routes. *Journal of Public Transportation*, *19 (3)*, 117–125.

Tveter, E., Rødseth, K., Hoff, K., Rødal, J. & Thune-Larsen, H. (2020). Forslag til nye kriterier for båter i inntektssystemet for fylkeskommunene. *Flexible Services and Manufacturing Journal - FLEX SERV MANUF J*, *24*, 90.

US Department of Energy. (2021). *Fuel cells*. Retrieved 07/11/2021, from energy.gov/eere/fuelcells/fuel-cells

Villa, D., Montoya, A. & Herrera, A. (2020). The electric riverboat charging station location problem. *Journal of Advanced Transportation*, *2020*.

Voanews. (2022). *Hydrogen-powered passenger boat to launch in san francisco*. Retrieved 21/05/2022, from https://learningenglish.voanews.com/a/hydrogen-powered-passenger-boat-to-launch-in-san-francisco/6543920.html

Wang, Z., Lo, H. & Lai, M. (2008). Mixed-fleet ferry routing and scheduling. *Lecture Notes in Economics and Mathematical Systems*, *600*, 181–194.

Wardman, M. (2001). A review of british evidence on time and service quality valuation. *Transportation Research Part E: Logistics and Transportation Review*, *37*, 107–128.

Wardman, M., Chintakayala, V. P. K. & de Jong, G. (2016). Values of travel time in europe: Review and meta-analysis. *Transportation Research Part A: Policy and Practice*, *94*, 93–111.

WETA. (2018). *Weta awards $13 million contract for new high-speed ferry*. Retrieved 02/12/2021, from https://weta.sanfranciscobayferry.com/sites/sfbf/files/pr/MANewVessel181004.pdf

Zhang, L., Zeng, Z. & Gao, K. (2021). Optimal design of mixed charging station for electric transit with joint consideration of normal charging and fast charging. *Smart Innovation, Systems and Technologies*, *231*, 85–94.

Zittel, W., Wurster, R. & Bolkow, L. (1996). Advantages and disadvantages of hydrogen. *Hydrogen in the Energy Sector*.

Appendix A

Literature Search Procedures and Results

A.1 Search process for Public Transport Networks

In the Scopus search for public transport literature, we let the first set of phrases be the *Transit Network Problem* and its sub-problems, *Transit Network Design*, *Frequency Setting* and *Vehicle Scheduling Problem*. We separated these terms with "OR" to make sure that at least one of the phrases was included. Additionally, we used the phrases *Public transport* and *Maritime transport*, again separated with "OR". The first set of words was chosen in order to discover articles within the relevant operations research topic, while the second set was selected to find articles within the relevant industry.

The initial search returned 107 articles. We further reduced the number of articles by limiting the result to English articles exclusively, within the subjects *Engineering*, *Mathematics* and *Decisions Sciences*, narrowing relevant articles to 81. Furthermore, we excluded the subjects *Material Sciences* and *Physics and Astronomy*, due to irrelevance to the problem. This left 77 articles. These articles' titles and abstracts were read in order to select the most relevant. This manual procedure resulted in two pieces for further review. After reading the articles and their citations, two additional public transport articles were deemed relevant.

The procedure above yielded no articles combining public transport and passenger vessels. Hence, we performed a second literature search to find articles covering waterborne public transportation. The first set of words in this search was *Passenger vessels* and *Ferry*, forcing transportation by sea. The second set of words was *Operations research* and *Optimization*, in order to obtain articles within the relevant study field. This time we added a third set of words: *Route*, *Schedule* and *Network*, to narrow the search to routing and scheduling problems. The search resulted in 124 articles. The same filters as in the previous search were applied, leaving 77 articles. The 77 articles' titles and abstracts were read, as before, to identify the most relevant articles. Only two articles of interest were found, but after reading the citations, one additional article was included for the review. The entire search procedure is illustrated in Figure A.1.

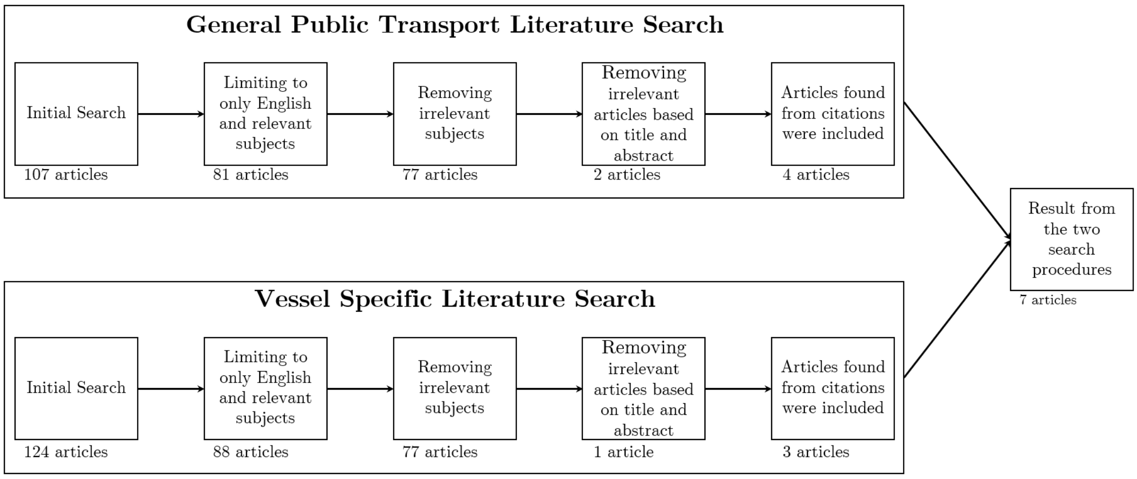

Figure A.1: Illustration of the Search Procedure covering Public Transport Literature

A.2 Search Procedure for subproblem literature

For the sub-problem, considering vessel scheduling to a fixed route, the initial set of phrases were chosen to be *Vessel scheduling*, *Vehicle scheduling*, *Vessel assignment* and *Vehicle assignment*, separated by the "OR"-operator. The other set of words only contained the phrase *Fixed route*. This search returned eight articles. After reading the titles and the abstracts, none of the articles were deemed relevant to our problem. We concluded that the second string only containing *Fixed route* was too restrictive, thus confining the search results. Hence, we performed another search with just the first string of words. The initial search gave 1 571 articles. We limited the relevant subjects to *Engineering*, *Mathematics* and *Decisions Science* and excluded irrelevant subjects such as *Material Science*, *Earth and Planetary Sciences*, etc. This resulted in 1 161 articles. Further, by considering the articles including the keywords *Optimization*, *Decision Making* and *Operations Research* we were left with only 261. After reading the headlines and abstracts, three articles were chosen for a full review.

To address the sub-problem concerning speed optimization for vessels, the first set of words only contained *Speed Optimization*. In order to enforce resulting articles to consider waterborne means of transportation, the second string was *Vessel*, *Ship* and *Maritime transport*. The search returned 193 articles. After limiting the articles to *Engineering*, *Mathematics* and *Decision Sciences*, and excluding articles within irrelevant subjects such as *Chemistry*, *Physics* etc., we were left with 163 articles. Selection based on the titles and abstracts of the articles yielded three articles for further review.

To address the last sub-problem, namely finding the optimal charging infrastructure locations, the first set of words only contained *Location Problem*. The second set of words consisted of *Charging* and *Infrastructure* to get problems that covered the relevant industry. The third set included *Optimization*, *Linear programming* and *Operations Research*, to only consider articles within operations research. The search resulted in 145 articles. After limiting the search to English articles within the subject areas *Engineering*, *Mathematics* and *Decision Sciences*, we were left with 116 articles. Further, the titles and abstracts of the 116 articles were read, and two articles were chosen for further review. The entire search procedure of the sub-problem related literature is illustrated in Figure A.2

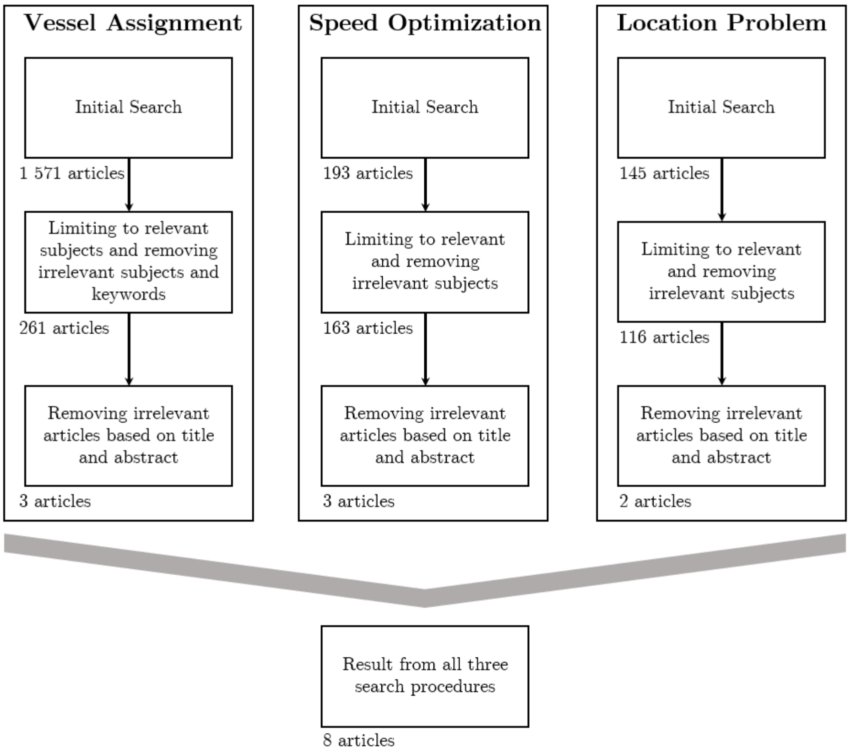

Figure A.2: Search procedure for literature covering relevant sub-problems

A.3 Results of Literature Review

#	Article	Mode of transportation
1	Shang et al. (2019)	Bus
2	Rinaldi et al. (2018)	Electric bus
3	Klier and Haase (2015)	General public transport
4	Aslaksen et al. (2020)	Ferry
5	Lai and Lo (2004)	Ferry
6	Aslaksen et al. (2021)	Ferry
7	Chuah et al. (2016)	Bus
8	Buba and Lee (2019)	Bus
9	Liu et al. (2022)	Electric bus
10	Arbex and da Cunha (2015)	Bus
11	Li et al. (2008)	Garbage truck
12	Sassi and Oulamara (2014)	Electric vehicle
13	Zhang et al. (2021)	Bus
14	Andersson et al. (2015)	Cargo ship
15	Ritari et al. (2021)	Hybrid cargo ship
16	Fagerholt et al. (2010)	Cargo ship
17	Villa et al. (2020)	Electric river boat
18	Rogge et al. (2018)	Electric bus
19	Brouer et al. (2014)	Cargo ship
20	Thun et al. (2017)	Cargo ship
21	This thesis	Electric HSV

Table A.1: Overview of the results from the literature review

#	Objective	Model	Sol. method	Demand	Time	Speed select.	Freq.	Energy constrs.
1	Min total system cost	Non-linear	Heuristic	N/A	Cont.	No	Yes	No
2	Min operator cost	Linear	Exact	N/A	Discrete	No	No	Yes
3	Max transported passengers	Linear	N/A	Endog.	N/A	No	Yes	No
4	Max customer satisfaction	Linear	Heuristic	Exog.	N/A	No	Yes	No
5	Min total system cost	Linear	Heuristic	Exog	Discrete	No	No	No
6	Max user utility	Linear	Heuristic	Exog.	N/A	No	Yes	No
7	Min distance	Linear	Heuristic	N/A	Cont.	No	No	No
8	Min total system cost	Linear	Heuristic	Exog.	Cont.	No	Yes	No
9	Min total system cost	Non-linear	Heuristic	Exog.	Cont.	No	Yes	Yes
10	Min total system cost	Linear	Heuristic	Exog.	N/A	No	Yes	No
11	Min operator cost	Linear	Heuristic	N/A	N/A	No	No	No
12	Max distance / Min charging cost	Linear	Heuristic	N/A	Discrete	No	No	Yes
13	Min operator cost	Linear	Exact	N/A	Discrete	No	No	Yes
14	Min operator cost	Linear	RH heuristic	N/A	Cont.	Yes	No	No
15	Min operator cost	Non-linear	Heuristic	N/A	Cont.	Yes	No	Yes
16	Min fuel emission	Both	Exact	N/A	Discrete	Yes	No	No
17	Min operator cost	Linear	Exact	N/A	Cont.	No	No	Yes
18	Min operator cost	Linear	Heuristic	N/A	Cont.	No	No	Yes
19	Max operator profits	Linear	Column generation	N/A	Cont.	Yes	Yes	No
20	Min operator cost	Linear	Branch & price	N/A	Cont.	No	Yes	No
21	Min total system cost	Linear	Heuristic	Endog.	Cont.	Yes	Yes	Yes

Table A.2: Comparison of important articles and their relation to the ZEVSNDP

Appendix B

Big-M Values

$$M^1 = \max_{p\in\mathcal{P},\ r\in\mathcal{R}_p} \{|\mathcal{C}_r| \cdot |\mathcal{F}_c|\} \tag{B.1}$$

$$M_p^2 = \overline{T}_p, \qquad p \in \mathcal{P} \tag{B.2}$$

$$M_{prc}^3 = \overline{T}_p - (T_{prc,1,|\mathcal{K}_c|} + T_{prc,|\mathcal{K}_c|,1}) \qquad p \in \mathcal{P}, r \in \mathcal{R}_p,\ c \in \mathcal{C}_r \tag{B.3}$$

$$M_p^4 = \frac{(\overline{B}_v - \underline{B}_v)}{P_i}, \qquad i \in \mathcal{I},\ v \in \mathcal{V} \tag{B.4}$$

$$M_p^5 = \frac{(\overline{B}_v - \underline{B}_v)}{P_i}, \qquad i \in \mathcal{I},\ v \in \mathcal{V} \tag{B.5}$$

$$M_p^6 = \frac{(\overline{B}_v - \underline{B}_v)}{P_i}, \qquad i \in \mathcal{I},\ v \in \mathcal{V} \tag{B.6}$$

$$M_{prckl}^7 = D_{prckl}, \qquad p \in \mathcal{P},\ r \in \mathcal{R}_p,\ c \in \mathcal{C}_r,\ k \in \mathcal{K}_c,\ l \in \mathcal{K}_c \tag{B.7}$$

$$M_{prc}^8 = \sum_{i\in\mathcal{I}_r} C_{pi}^{VC} P_i \overline{T}_p, \qquad p \in \mathcal{P},\ r \in \mathcal{R}_p,\ c \in \mathcal{C}_r \tag{B.8}$$

$$M_{prcf}^9 = \sum_{k\in\mathcal{K}_c} \sum_{l\in\mathcal{K}_c} D_{prcklf}, \qquad p \in \mathcal{P},\ r \in \mathcal{R}_p,\ c \in \mathcal{C}_r,\ f \in \mathcal{F}_c \tag{B.9}$$

$$M_{prcf}^{10} = \sum_{k\in\mathcal{K}_c} \sum_{l\in\mathcal{K}_c} \overline{T}_p D_{prcklf}, \qquad p \in \mathcal{P},\ r \in \mathcal{R}_p,\ c \in \mathcal{C}_r,\ f \in \mathcal{F}_c \tag{B.10}$$

Appendix C

Complete Mathematical Formulations

C.1 Complete LP-model

Sets

$\mathcal{C}$	Set of subroutes
$\mathcal{S}$	Set of discrete speed levels
$\mathcal{K}$	Set of sailing legs
$\mathcal{K}_c$	Set of sailing legs in subroute c

Parameters

$\overline{T}$	Length of planning period
T_{cks}	Sailing time of leg k in subroute c with speed s
$\underline{T}^W_{ck}$	Minimum waiting time in port at the beginning of leg k in subroute c to allow passengers to enter and exit the vessel
T^U_{ckl}	Travel time from port at the beginning of leg k to port beginning at leg l in subroute c with the fastest vessel type available, sailing at its fastest speed level with no charging or waiting time beyond the minimum requirements
W_c	Average waiting time at port in subroute c
D_{ckl}	Total demand from port at the beginning of leg k to port at the beginning of leg l in subroute c
D^F_{ckl}	Frequency dependent demand from port at the beginning of leg k to port at the beginning of leg l in subroute c
N_c	Number of vessels in subroute c
Q	Passenger capacity of selected vessel type
F_c	Service frequency in subroute c
E_{cks}	Energy consumption on leg k in subroute c sailing at speed level s
$\overline{B}$	Maximum battery level
$\underline{B}$	Minimum battery level
$\overline{P}_{ck}$	Installed charging power in port at the beginning of leg k in subroute c

C^{FC}	Fixed cost of vessel investment
C^{INF}	Fixed cost of investing in charging infrastructure
C^{CREW}	Crew cost for the chosen amount of vessels during the planning period
C^{VC}_{ck}	Cost per unit of energy charged in port at the beginning of leg k in subroute c
C^{ALT1}	Total alternative travel cost due to unvisited ports
C^{ALT2}_{ckl}	Alternative cost per passenger not transported between port at the beginning of leg k to port at the beginning of leg l in subroute c
C^{PW}	Value of passenger time while waiting at port
C^{SW}	Value of passenger time while sailing

Variables

x_{cks}	Weight variable for speed s on leg k in subroute c
l_{ckl}	Number of passengers traversing leg k with destination port at the end of leg l in subroute c
q_{ckl}	Number of passengers picked up in port at the beginning of leg k with destination at the port at the beginning of leg l in subroute c
u_{ckl}	Unmet demand between port at the beginning of leg k and port at the beginning of leg l in subroute c
t^{RT}_c	Total round trip time in subroute c
c_{ck}	Charging time in subroute c before traversing leg k
w_{ck}	Time spent in port before sailing leg k in subroute c
t_{ckl}	Sailing time from port at the beginning of leg k to port at the beginning of leg l in subroute c
b_{ck}	Battery level when starting leg k in subroute c

Objective function

$$\begin{aligned}\min z = {} & C^{FC} + C^{INF} + C^{CREW} \\ & + \sum_{c\in\mathcal{C}}\sum_{k\in\mathcal{K}_c} C^{VC}_{ck}\overline{P}_{ck}F_c c_{ck} + C^{ALT1} + \sum_{c\in\mathcal{C}}\sum_{k\in\mathcal{K}_c}\sum_{l\in\mathcal{K}_c} C^{ALT2}_{ckl}u_{ckl} \\ & + C^{PW}\sum_{c\in\mathcal{C}} W_c(\sum_{k\in\mathcal{K}_c}\sum_{l\in\mathcal{K}_c} q_{ckl}) + C^{SW}\sum_{c\in\mathcal{C}}\sum_{k\in\mathcal{K}_c}\sum_{l\in\mathcal{K}_c}(t_{ckl} - T^{U}_{ckl})D_{ckl}\end{aligned} \tag{C.1}$$

Constraints

$$t^{RT}_c = \sum_{k\in\mathcal{K}_c}\sum_{s\in\mathcal{S}} T_{cks}x_{cks} + \sum_{k\in\mathcal{K}_c}(c_{ck} + w_{ck}), \qquad c\in\mathcal{C} \tag{C.2}$$

$$F_c t^{RT}_c = N_c\overline{T}, \qquad c\in\mathcal{C} \tag{C.3}$$

$$w_{ck} \geq \underline{T}^{W}_{ck}, \qquad c\in\mathcal{C},\ k\in\mathcal{K}_c \tag{C.4}$$

$$\sum_{s\in\mathcal{S}} x_{cks} = 1, \qquad c\in\mathcal{C},\ k\in\mathcal{K}_c \tag{C.5}$$

$$t_{ckl} = \sum_{s\in\mathcal{S}}\sum_{\hat{k}=k}^{l} t_{c\hat{k}s}x_{c\hat{k}s} + \sum_{\hat{k}=k+1}^{l-1}(c_{c\hat{k}} + w_{c\hat{k}}), \qquad c\in\mathcal{C},\ k\in\mathcal{K}_c,\ l\in\mathcal{K}_c \mid l > k \tag{C.6}$$

$$t_{ckl} = \sum_{s \in \mathcal{S}} \sum_{\hat{k}=k}^{|\mathcal{K}_c|} t_{c\hat{k}s} x_{c\hat{k}s} + \sum_{\hat{k}=k+1}^{|\mathcal{K}_c|} (c_{c\hat{k}} + w_{c\hat{k}}) + \sum_{s \in \mathcal{S}} \sum_{\hat{k}=1}^{l-1} t_{c\hat{k}s} x_{c\hat{k}s} + \sum_{\hat{k}=1}^{l-1} (c_{c\hat{k}} + w_{c\hat{k}}), \quad c \in \mathcal{C},\ k \in \mathcal{K}_c,\ l \in \mathcal{K}_c \mid l < k \tag{C.7}$$

$$b_{ck} = b_{c,k-1} - \sum_{s \in \mathcal{S}} E_{cks} x_{cks} + \overline{P}_{ck} c_{ck}, \quad c \in \mathcal{C},\ k \in \mathcal{K}_c \setminus \{1\} \tag{C.8}$$

$$b_{c1} = b_{c,|\mathcal{K}_c|} - \sum_{s \in \mathcal{S}} E_{c|\mathcal{K}_c|s} x_{c|\mathcal{K}_c|s} + \overline{P}_{c1} c_{c1}, \quad c \in \mathcal{C} \tag{C.9}$$

$$b_{ck} \leq \overline{B}, \quad c \in \mathcal{C},\ k \in \mathcal{K}_c \tag{C.10}$$

$$b_{ck} - \sum_{s \in \mathcal{S}} E_{cks} x_{cks} \geq \underline{B}, \quad c \in \mathcal{C},\ k \in \mathcal{K}_c \tag{C.11}$$

$$c_{ck} \leq M \overline{P}_{ck}, \quad c \in \mathcal{C},\ k \in \mathcal{K}_c \tag{C.12}$$

$$\sum_{l \in \mathcal{K}_c} l_{ckl} \leq QF_c, \quad c \in \mathcal{C},\ k \in \mathcal{K}_c \tag{C.13}$$

$$q_{ckl} = l_{ckl} - l_{c,k-1,l}, \quad c \in \mathcal{C},\ k \in \mathcal{K}_c \setminus \{1\},\ l \in \mathcal{K}_c \mid l \neq k \tag{C.14}$$

$$q_{c1l} = l_{c1l} - l_{c,|\mathcal{K}_c|,l}, \quad c \in \mathcal{C},\ l \in \mathcal{K}_c \setminus \{1\} \tag{C.15}$$

$$q_{ckl} + u_{ckl} = D_{ckl}, \quad c \in \mathcal{C},\ k \in \mathcal{K}_c\ l \in \mathcal{K}_c \tag{C.16}$$

$$l_{c,k-1,l} \leq l_{ckl}, \quad c \in \mathcal{C},\ k \in \mathcal{K}_c \setminus \{1\},\ l \in \mathcal{K}_c \mid l \neq k \tag{C.17}$$

$$l_{c,|\mathcal{K}_c|,l} \leq l_{c1l}, \quad c \in \mathcal{C},\ l \in \mathcal{K}_c \setminus \{1\} \tag{C.18}$$

$$q_{ckl} \leq D^F_{ckl}, \quad c \in \mathcal{C},\ k \in \mathcal{K}_c\ l \in \mathcal{K}_c \tag{C.19}$$

Declaration of variables

$$x_{cks} \in \mathbb{R}^+, \quad c \in \mathcal{C},\ k \in \mathcal{K}_c,\ s \in \mathcal{S} \tag{C.20}$$

$$l_{ckl} \in \mathbb{R}^+, \quad c \in \mathcal{C},\ k \in \mathcal{K}_c,\ l \in \mathcal{K}_c \tag{C.21}$$

$$q_{ckl} \in \mathbb{R}^+, \quad c \in \mathcal{C},\ k \in \mathcal{K}_c,\ l \in \mathcal{K}_c \tag{C.22}$$

$$u_{ckl} \in \mathbb{R}^+, \quad c \in \mathcal{C},\ k \in \mathcal{K}_c,\ l \in \mathcal{K}_c \tag{C.23}$$

$$t^{RT}_c \in \mathbb{R}^+, \quad c \in \mathcal{C} \tag{C.24}$$

$$c_{ck} \in \mathbb{R}^+, \quad c \in \mathcal{C},\ k \in \mathcal{K}_c \tag{C.25}$$

$$w_{ck} \in \mathbb{R}^+, \quad c \in \mathcal{C},\ k \in \mathcal{K}_c \tag{C.26}$$

$$t_{ckl} \in \mathbb{R}^+, \quad c \in \mathcal{C},\ k \in \mathcal{K}_c,\ l \in \mathcal{K}_c \tag{C.27}$$

$$b_{ck} \in \mathbb{R}^+, \quad c \in \mathcal{C},\ k \in \mathcal{K}_c \tag{C.28}$$

C.2 Single Period MIP-model with Fixed Strategic Decisions

Sets

$\mathcal{P}$	Set of planning periods
$\mathcal{R}_p$	Set of potential routes in period p
$\mathcal{C}_r$	Set of subroutes in route r
$\mathcal{K}_c$	Set of legs in route c
$\mathcal{I}$	Set of all ports
$\mathcal{I}_c$	Set of ports in route c
$\mathcal{F}_c$	Set of potential frequencies in subroute c
$\mathcal{S}$	Set of discrete speed levels

Parameters

$\overline{T_p}$	Length of planning period p
T_{prckvs}	Sailing time of leg k in subroute c in route r in period p with speed s and vessel type v
$\underline{T}^W_{prck}$	Minimum waiting time in port at the beginning of leg k in subroute c, in route r, in period p to allow passengers to enter and exit the vessel
T^U_{prckl}	Travel time from port at the beginning of leg k to port beginning at leg l in subroute c in route r in period p with the fastest vessel type available, sailing at its fastest speed level, with no charging or waiting time beyond the minimum requirements
W_{prcf}	Average waiting time at frequency f in time period p for subroute c in route r
D_{prckl}	Maximum demand from port at the beginning of leg k to port at the beginning of leg l in subroute c in period p with route r
D_{prcklf}	Demand from port at the beginning of leg k to port at the beginning of leg l in subroute c in period p with route r at frequency f
N	Number of vessels acquired
Q	Passenger capacity of chosen vessel type
E_{prcks}	Energy consumption on leg k in subroute c in route r in period p sailing at speed s
$\overline{B}$	Maximum battery level of chosen vessel type
$\underline{B}$	Minimum battery level of chosen vessel type
P_{prck}	Available charging power in port at the beginning of leg k in subroute c, in route r, in period p
C^{FC}	Fixed cost from the vessel investment vessel of type v
C^{INF}	Fixed cost of investing in charging infrastructure
C^{VC}_{prck}	Cost per unit of energy charged in port at the beginning of leg k, in subroute c, in route r, in period p
C^{ALT1}_{pr}	Alternative cost per passenger not transported due to unvisited ports in route r in period p
C^{ALT2}_{prckl}	Alternative cost per passenger not transported between port at the beginning of leg k to port at the beginning of leg l in subroute c in route r in period p
C^{PW}	Value of passenger time while waiting at port
C^{SW}	Value of passenger time while sailing

Variables

x_{prckfs}	Weight variable for speed s on leg k in subroute c in route r served with frequency f in period p
l_{prckl}	Number of passengers traversing leg k with destination port at the end of leg l in subroute c, in route r, in period p
q_{prcklf}	Number of passengers picked up in port at the beginning of leg k with destination at the port in the beginning of leg l in subroute c with route r in period p with frequency f
u_{prckl}	Unmet demand between port at the beginning of leg k and port at the beginning of leg l in subroute c with route r in period p
t^{RT}_{prcf}	Round trip time in subroute c, in route r, in period p, served with frequency f
c_{prckf}	Charging time in port at the beginning of leg k in subroute c served with frequency f, in route r, in period p
w_{prckf}	Waiting time in port at the beginning of leg k in subroute c served with frequency f, in route r, in period p
t_{prckl}	Transit time from port at the beginning of leg k to port at the beginning of leg l in subroute c, in route r, in period p
b_{prck}	Battery level before sailing leg k, in subroute c, in route r, in oeriod p
g_{prc}	Vessels used in subroute $c, inorute$r, in period p
z_{prcf}	1 if frequency f is chosen in subroute c, in route r, in period p
β_{pr}	1 if route r is chosen in period p

Auxiliary Variables

v_{prcf}	Auxiliary variable
p_{prcf}	Auxiliary variable
o_{prcf}	Auxiliary variable
s_{prcf}	Auxiliary variable

Objective function

$$\begin{aligned}\min z = & C^{FC} + C^{INF} + \sum_{p\in\mathcal{P}}\sum_{r\in\mathcal{R}_p}\sum_{c\in\mathcal{C}_r}\sum_{f\in\mathcal{F}_c} f\, v_{prcf} \\ & + \sum_{p\in\mathcal{P}}\sum_{r\in\mathcal{R}_p} C^{ALT1}_{pr}\beta_{pr} + \sum_{p\in\mathcal{P}}\sum_{r\in\mathcal{R}_p}\sum_{c\in\mathcal{C}_r}\sum_{k\in\mathcal{K}_c}\sum_{l\in\mathcal{K}_c} C^{ALT2}_{prckl}\, u_{prckl} \\ & + C^{PW}\sum_{p\in\mathcal{P}}\sum_{r\in\mathcal{R}_p}\sum_{c\in\mathcal{C}_r}\sum_{f\in\mathcal{F}_c} W_{prcf}\, p_{prcf} + C^{SW}\sum_{p\in\mathcal{P}}\sum_{r\in\mathcal{R}_p}\sum_{c\in\mathcal{C}_r}\sum_{f\in\mathcal{F}_c} o_{prcf}\end{aligned} \tag{C.29}$$

Constraints

$$\sum_{r\in\mathcal{R}_p}\sum_{c\in\mathcal{C}_r} g_{prc} \leq N, \qquad p\in\mathcal{P} \tag{C.30}$$

$$\sum_{r\in\mathcal{R}_p} \beta_{pr} = 1, \qquad p\in\mathcal{P} \tag{C.31}$$

$$g_{prc} \leq \sum_{f\in\mathcal{F}_c} f\, z_{prcf}, \qquad p\in\mathcal{P},\ r\in\mathcal{R}_p,\ c\in\mathcal{C}_r \tag{C.32}$$

$$\sum_{f\in\mathcal{F}_c} z_{prcf} = \beta_{pr}, \qquad p\in\mathcal{P},\ r\in\mathcal{R}_p,\ c\in\mathcal{C}_r \tag{C.33}$$

$$t^{RT}_{prcf} = \sum_{k\in\mathcal{K}_c}\sum_{s\in\mathcal{S}} T_{prcks}\, x_{prckfs} + \sum_{k\in\mathcal{K}_c} (c_{prckf} + w_{prckf}), \qquad p\in\mathcal{P},\ r\in\mathcal{R}_p,\ c\in\mathcal{C}_r,\ f\in\mathcal{F}_c \tag{C.34}$$

$$s_{prcf} \geq t^{RT}_{prcf} - M(1 - z_{prcf}), \qquad p\in\mathcal{P},\ r\in\mathcal{R}_p,\ c\in\mathcal{C}_r,\ f\in\mathcal{F}_c \tag{C.35}$$

$$s_{prcf} \leq M z_{prcf}, \qquad p\in\mathcal{P},\ r\in\mathcal{R}_p,\ c\in\mathcal{C}_r,\ f\in\mathcal{F}_c \tag{C.36}$$

$$\sum_{f\in\mathcal{F}_c} f\, s_{prcf} = \overline{T}_p\, g_{prc}, \qquad p\in\mathcal{P},\ r\in\mathcal{R}_p,\ c\in\mathcal{C}_r \tag{C.37}$$

$$w_{prckf} \geq T^{W}_{prck}\, z_{prcf}, \qquad p\in\mathcal{P},\ r\in\mathcal{R}_p,\ c\in\mathcal{C}_r,\ k\in\mathcal{K}_c,\ f\in\mathcal{F}_c \tag{C.38}$$

$$w_{prckf} \leq M\, z_{prcf}, \qquad p\in\mathcal{P},\ r\in\mathcal{R}_p,\ c\in\mathcal{C}_r,\ k\in\mathcal{K}_c,\ f\in\mathcal{F}_c \tag{C.39}$$

$$\sum_{s\in\mathcal{S}} x_{prckfs} = z_{prcf}, \qquad p\in\mathcal{P},\ r\in\mathcal{R}_p,\ c\in\mathcal{C}_r,\ k\in\mathcal{K}_c,\ f\in\mathcal{F}_c \tag{C.40}$$

$$\begin{aligned} t_{prckl} = \sum_{f\in\mathcal{F}_c} s_{prcf} - \sum_{f\in\mathcal{F}_c} \Bigg[&\sum_{\hat{k}=l}^{|\mathcal{K}_c|} \Big(\sum_{s\in\mathcal{S}} T_{prc\hat{k},s} x_{prc\hat{k}fs} + w_{prc\hat{k}f} + c_{prc\hat{k}f} \Big) \\ &+ \sum_{k'}^{k-1} \sum_{s\in\mathcal{S}} T_{prck's} x_{prck'fs} + \sum_{\hat{k}=1}^{k} w_{prc\hat{k}f} + c_{prc\hat{k}f} \Bigg], \\ & p\in\mathcal{P},\ r\in\mathcal{R}_p,\ c\in\mathcal{C}_r,\ k\in\mathcal{K}_c,\ l\in\mathcal{K}_c \,|\, l > k \end{aligned} \tag{C.41}$$

$$\begin{aligned} t_{prckl} = \sum_{f\in\mathcal{F}_c} s_{prcf} - \sum_{f\in\mathcal{F}_c} \Bigg[\sum_{\hat{k}=l}^{k-1} \sum_{s\in\mathcal{S}} T_{prc\hat{k},s} x_{prc\hat{k}fs} + \sum_{\hat{k}=l}^{k} w_{prc\hat{k}f} + c_{prc\hat{k}f} \Bigg], \\ p\in\mathcal{P},\ r\in\mathcal{R}_p,\ c\in\mathcal{C}_r,\ k\in\mathcal{K}_c,\ l\in\mathcal{K}_c \,|\, l < k \end{aligned} \tag{C.42}$$

$$\begin{aligned} b_{prck} =& b_{prc,k-1} - \sum_{f\in\mathcal{F}_c}\sum_{s\in\mathcal{S}} E_{prc,k-1,s} x_{prc,k-1,fs} + \sum_{f\in\mathcal{F}_c} P_{prck} c_{prckf}, \\ & p\in\mathcal{P},\ r\in\mathcal{R}_p,\ c\in\mathcal{C}_r,\ k\in\mathcal{K}_c\backslash\{1\} \end{aligned} \tag{C.43}$$

$$\begin{aligned} b_{prc,1} =& b_{prc,|\mathcal{K}_c|} - \sum_{f\in\mathcal{F}_c}\sum_{s\in\mathcal{S}} E_{prc,|\mathcal{K}_c|,s} x_{prc,|\mathcal{K}_c|,fs} + \sum_{f\in\mathcal{F}_c} P_{prc,1,f} c_{prc,1,f}, \\ & p\in\mathcal{P},\ r\in\mathcal{R}_p,\ c\in\mathcal{C}_r \end{aligned} \tag{C.44}$$

$$b_{prck} \leq \overline{B}, \qquad p\in\mathcal{P},\ r\in\mathcal{R}_p,\ c\in\mathcal{C}_r,\ k\in\mathcal{K}_c \tag{C.45}$$

$$b_{prck} \geq \underline{B}, \qquad p\in\mathcal{P},\ r\in\mathcal{R}_p,\ c\in\mathcal{C}_r,\ k\in\mathcal{K}_c \tag{C.46}$$

$$c_{prckf} \leq M\, P_{prck}\, z_{prcf}, \qquad p\in\mathcal{P},\ r\in\mathcal{R}_p,\ c\in\mathcal{C}_r,\ k\in\mathcal{K}_c,\ f\in\mathcal{F}_c \tag{C.47}$$

$$l_{prckl} \leq M g_{prc}, \qquad p\in\mathcal{P},\ r\in\mathcal{R}_p,\ c\in\mathcal{C}_r,\ k\in\mathcal{K}_c,\ l\in\mathcal{K}_c \tag{C.48}$$

$$\sum_{l\in\mathcal{K}_c} l_{prckl} \leq Q \sum_{f\in\mathcal{F}_c} f\, z_{prcf}, \qquad p\in\mathcal{P},\ r\in\mathcal{R}_p,\ c\in\mathcal{C}_r,\ k\in\mathcal{K}_c \tag{C.49}$$

$$\sum_{f \in \mathcal{F}_c} q_{prcklf} = l_{prckl} - l_{prc,k-1,l}, \qquad p \in \mathcal{P},\ r \in \mathcal{R}_p,\ c \in \mathcal{C}_r,\ k \in \mathcal{K}_c \backslash \{1\},\ l \in \mathcal{K}_c \,|\, l \neq k \tag{C.50}$$

$$\sum_{f \in \mathcal{F}_c} q_{prc,1,lf} = l_{prc,1,l} - l_{prc,|\mathcal{K}_c|,l}, \qquad p \in \mathcal{P},\ r \in \mathcal{R}_p,\ c \in \mathcal{C}_r,\ l \in \mathcal{K}_c \,|\, l \neq 1 \tag{C.51}$$

$$q_{prcklf} \leq D_{prcklf}\, z_{prcf}, \qquad p \in \mathcal{P},\ r \in \mathcal{R}_p,\ c \in \mathcal{C}_r,\ k \in \mathcal{K}_c,\ l \in \mathcal{K}_c \,|\, l \neq k,\ f \in \mathcal{F}_c \tag{C.52}$$

$$\sum_{f \in \mathcal{F}_c} q_{prcklf} + u_{prckl} = D_{prckl}, \qquad p \in \mathcal{P},\ r \in \mathcal{R}_p,\ c \in \mathcal{C}_r,\ k \in \mathcal{K}_c,\ l \in \mathcal{K}_c \,|\, l \neq k \tag{C.53}$$

$$l_{prc,k-1,l} \leq l_{prckl}, \qquad p \in \mathcal{P},\ r \in \mathcal{R}_p,\ c \in \mathcal{C}_r,\ k \in \mathcal{K}_c \backslash \{1\},\ l \in \mathcal{K}_c \,|\, l \neq k \tag{C.54}$$

$$l_{prc,1,l} \leq l_{prc,|\mathcal{K}_c|,l}, \qquad p \in \mathcal{P},\ r \in \mathcal{R}_p,\ c \in \mathcal{C}_r,\ l \in \mathcal{K}_c \,|\, l \neq 1 \tag{C.55}$$

$$v_{prcf} \geq \sum_{k \in \mathcal{K}_c} C^{VC}_{prck}\, P_{prck}\, c_{prckf} - M(1 - z_{prcf}), \quad p \in \mathcal{P},\ r \in \mathcal{R}_p,\ c \in \mathcal{C}_r,\ f \in \mathcal{F}_c \tag{C.56}$$

$$v_{prcf} \leq M z_{prcf}, \qquad p \in \mathcal{P},\ r \in \mathcal{R}_p,\ c \in \mathcal{C}_r,\ f \in \mathcal{F}_c \tag{C.57}$$

$$p_{prcf} \geq \sum_{k \in \mathcal{K}_c} \sum_{l \in \mathcal{K}_c} q_{prcklf} - M(1 - z_{prcf}), \qquad p \in \mathcal{P},\ r \in \mathcal{R}_p,\ c \in \mathcal{C}_r,\ f \in \mathcal{F}_c \tag{C.58}$$

$$p_{prcf} \leq M z_{prcf}, \qquad p \in \mathcal{P},\ r \in \mathcal{R}_p,\ c \in \mathcal{C}_r,\ f \in \mathcal{F}_c \tag{C.59}$$

$$o_{prcf} \geq \sum_{k \in \mathcal{K}_c} \sum_{l \in \mathcal{K}_c} (t_{prckl} - T^{U}_{prckl}) D_{prcklf} - M(1 - z_{prcf}), \qquad p \in \mathcal{P},\ r \in \mathcal{R}_p,\ c \in \mathcal{C}_r,\ f \in \mathcal{F}_c \tag{C.60}$$

$$o_{prcf} \leq M z_{prcf}, \qquad p \in \mathcal{P},\ r \in \mathcal{R}_p,\ c \in \mathcal{C}_r,\ f \in \mathcal{F}_c \tag{C.61}$$

$$\beta_{pr} \in \{0, 1\}, \qquad p \in \mathcal{P},\ r \in \mathcal{R}_p \tag{C.62}$$

$$z_{prcf} \in \{0, 1\}, \qquad p \in \mathcal{P},\ r \in \mathcal{R}_p,\ c \in \mathcal{C}_r,\ f \in \mathcal{F}_c \tag{C.63}$$

$$g_{prc} \in \mathbb{Z}^{+}, \qquad p \in \mathcal{P},\ r \in \mathcal{R}_p,\ c \in \mathcal{C}_r \tag{C.64}$$

$$x_{prcks} \in \mathbb{R}^{+}, \qquad p \in \mathcal{P},\ r \in \mathcal{R}_p,\ c \in \mathcal{C}_r,\ k \in \mathcal{K}_c,\ s \in \mathcal{S} \tag{C.65}$$

$$l_{prckl} \in \mathbb{R}^{+}, \qquad p \in \mathcal{P},\ r \in \mathcal{R}_p,\ c \in \mathcal{C}_r,\ k \in \mathcal{K}_c,\ l \in \mathcal{K}_c \tag{C.66}$$

$$q_{prcklf} \in \mathbb{R}^{+}, \qquad p \in \mathcal{P},\ r \in \mathcal{R}_p,\ c \in \mathcal{C}_r,\ k \in \mathcal{K}_c,\ l \in \mathcal{K}_c,\ f \in \mathcal{F}_c \tag{C.67}$$

$$u_{prckl} \in \mathbb{R}^{+}, \qquad p \in \mathcal{P},\ r \in \mathcal{R}_p,\ c \in \mathcal{C}_r,\ k \in \mathcal{K}_c,\ l \in \mathcal{K}_c \tag{C.68}$$

$$t^{RT}_{prcf} \in \mathbb{R}^{+}, \qquad p \in \mathcal{P},\ r \in \mathcal{R}_p,\ c \in \mathcal{C}_r,\ f \in \mathcal{F}_c \tag{C.69}$$

$$c_{prck} \in \mathbb{R}^{+}, \qquad p \in \mathcal{P},\ r \in \mathcal{R}_p,\ c \in \mathcal{C}_r,\ k \in \mathcal{K}_c \tag{C.70}$$

$$w_{prck} \in \mathbb{R}^+, \qquad p \in \mathcal{P},\ r \in \mathcal{R}_p,\ c \in \mathcal{C}_r,\ k \in \mathcal{K}_c \tag{C.71}$$

$$t_{prckl} \in \mathbb{R}^+, \qquad p \in \mathcal{P},\ r \in \mathcal{R}_p,\ c \in \mathcal{C}_r,\ k \in \mathcal{K}_c,\ l \in \mathcal{K}_c \tag{C.72}$$

$$b_{prck} \in \mathbb{R}^+, \qquad p \in \mathcal{P},\ r \in \mathcal{R}_p,\ c \in \mathcal{C}_r,\ k \in \mathcal{K}_c \tag{C.73}$$

$$v_{prcf} \in \mathbb{R}^+, \qquad p \in \mathcal{P},\ r \in \mathcal{R}_p,\ c \in \mathcal{C}_r,\ f \in \mathcal{F}_c \tag{C.74}$$

$$p_{prcf} \in \mathbb{R}^+, \qquad p \in \mathcal{P},\ r \in \mathcal{R}_p,\ c \in \mathcal{C}_r,\ f \in \mathcal{F}_c \tag{C.75}$$

$$o_{prcf} \in \mathbb{R}^+, \qquad p \in \mathcal{P},\ r \in \mathcal{R}_p,\ c \in \mathcal{C}_r,\ f \in \mathcal{F}_c \tag{C.76}$$

$$s_{prcf} \in \mathbb{R}^+, \qquad p \in \mathcal{P},\ r \in \mathcal{R}_p,\ c \in \mathcal{C}_r,\ f \in \mathcal{F}_c \tag{C.77}$$

Appendix D

Input Data

Abbreviation	Port name
Alv	Alvora
Ann	Ånnøy
Ask	Askrova
Bar	Barekstad
Bat	Batalden
Fan	Fanøy
Fer	Ferøyna
Flo	Florø
Kin	Kinn
Ner	Nærøy
Rog	Rognaldsvåg
Sel	Selvåg
Ska	Skorpa
Ske	Skorpeide
Son	Søndre Nekkøy
Sta	Stavang
Sva	Svanøybukt
Vei	Veiesund
Vev	Vevling
Vil	Villevik

Table D.1: Port names with corresponding abbreviations used in subsequent tables

	Alv	Ann	Ask	Bar	Bat	Fan	Fer	Flo	Kin	Ner	Rog	Sel	Ska	Ske	Son	Sta	Sva	Vei	Vev	Vil
Alv	-	7.0	8.4	10.8	11.4	10.6	5.9	7.5	11.4	8.1	11.1	8.1	9.9	8.3	6.4	2.6	5.3	3.3	9.8	8.3
Ann	7.0	-	7.4	5.7	4.7	3.8	1.4	3.1	5.0	2.7	4.6	2.0	3.3	1.6	1.3	9.0	8.7	4.6	3.1	4.1
Ask	8.4	7.4	-	11.8	12.3	10.7	7.0	8.2	6.9	9.1	7.3	7.7	9.0	7.7	6.4	6.8	5.5	7.5	10.2	9.9
Bar	10.8	5.7	11.8	-	3.3	4.3	5.7	6.2	9.1	3.5	8.2	5.9	7.1	5.4	5.9	12.3	12.6	8.6	3.5	4.9
Bat	11.4	4.7	12.3	3.3	-	1.5	6.1	7.2	6.3	4.8	6.0	6.0	7.1	5.3	5.5	13.2	13.1	9.1	1.8	6.3
Fan	10.6	3.8	10.7	4.3	1.5	-	5.1	6.4	5.1	4.2	5.0	5.0	6.1	4.4	4.5	12.1	12.3	9.2	0.8	5.6
Fer	5.9	1.4	7.0	5.7	6.1	5.1	-	2.2	6.1	2.9	5.7	3.0	4.6	2.9	1.5	7.4	7.6	4.8	4.6	3.4
Flo	7.5	3.1	8.2	6.2	7.2	6.4	2.2	-	8.2	3.1	7.7	54.1	6.5	4.8	3.6	9.0	9.1	4.7	5.9	2.8
Kin	11.4	5.0	6.9	9.1	6.3	5.1	6.1	8.2	-	7.2	0.6	4.0	1.9	3.5	5.0	12.2	11.5	9.4	4.8	8.4
Ner	8.1	2.7	9.1	3.5	4.8	4.2	2.9	3.1	7.2	-	6.8	4.5	5.5	3.8	3.7	10.3	11.0	7.1	3.4	1.4
Rog	11.1	4.6	7.3	8.2	6.0	5.0	5.7	7.7	0.6	6.8	-	3.7	1.5	3.1	4.8	12.8	12.1	9.4	4.6	7.8
Sel	8.1	2.0	7.7	5.9	6.0	5.0	3.0	5.1	4.0	4.5	3.7	-	2.8	1.3	1.8	9.1	9.0	5.9	4.0	6.0
Ska	9.9	3.3	9.0	7.1	7.1	6.1	4.6	6.5	1.9	5.5	1.5	2.8	-	1.8	3.4	11.1	11.1	7.6	5.6	6.9
Ske	8.3	1.6	7.7	5.4	5.3	4.4	2.9	4.8	3.5	3.8	3.1	1.3	1.8	-	2.0	9.8	9.5	6.5	3.4	5.2
Son	6.4	1.3	6.4	5.9	5.5	4.5	1.5	3.6	5.0	3.7	4.8	1.8	3.4	2.0	-	7.7	7.6	4.5	3.7	4.4
Sta	2.6	9.0	6.8	12.3	13.2	12.1	7.4	9.0	12.2	10.3	12.8	9.1	11.1	9.8	7.7	-	1.4	4.3	12.1	10.4
Sva	5.3	8.7	5.5	12.6	13.1	12.3	7.6	9.1	11.5	11.0	12.1	9.0	11.1	9.5	7.6	3.4	-	5.1	11.7	12.6
Vei	3.3	4.6	7.5	8.6	9.1	9.2	4.8	4.7	9.4	7.1	9.4	5.9	7.6	6.5	4.5	4.3	5.1	-	8.3	7.0
Vev	9.8	3.1	10.2	3.5	1.8	0.8	4.6	5.9	4.8	3.4	4.6	4.0	5.6	3.4	3.7	12.1	11.7	8.3	-	4.7
Vil	8.3	4.1	9.9	4.9	6.3	5.6	3.4	2.8	8.4	1.4	7.8	6.0	6.9	5.2	4.4	10.4	12.6	7.0	4.7	-

Table D.2: Distances in nautical miles between ports

	Alv	Ann	Ask	Bar	Bat	Fan	Fer	Flo	Kin	Ner	Rog	Sel	Ska	Ske	Son	Sta	Sva	Vei	Vev	Vil
Alv	-	0.0	0.0	0.0	0.0	0.0	0.0	0.0	0.0	0.0	0.0	0.0	0.0	0.0	0.0	0.0	0.0	0.0	0.0	0.0
Ann	0.0	-	0.0	0.0	0.0	0.0	0.0	1.6	0.0	0.0	0.0	0.0	0.0	0.0	0.0	0.0	0.0	0.0	0.0	0.0
Ask	0.0	0.0	-	0.0	0.0	0.0	0.0	5.2	0.0	0.0	0.0	0.0	0.0	0.0	0.0	0.0	0.0	0.0	0.0	0.0
Bar	0.0	0.0	0.0	-	0.0	0.2	0.0	6.9	0.0	0.0	0.0	0.0	0.0	0.0	0.0	0.0	0.0	0.0	0.0	0.2
Bat	0.0	0.0	0.0	0.0	-	0.0	0.0	0.3	0.0	0.0	0.0	0.0	0.0	0.0	0.0	0.0	0.0	0.0	0.0	0.0
Fan	0.0	0.0	0.0	0.2	0.0	-	0.0	6.0	0.0	0.0	0.0	0.0	0.0	0.0	0.0	0.0	0.0	0.0	0.0	0.0
Fer	0.0	0.0	0.0	0.0	0.0	0.0	-	0.2	0.0	0.0	0.0	0.0	0.0	0.0	0.0	0.0	0.0	0.0	0.0	0.0
Flo	0.0	0.7	27.0	12.3	0.2	13.4	4.7	-	3.2	1.3	24.5	0.1	3.2	0.0	0.3	0.0	10.4	10.0	0.1	8.9
Kin	0.0	0.0	0.0	0.0	0.0	0.0	0.0	2.0	-	0.0	0.0	0.0	0.0	0.0	0.0	0.0	0.0	0.0	0.0	0.0
Ner	0.0	0.0	0.0	0.0	0.0	0.0	0.0	0.1	0.0	-	0.0	0.0	0.0	0.0	0.0	0.0	0.0	0.0	0.0	0.0
Rog	0.0	0.0	0.0	0.0	0.0	0.0	0.0	9.8	0.0	0.0	-	0.0	0.1	0.0	0.0	0.0	0.0	0.0	0.0	0.0
Sel	0.0	0.0	0.0	0.0	0.0	0.0	0.0	0.0	0.0	0.0	0.0	-	0.0	0.0	0.0	0.0	0.0	0.0	0.0	0.0
Ska	0.0	0.0	0.0	0.0	0.0	0.0	0.0	1.7	0.0	0.0	0.1	0.0	-	0.0	0.0	0.0	0.0	0.0	0.0	0.0
Ske	0.0	0.0	0.0	0.0	0.0	0.0	0.0	0.1	0.0	0.0	0.0	0.0	0.0	-	0.0	0.0	0.0	0.0	0.0	0.0
Son	0.0	0.0	0.0	0.0	0.0	0.0	0.0	0.0	0.0	0.0	0.0	0.0	0.0	0.0	-	0.0	0.0	0.0	0.0	0.0
Sta	0.0	0.0	0.0	0.0	0.0	0.0	0.0	0.0	0.0	0.0	0.0	0.0	0.0	0.0	0.0	-	0.0	0.0	0.0	0.0
Sva	0.0	0.0	0.0	0.0	0.0	0.0	0.0	7.9	0.0	0.0	0.0	0.0	0.0	0.0	0.0	0.0	-	0.1	0.0	0.0
Vei	0.0	0.0	0.0	0.0	0.0	0.0	0.0	1.1	0.0	0.0	0.0	0.0	0.0	0.0	0.0	0.0	0.0	-	0.0	0.0
Vev	0.0	0.0	0.0	0.0	0.0	0.0	0.0	0.0	0.0	0.0	0.0	0.0	0.0	0.0	0.0	0.0	0.0	0.0	-	0.0
Vil	0.0	0.0	0.0	0.0	0.0	0.0	0.0	4.4	0.0	0.1	0.0	0.0	0.0	0.0	0.0	0.0	0.0	0.0	0.0	-

Table D.3: Observed daily average demand for transportation in the Florø area for the peak time period, between 01:00 PM and 05:00 PM

Appendix E

Illustrations of Route Choices

E.1 Test Instance AP-ZE

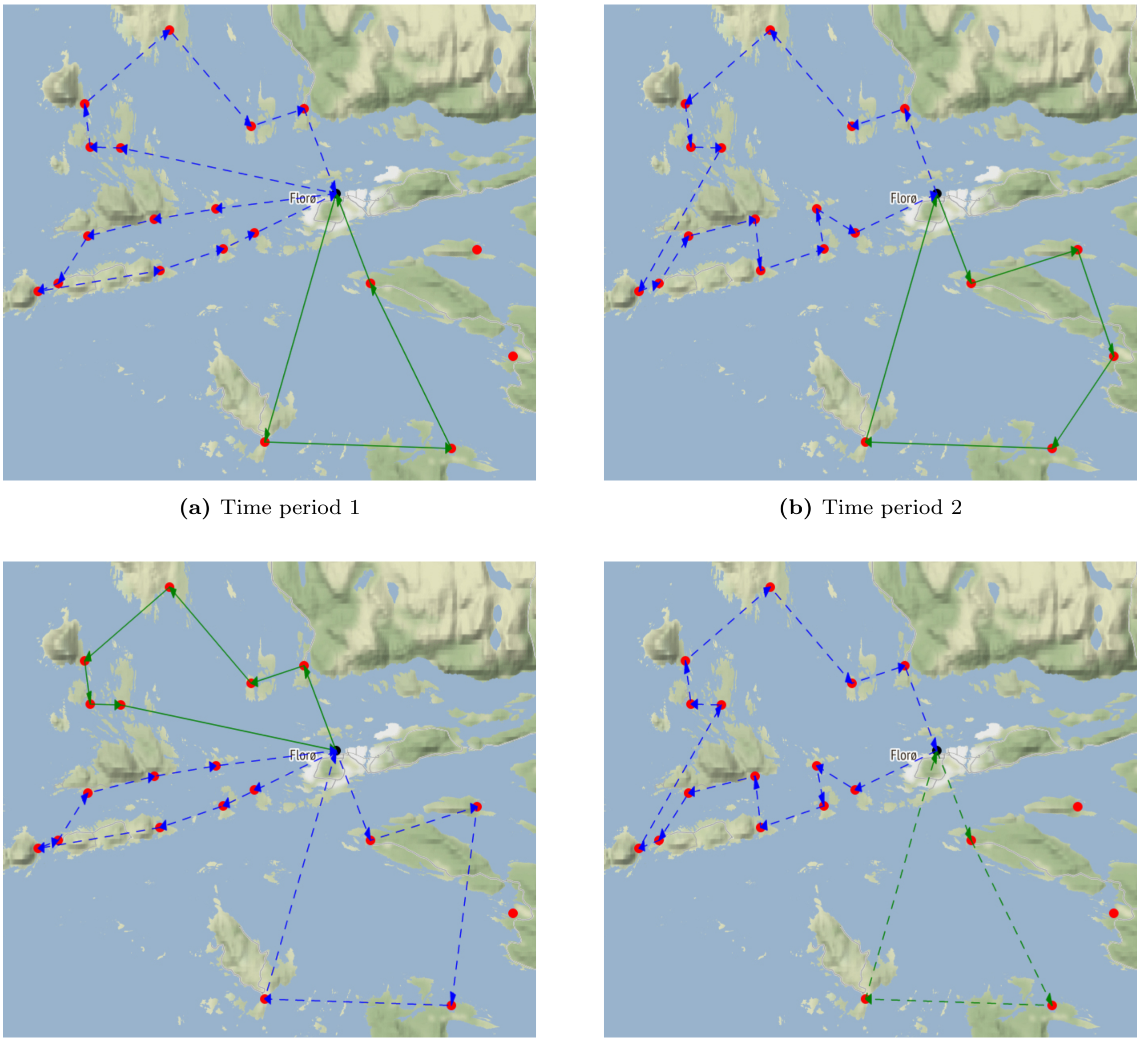

(a) Time period 1

(b) Time period 2

(c) Time period 3

(d) Time period 4

Figure E.1: Route choices in the AP-ZE instance. Different colored lines indicate separate sub-routes and the arrow at the end indicate the direction it is sailed. Dashed lines indicate a frequency of 1, whereas solid lines indicate a frequency of 2.

E.2 Test Instance `AP-C`

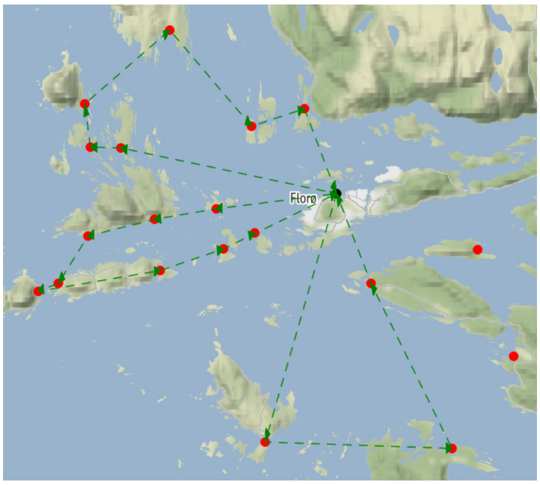

(a) Time period 1

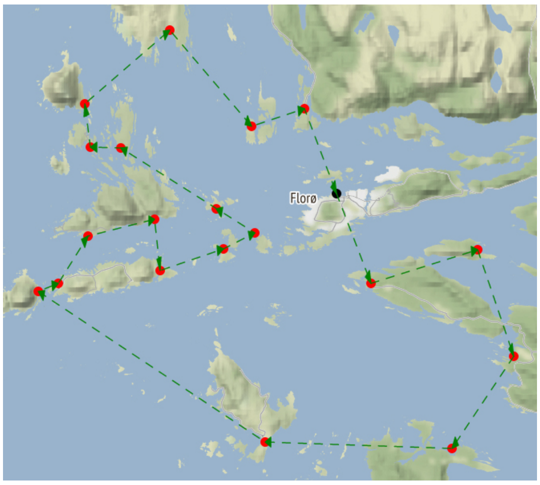

(b) Time period 2

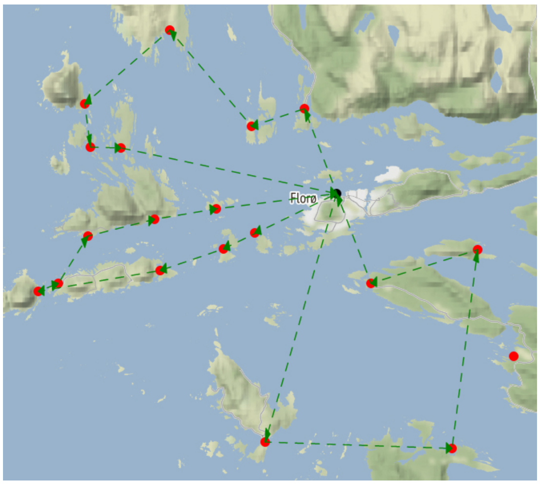

(c) Time period 3

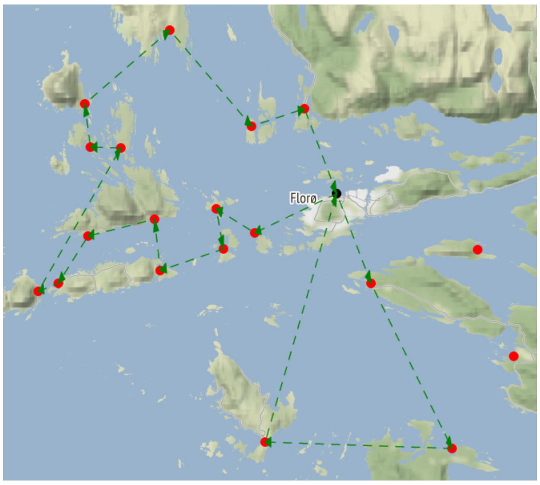

(d) Time period 4

Figure E.2: Route choices in the `AP-C` instance. Different colored lines indicate separate subroutes and the arrow at the end indicate the direction it is sailed. Dashed lines indicate a frequency of 1, whereas solid lines indicate a frequency of 2.

E.3 Test Instance `NP-ZE`

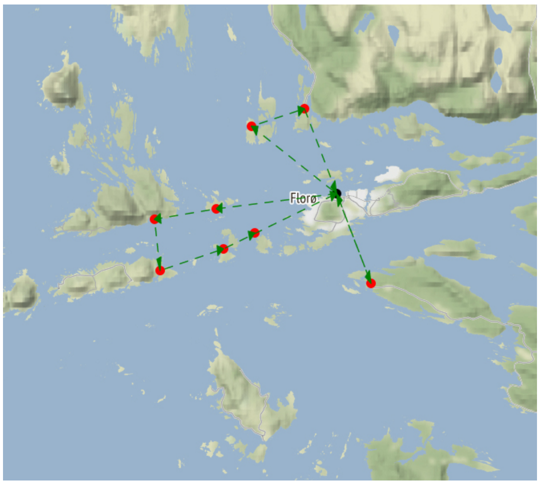

(a) Time period 1

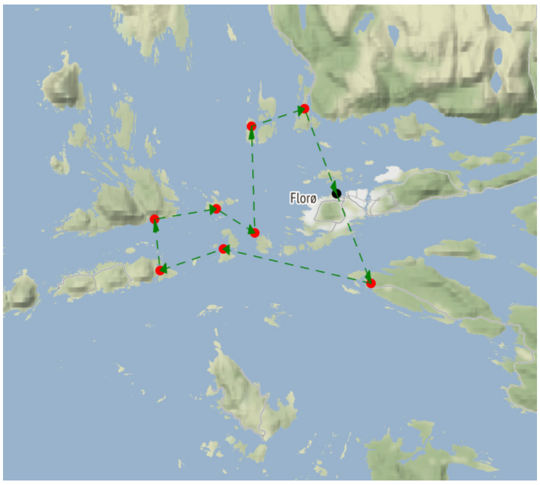

(b) Time period 2

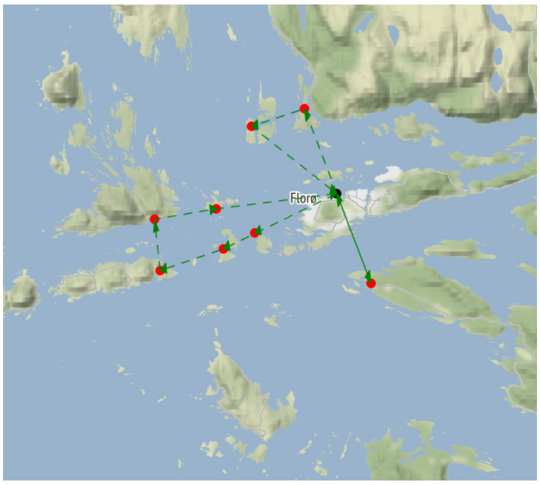

(c) Time period 3

(d) Time period 4

Figure E.3: Route choices in the `NP-ZE` instance. Different colored lines indicate separate subroutes and the arrow at the end indicate the direction it is sailed. Dashed lines indicate a frequency of 1, whereas solid lines indicate a frequency of 2.

E.4 Test Instance `NP-C`

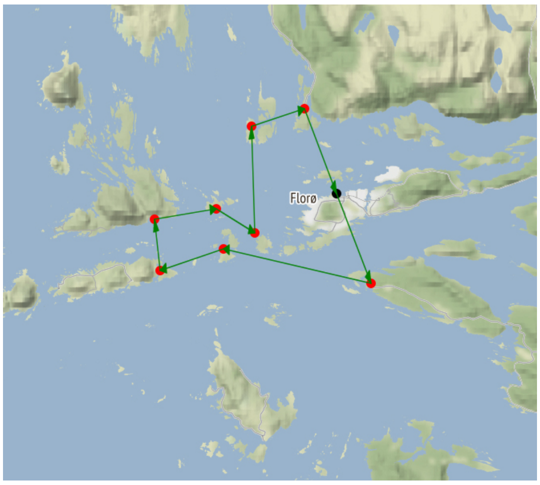

(a) Time period 1

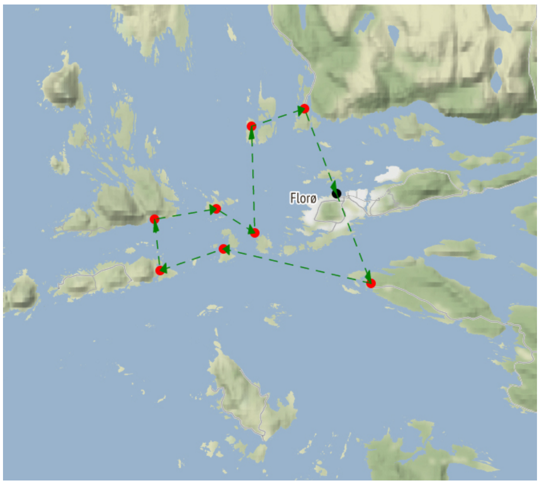

(b) Time period 2

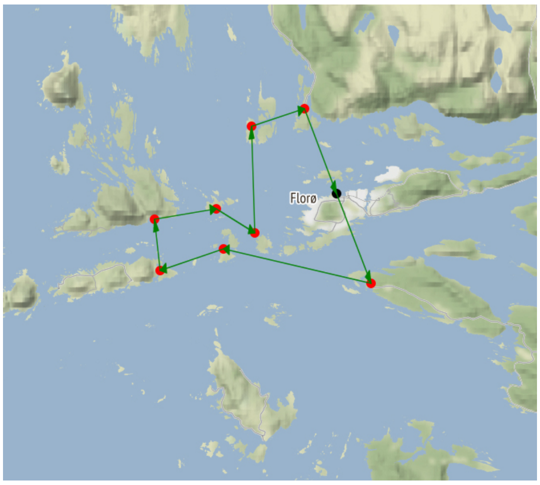

(c) Time period 3

(d) Time period 4

Figure E.4: Route choices in the `NP-C` instance. Route choices in the `NP-ZE` instance. Different colored lines indicate separate subroutes and the arrow at the end indicate the direction it is sailed. Dashed lines indicate a frequency of 1, whereas solid lines indicate a frequency of 2.

E.5 Test Instance HD-ZE

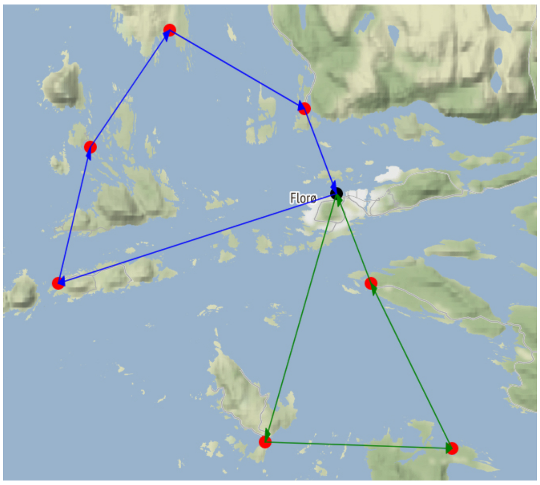

(a) Time period 1

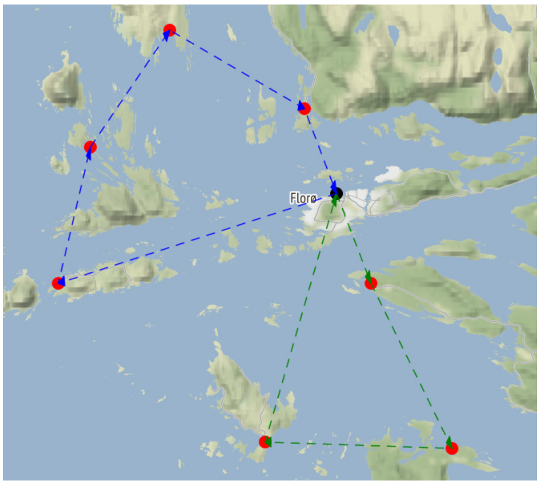

(b) Time period 2

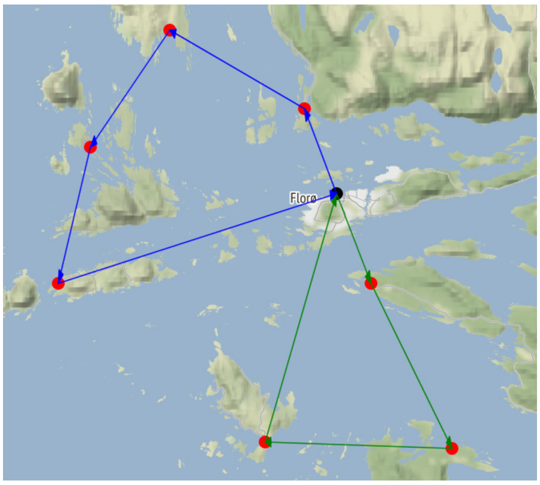

(c) Time period 3

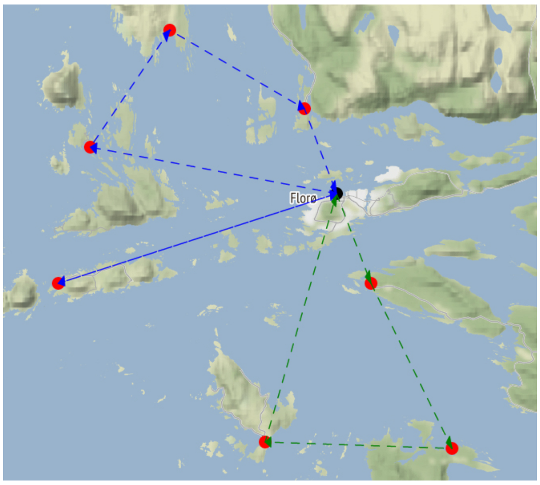

(d) Time period 4

Figure E.5: Route choices in the HD-ZE instance. Route choices in the NP-C instance. Route choices in the NP-ZE instance. Different colored lines indicate separate subroutes and the arrow at the end indicate the direction it is sailed. Dashed lines indicate a frequency of 1, whereas solid lines indicate a frequency of 2.

E.6 Test Instance HD-C

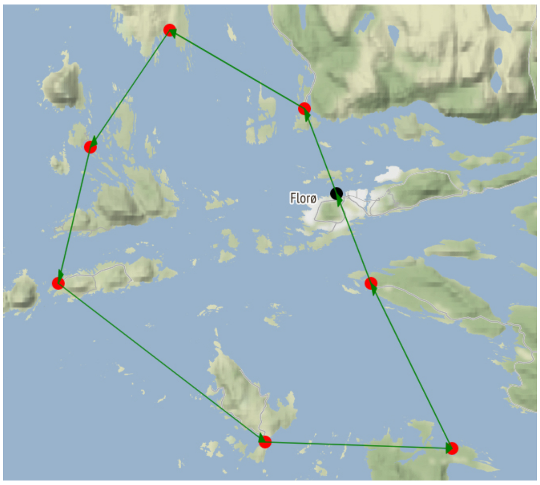

(a) Time period 1

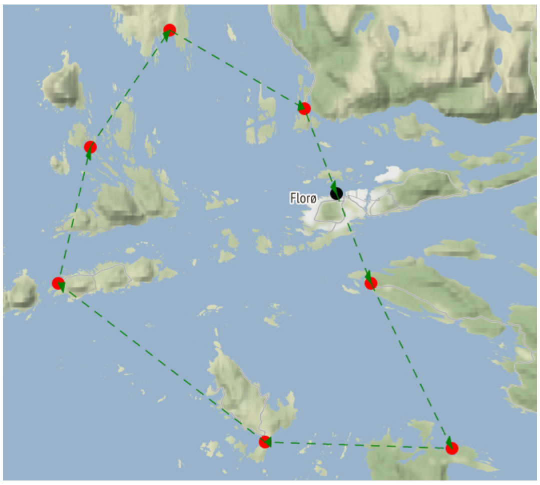

(b) Time period 2

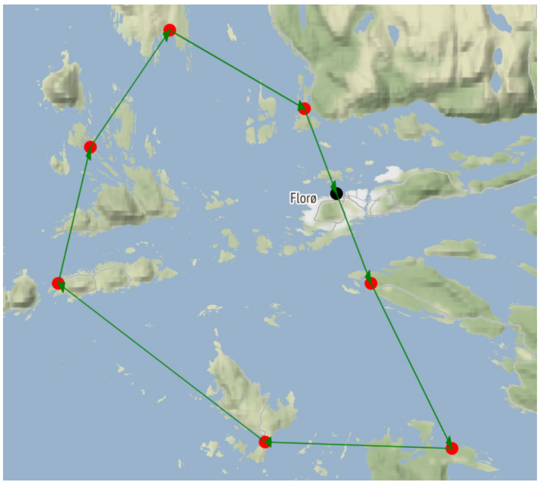

(c) Time period 3

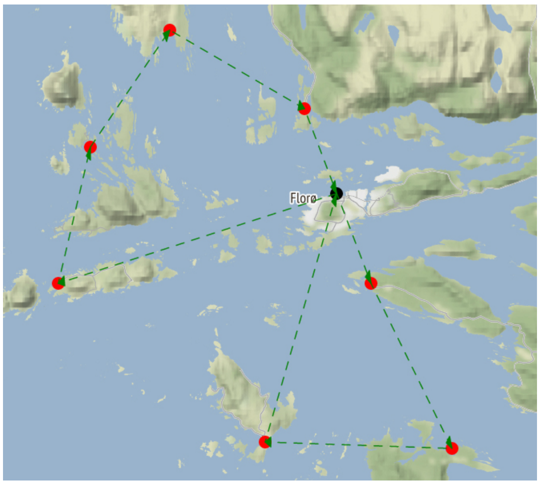

(d) Time period 4

Figure E.6: Route choices in the HD-C instance. Route choices in the HD-ZE instance. Route choices in the NP-C instance. Route choices in the NP-ZE instance. Different colored lines indicate separate subroutes and the arrow at the end indicate the direction it is sailed. Dashed lines indicate a frequency of 1, whereas solid lines indicate a frequency of 2.

Håkon F. Havre, Ulrik Lien, Mattias M. Ness

Network Design for Zero Emission Passenger Vessel Services

NTNU

Norwegian University of
Science and Technology